

Evaluation of diagnostic methods for vector-borne viral infections and development of tools for the study of yellow fever infections

Inaugural-Dissertation to obtain the academic degree
Doctor rerum naturalium (Dr. rer. Nat.)

submitted to the

Department of Biology, Chemistry and Pharmacy
of the Freie Universität of Berlin



by

Camille Escadafal

from Châtenay-Malabry (France)

2014

The presented Ph.D. thesis was conducted from September 2011 to May 2014 at Robert Koch Institute, Berlin, Germany under the supervision of Prof. Dr. Matthias Niedrig.

1st reviewer: Prof. Dr. Matthias Niedrig
Robert Koch Institute, Berlin

2nd reviewer: Prof. Dr. Rupert Mutzel
Freie Universität Berlin

Date of defense: 18th July 2014

DECLARATION OF AUTHORSHIP

I certify that the work presented here is, to the best of my knowledge and belief, original and the result of my own investigations, except as acknowledged. The present work has not been submitted, either in part or completely, for a degree at this or any other University.

Date : _____

Signature: _____

ACKNOWLEDGEMENTS

It is a pleasure for me to thank the persons who have supported me during the achievement of this PhD thesis:

*My supervisor at the Robert Koch Institute, **Professor Matthias Niedrig**, for offering me such a great working experience and learning opportunity. At his side, I have learned a lot in the field of virology but also about human relationships. I also thank him for his kindness, support and liberty of initiative he gave me throughout all this work.*

*My supervisor at the Freie Universität, **Professor Rupert Mützel**, for listening and advising me and facilitating every stage of the process.*

***Nina Stock**, for her availability, her support, her joyful energy and her friendship.*

***Pranav Patel**, for his help and for sharing knowledge and fructifying ideas.*

***Oliver Donoso-Mantke**, for being the greatest coordinator I ever had!*

***Pauline Prüger**, for her constant dedication and for her communicative thirst of knowledge.*

***Dia Roy Chowdhury** and **Ravish Paliwal**, for their words and laughs of solidarity throughout our collective adventure.*

***Nadine Litzba**, for sharing her knowledge in science and her wisdom in life.*

***Peter Hagerdorn**, for introducing me to the fascinating world of ticks!*

***Regina Schädler**, for being such a great support since my first day in Berlin.*

***Andrea Sanchini** and **Sergejs Nikisins**, for providing an improved version of the EUPHEM fellow in Berlin and a fun multicultural work environment!*

***Marion Mielke**, for sweeping away bad moods each morning.*

***Anette Teichmann**, for her joyful assistance.*

*My parents, **Richard** and **Colette**, for supporting me in all my choices.*

*My husband, **Omar Latsouck**, for his every day comfort, love and indulgence.*

ABSTRACT

Vector-borne diseases represent over 17% of all infectious diseases in humans causing one billion deaths each year. Public health efforts to strengthen vector-borne disease detection, surveillance and control have been intensified and laboratories play a key role in this process. Since diagnostic methods for vector-borne infections are often not standardized, it is essential to evaluate the quality of diagnostic methods currently in use in laboratories by organizing external quality assurance (EQA) programs.

The first chapter of this dissertation presents the organization and analysis of five EQA studies on the serological and/or molecular detection of hantavirus, yellow fever virus, Rift Valley fever virus and Crimean-Congo hemorrhagic fever virus. The analysis of all study results enabled to identify important weak points in the diagnostic procedures performed by the different participating laboratories and propose recommendations for the future development of EQAs.

The next chapters of the dissertation focus on the study and the development of diagnostic tools for yellow fever virus (YFV) infections. The second chapter describes the development of an isothermal molecular method for YFV detection using recombinase polymerase amplification (RPA). The YFV RPA assay proved to be a specific and sensitive detection method during testing with a low detection limit and rapid processing time by using a portable instrument. Therefore the RPA method can provide an affordable alternative to current PCR-based technologies allowing an early and accurate molecular diagnosis of YFV infections in low-resource remote endemic areas.

A second diagnostic approach for YFV infections was investigated by producing antibodies for the specific detection of the non-structural 1 (NS1) protein which is already used as an early diagnostic marker for dengue infections. Production and characterization of three polyclonal anti-NS1 sera from guinea pig was performed and allowed specific detection of the YFV NS1 in immunofluorescence and Western blot assays. Even though the development of an ELISA assay could not be brought to success within the frame of this study, preliminary results confirm the NS1 protein as a promising diagnostic marker for early detection of YFV infections and provide a basis for the further development of a quantitative assay for YFV NS1 detection.

The third and last chapter of this dissertation describes the development of tools for the study of the pathogenesis of YFV infections in live cell imaging microscopy. For that purpose, fluorescent labeling of viral proteins of the 17D vaccine strain was performed by using the tetracysteine (TC-) tag technology (FIASH). The project had been initiated at the Robert Koch

Institute where four full-length YFV-17D plasmids with the TC-tag in the envelope or the capsid (C) protein had been constructed. In this work, the potential use of the four YFV-17D constructs as models for the study of YFV pathogenesis was investigated. One construct with the TC-tag in the C protein lead to the production of live infectious virus particles and showed similar growth characteristics compared to the parental 17D-virus. However, further experiments revealed that the TC-tagged virus was not able to produce fluorescence after staining with the FIAsH-reagent.

In summary, the various results of this PhD work are a significant contribution to the development of international EQA programs for diagnostic methods of vector-borne viral infections and to the enlargement of the methodological spectrum for the investigation and diagnostics of yellow fever virus.

ZUSAMMENFASSUNG

Vektorübertragene Krankheiten verursachen über 17% aller Infektionskrankheiten im Menschen und dadurch eine Milliarde Todesfälle pro Jahr. Bestrebungen des Gesundheitswesens zur Erkennung, Überwachung und Kontrolle vektorübertragener Krankheiten sind kontinuierlich verstärkt worden und mikrobiologische Labore spielen dabei eine Schlüsselrolle. Da diagnostische Methoden zur Detektion vektorübertragener Krankheiten häufig nicht standardisiert sind, ist es von großer Bedeutung die Qualität der derzeit in den Laboren verwendeten Methoden durch die Durchführung externer Qualitätskontrollen (EQA) zu evaluieren.

Das erste Kapitel dieser Dissertation beschreibt die Organisation und Analyse von fünf EQA Studien zur serologischen und/oder molekularbiologischen Detektion von Hantaviren, Gelbfiebertviren, Rift Valley Fieber- und Krim-Kongo Hämorrhagisches Fiebertviren. Die Analyse aller Untersuchungsergebnisse zeigt Schwachpunkte in den diagnostischen Prozessen der teilnehmenden Labore auf und liefert Verbesserungsvorschläge für die zukünftige Entwicklung von EQAs.

Die weiteren Kapitel dieser Arbeit konzentrieren sich auf die Untersuchung und Entwicklung diagnostischer Methoden zum Nachweis von Gelbfiebertviren (GFV). Das zweite Kapitel beschreibt die Entwicklung einer molekularen, isothermalen Methode zur GFV Detektion mittels *recombinase polymerase amplification* (RPA). Hierbei erwies sich der GFV RPA Assay als spezifische und sensitive Nachweismethode mit einem niedrigen Detektionslimit und kurzer Bearbeitungszeit, die in einem tragbaren Gerät durchgeführt werden kann. Die RPA Methode bietet daher eine erschwingliche Alternative zu gegenwärtigen PCR-basierten Technologien, die eine frühe und genaue Diagnose von GFV Infektionen besonders in unterversorgten und entlegenen Endemiegebieten ermöglicht.

Ein zweiter diagnostischer Ansatz zum Nachweis von GFV Infektionen wurde durch die Produktion von Antikörpern zur spezifischen Detektion des NS1-Proteins untersucht. Das NS1-Protein wird bereits als früher diagnostischer Marker bei Infektionen mit dem Denguevirus verwendet. Insgesamt wurden drei polyklonale anti-NS1 Seren in Meerschweinchen hergestellt und charakterisiert, die eine spezifische Detektion des GFV NS1-Proteins im Immunfluoreszenztest und Western Blot ermöglichen. Obwohl die Entwicklung eines ELISA-Tests im Rahmen dieser Arbeit nicht erfolgreich abgeschlossen werden konnte, bestätigen die vorläufigen Ergebnisse das diagnostische Potential des NS1-Proteins für eine frühe Detektion von GFV-Infektionen und liefern eine Grundlage für die weitere Entwicklung eines quantitativen Tests zum Nachweis des GFV NS1-Proteins.

Das dritte und letzte Kapitel dieser Dissertation beschreibt die Entwicklung eines Tools zur Untersuchung der GFV-Pathogenese mittels *live cell imaging*-Mikroskopie. Dazu wurden virale Proteine des GFV Impfstammes 17D unter Anwendung der Tetracystein (TC)-Technologie fluoreszenzmarkiert. Das Projekt wurde zuvor am Robert Koch-Institut initiiert, wo vier GFV-17D Volllängeklone hergestellt wurden, die den TC-Marker im Hüll- oder Capsid (C)-Protein tragen. In dieser Arbeit wurde die Möglichkeit untersucht, diese vier GFV-17D Konstrukte als Modellviren zur Untersuchung der GFV-Pathogenese zu verwenden. Ein Konstrukt mit dem TC-Tag im C-Protein führte zur Produktion infektiöser viraler Partikel und wies vergleichbare Wachstumseigenschaften zu dem ursprünglichen 17D Volllängeklon auf. Allerdings zeigten weiterführende Experimente, dass das Virus mit dem TC-Tag keine spezifische Fluoreszenz nach einer Färbung mit dem FIAsH Reagens aufwies.

Zusammengefasst liefern die verschiedenen Ergebnisse dieser Doktorarbeit einen bedeutenden Beitrag zur Entwicklung internationaler EQA Programme für diagnostische Methoden zur Erkennung vektorübertragener viraler Erkrankungen sowie zur Erweiterung des methodologischen Spektrums für die Untersuchung und Diagnose von Gelbfieberviren.

ABBREVIATIONS

APS	Ammonium Persulfate
BSA	Bovine serum albumin
bp	Base pair
CCHFV	Crimean-Congo hemorrhagic fever virus
CDC	Centre of Disease Control and Prevention
CMC	Carboxy methyl cellulose
CO₂	Carbone dioxide
CPE	Cytopathic effects
Ct	Threshold cycle
ddNTP	Dideoxynucleotide
DENV	Dengue virus
DNA	Deoxyribonucleic acid
DOBV	Dobrava-Belgrade virus
DTT	Dithiothreitol
EIA	Enzyme immunoassay
ELISA	Enzyme-linked immunosorbent assay
ECDC	European Centre of Disease Control and Prevention
EQA	External Quality Assurance
ENIVD	European Network for Diagnostics of “Imported” Viral Diseases
FITC	Fluorescein isothiocyanate
FBS	Fetal bovine serum
Geq	Genome equivalents
Geq/rxn	Genome equivalent copies per reaction
GFP	Green fluorescent protein
H₂O	Water
HIV	Human immunodeficiency virus
HRP	Horseradish peroxydase
HDA	Helicase dependent amplification
IBA	Immunoblot assays
IFA	Immunofluorescence assay
IgG	Immunoglobulin G
IgM	Immunoglobulin M
ivRNA	In vitro transcribed RNA
JEV	Japanese Encephalitis virus
kDa	Kilodalton
KLH	Keyhole limpet hemocyanin

LAMP	Loop-mediated amplification
LFS	Lateral flow stripe
LNA	Locked nucleotide
MgCl₂	Magnesium chloride
MOI	Multiplicity of infection
NALF	Nucleic acid based lateral flow assay
NASBA	Nucleic acid sequence based amplification
NS	Non-structural protein
NAT	Nucleic acid testing
OD	Optical density
PAA	Polyacrylamide
PBS	Phosphate buffered saline
PBST	PBS with Tween 20
PCR	Polymerase chain reaction
PFU	Plaque forming units
PRNT	Plaque reduction neutralization tests
PUUV	Puumala virus
real-time qPCR	Quantitative real-time PCR
real-time RT-qPCR	Quantitative real-time RT-PCR
RKI	Robert Koch Institute
RNA	Ribonucleic acid
rNTP	Ribonucleoside tri-phosphate
RPA	Recombinase polymerase amplification
RT	Room temperature
RT-PCR	Reverse transcriptase-polymerase chain reaction
RVFV	Rift valley fever virus
SAEs	Severe adverse events
SDS	Sodium dodecyl sulfate
SDA	Strand displacement amplification
Taq	<i>Thermus aquaticus</i>
TBEV	Tick-borne encephalitis virus
TBST	Tris-Buffered Saline and 0,05% Tween 20
TC	Tetracysteine
WHO	World health organization
WB	Western blot
WNV	West Nile virus
YF	Yellow fever
YFV	Yellow fever virus
xFP	Fluorescent proteins

PUBLICATIONS

Related to the PhD dissertation

1. **Escadafal C**, Avsic-Zupanc T, Vapalahti O, Niklasson B, Teichmann A, et al. (2012) Second external quality assurance study for the serological diagnosis of hantaviruses in Europe. PLoS Negl Trop Dis 6: e1607.
2. **Escadafal C**, Olschlager S, Avsic-Zupanc T, Papa A, Vanhomwegen J, et al. (2012) First international external quality assessment of molecular detection of Crimean-Congo hemorrhagic fever virus. PLoS Negl Trop Dis 6: e1706.
3. Domingo C, **Escadafal C**, Rumer L, Mendez JA, Garcia P, et al. (2012) First international external quality assessment study on molecular and serological methods for yellow fever diagnosis. PLoS One 7: e36291.
4. **Escadafal C**, Paweska JT, Grobbelaar A, le Roux C, Bouloy M, et al. (2013) International External Quality Assessment of Molecular Detection of Rift Valley Fever Virus. PLoS Negl Trop Dis 7(5): e2244.
5. **Escadafal C**, Faye O, Sall AA, Faye O, Weidmann M, et al. (2014) Rapid Molecular Assays for the Detection of Yellow Fever Virus in Low-Resource Settings. PLoS Negl Trop Dis 8(3): e2730. doi: 10.1371/journal.pntd.0002730
6. Stock NK, **Escadafal C**, Achazi K, Cissé M, and Niedrig M. Development, characterization and application of polyclonal peptide antibodies for the detection of yellow fever virus proteins. (In preparation for submission to the Journal of Virological Methods)

Other publications

7. Donoso Mantke O, **Escadafal C**, Niedrig M, Pfeffer M, Working Group For Tick-Borne Encephalitis Virus C (2011) Tick-borne encephalitis in Europe, 2007 to 2009. Euro Surveill 16.
8. Sambri V, Capobianchi M, Cavrini F, Charrel R, Donoso-Mantke O, **Escadafal C**, et al. (2013) Diagnosis of West Nile Virus Human Infections: Overview and Proposal of Diagnostic Protocols Considering the Results of External Quality Assessment Studies. Viruses 5: 2329-2348
9. Chapter on Tick-borne encephalitis viruses - Manual of Security Sensitive Microbes and Toxins on behalf of Taylor & Francis Group - Cat #: K15299 – (Published on April 16, 2014 by CRC Press)

"The stupidest virus is cleverer than the cleverest virologist." George Klein (1925-....)

TABLE OF CONTENTS

DECLARATION OF AUTHORSHIP	I
ACKNOWLEDGEMENTS	III
ABSTRACT	IV
ZUSAMMENFASSUNG	VI
ABBREVIATIONS	VIII
PUBLICATIONS	X
INTRODUCTION	4
A BACKGROUND	4
A.1 <i>Vector-borne viruses</i>	4
A.1.1 Introduction	4
A.1.2 Transmission and emergence of vector-borne viruses	5
A.1.3 Diagnosis of arbovirus infections	11
A.1.4 Prevention and treatment	13
A.2 <i>Yellow fever virus</i>	14
A.2.1 Introduction	14
A.2.2 Virus structure	15
A.2.3 Flavivirus life cycle	17
A.2.4 Transmission cycle	18
A.2.5 The disease	20
A.2.6 Diagnosis	22
A.2.7 Treatment and prevention	23
A.2.8 The yellow fever vaccine history	23
B OBJECTIVES AND OUTLINE OF THE DISSERTATION	26
CHAPTER 1 EXTERNAL QUALITY ASSESSMENT OF DIAGNOSTIC METHODS FOR VECTOR-BORNE VIRAL INFECTIONS	28
A INTRODUCTION	28
B METHODS	30
B.1 <i>Planning</i>	30
B.2 <i>Panel preparation and distribution</i>	31
B.3 <i>Announcement</i>	31
B.4 <i>Evaluation of results</i>	32
C RESULTS	33
C.1 <i>Summary</i>	33

C.2	<i>Molecular Assays</i>	34
C.3	<i>Serological Assays</i>	37
D	DISCUSSION	40
CHAPTER 2	DEVELOPMENT OF DIAGNOSTIC METHODS FOR YELLOW FEVER INFECTIONS	44
A	RECOMBINASE POLYMERASE AMPLIFICATION	44
A.1	<i>Introduction</i>	44
A.2	<i>Methods</i>	49
A.2.1	Viruses and mosquito pools	49
A.2.2	RNA extraction and sample preparation	50
A.2.3	Primer and probe design for RPA	50
A.2.4	Real-time RT-PCR	50
A.2.5	Real-time RT-RPA	51
A.2.6	Lateral-flow strip RT-RPA assay	52
A.2.7	Analytical specificity of real-time and LFS RT-RPA	52
A.2.8	Analytical sensitivity of real-time and LFS RT-RPA	55
A.2.9	Testing of mosquito pools with real-time RT-RPA and RT-PCR	55
A.3	<i>Results</i>	55
A.3.1	Analytical specificity of real-time and LFS RT-RPA	55
A.3.2	Analytical sensitivity of real-time and LFS RT-RPA	58
A.3.3	Testing of mosquito pools with real-time RT-RPA	58
A.4	<i>Discussion</i>	58
B	DETECTION OF YELLOW FEVER VIRUS NS1 ANTIGEN	61
B.1	<i>Introduction</i>	61
B.2	<i>Methods</i>	63
B.2.1	Peptide immunogen design	63
B.2.2	Production of polyclonal antisera	64
B.2.3	Indirect immunofluorescence assay	64
B.2.4	Cultivation of adherent cells	66
B.2.5	Plaque Reduction Neutralization Test	67
B.2.6	Preparation of cell culture supernatants positive for YFV NS1 protein	68
B.2.7	Western blot	68
B.2.8	ELISA	71
B.3	<i>Results</i>	73
B.3.1	Peptide immunogen design and production of polyclonal antisera	73
B.3.2	Indirect immunofluorescence assay	74
B.3.3	Plaque reduction neutralization test	76
B.3.4	Western blot	77
B.3.5	ELISA	79

B.4	Discussion	82
CHAPTER 3	DEVELOPMENT OF TOOLS FOR THE LIVE-CELL IMAGERY OF YELLOW FEVER INFECTIONS	89
A	INTRODUCTION	89
B	METHODS	93
B.1	<i>Sequencing of the cDNA plasmid clones</i>	93
B.1.1	Polymerase chain reaction (PCR)	93
B.1.2	Agarose gel electrophoresis	94
B.1.3	Gel extraction for purification of DNA fragments	95
B.1.4	Sample preparation for DNA sequencing	95
B.2	<i>Preparation of viral RNA from cDNA clones and Transfection of cells with the viral RNA</i>	96
B.2.1	Linearization of the cDNA plasmids	96
B.2.2	DNA purification	96
B.2.3	In-vitro transcription of the cDNA into viral RNA	96
B.2.4	Determining the concentration of nucleic acids solution	97
B.2.5	Cell counting	97
B.2.6	Transfection of viral RNA in Vero E6 cells	97
B.3	<i>Monitoring of virus production after RNA transfection</i>	99
B.3.1	Sampling procedure after transfection	99
B.3.2	Real-time reverse transcription polymerase chain reaction (RT-PCR)	99
B.3.3	Viral titration by plaque assay	99
B.3.4	Indirect immunofluorescence assay	100
B.3.5	Preparation of virus stock	100
B.4	<i>Virus characterization by Growth kinetics on Vero cells</i>	101
B.5	<i>Labeling of the TC-tagged virus with FIAsH reagent</i>	102
C	RESULTS	103
C.1	<i>Sequencing of the cDNA plasmid clones</i>	103
C.2	<i>Transfection of cells with the viral RNA from cDNA clones</i>	103
C.3	<i>Monitoring of Virus Production after RNA Transfection</i>	104
C.4	<i>Virus characterization by Growth kinetics on Vero cells</i>	106
C.5	<i>Labeling of the TC-tagged virus with FIAsH reagent</i>	108
D	DISCUSSION	109
	GENERAL CONCLUSION	113
	REFERENCES	119
	LIST OF MATERIALS	131
	CURRICULUM VITAE	142

INTRODUCTION

A BACKGROUND

A.1 VECTOR-BORNE VIRUSES

A.1.1 Introduction

Viruses are unique and fascinating biological entities. They exist in a gap between the living and non-living, and have consistently challenged our definitions of life. But most of all, viruses inspire great fear in us. Borne by water, food, air, blood, or mosquitoes, viruses are estimated to cause over 60% of infectious diseases, ranging from the trivial common cold or diarrhea, to the most lethal diseases such as encephalitis and hemorrhagic fevers [1]. Their potential of causing great damage to plants or animals coupled with their small size (20 to 400 nanometers) indicates they are highly efficient and sophisticated machineries.

Therefore it is essential to study and to understand the nature of viruses and how they cause illness. With this knowledge we are able to provide effective means of diagnosis, treatment and prevention of viral infections through the development of accurate diagnostic methods, antiviral drugs and vaccines.

Paradoxically, the more science progresses, the more we realize that the study of infectious diseases along with the battle against viral diseases is without end. Even though smallpox was eradicated in 1981 by launching massive vaccination programs, this has only been possible thanks to the combination of several key factors proper to the biology and the ecology of this virus [2]. Unlike smallpox, vector-borne viruses can never be eradicated as the vectors transmitting the disease (mosquitoes, ticks, rodents...) cannot be totally eliminated. For this reason the focus needs to be on prevention and treatment by improving vector control and developing effective vaccines, drugs and diagnostic methods.

Vector-borne viruses are often assimilated to arthropod-borne viruses, also named arboviruses. Nevertheless, some vector-borne viruses are transmitted by rodents and are infective to humans without the intervention of arthropod vectors. Transmission occurs by direct contact with rodent body fluids or excretions. Major rodent-borne viruses, include hantaviruses (*Bunyaviridae* family), Lassa fever virus and South American hemorrhagic fever viruses (i.e. Junin, Machupo, Guanarito and Sabia virus) (*Arenaviridae* family).

Arthropod-borne viruses have been defined by the World Health Organization (WHO) as a group of viruses that survives in nature through biological transmission between susceptible vertebrate hosts by hematophagous (blood-feeding) arthropods including mosquitoes, ticks, midges and sandflies. The term “arbovirus” has no taxonomic significance and is referring to the common biological and ecological characteristics of a heterogeneous group of viruses. The arboviruses include a wide variety of RNA viruses, a majority of which belongs to the *Bunyaviridae*, *Flaviviridae* and *Togaviridae* families and a minority to the *Reoviridae* and *Orthomyxoviridae* families. These virus groups have very diverse genome structures and replication strategies, suggesting that viral transmission by arthropods has arisen successively during virus evolution. Only one DNA arbovirus has been reported, the *African swine fever virus*. This indicates that the greater genetic plasticity and higher mutation rate of RNA genomes are more suitable to arboviruses which are able to replicate alternatively in vertebrate and non-vertebrate hosts.

Over 545 suspected arbovirus species are catalogued and more than 150 are documented to cause disease in humans, with clinical signs ranging from flu-like symptoms, muscle and joint pain (e.g. dengue and chikungunya disease) to hemorrhagic symptoms (e.g. Crimean-Congo hemorrhagic fever and yellow fever) and/or neurological illness (e.g. tick-borne and West Nile encephalitis) [3]. However, most human arboviral infections are asymptomatic and therefore remain unnoticed. Table 1 gives an overview of the most important arboviruses worldwide based on their taxonomy, ecology, geographical distribution and impact on human health.

A.1.2 Transmission and emergence of vector-borne viruses

An arbovirus transmission cycle always involves the virus and at least one primary arthropod vector and one non-human primary vertebrate host. The complex relationship between these three components is influenced by several factors such as the susceptibility of the host for the virus, the appetite of the vector for the host and the vectors' competence for the particular virus [4-6]. The virus multiplies in the tissues of the arthropod generating high virus concentrations in the salivary glands which can then be transmitted to vertebrates by arthropod bites [7]. Most arboviruses are zoonotic and have a maintenance enzootic cycle involving birds or mammals as reservoir hosts (Figure 1). While the virus infects the host, it undergoes a process called amplification, where the virus replicates at sufficient levels to induce viremia. The high virus concentration in the host's blood allows the host to transmit the virus to other organisms if its blood is consumed by them. When uninfected vectors become infected from feeding, they are then capable of transmitting the virus to uninfected

hosts, continuing amplification of virus populations. Humans do not amplify the virus sufficiently to infect further arthropods. For this reason humans are infected accidentally and are most often dead-end hosts [8]. Only a few viruses such as dengue, yellow fever and chikungunya viruses implicate humans as amplifying hosts in their transmission cycle. These viruses can be involved in urban transmission cycles and lead to arbovirus outbreaks without the requirement of an animal reservoir [9]. Based on their level of occurrence, each virus listed in Table 1 has been classified as sporadic, endemic or epidemic. Sporadic viruses cause isolated cases; endemic viruses are continuously present in reservoir hosts whereas epidemic viruses can cause seasonal increased disease occurrence and potential outbreaks. The risk of an arbovirus outbreak is increased by large population movements, introduction of a virus in a new area or climatic events such as heavy rainfall [10].

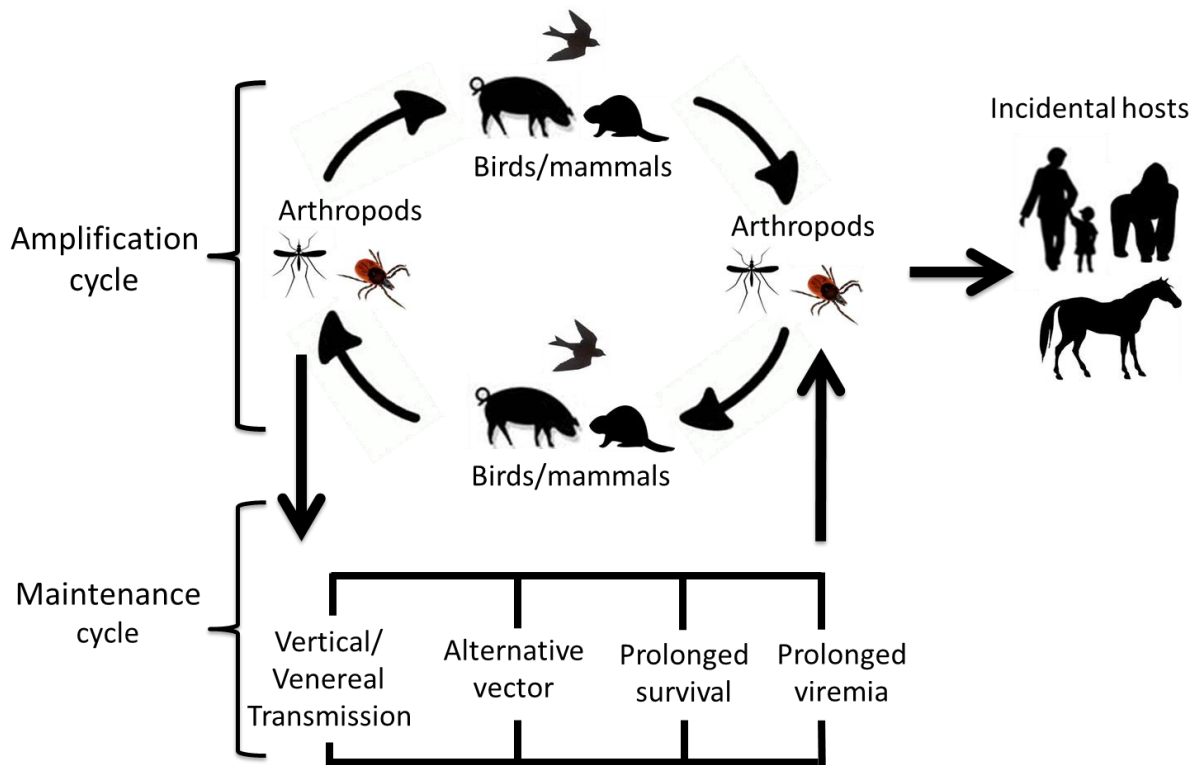


Figure 1: Main pattern of the transmission cycle of arboviruses

In the past three decades, many vector-borne diseases, and in particular arboviral diseases have emerged. From 1990 to 2000, the proportion of vector-borne diseases approached 30% of all emerging diseases [11]. Many arboviruses have recently increased in importance as human and veterinary pathogens through several mechanisms such as geographic expansion of the pathogens and their respective vectors [12]. Arbovirus transmission is suspected to progress as these mechanisms are enhanced by the increase in human travel and animal trade as well as deforestation and global warming [13]. The study of

determining the factors influencing disease emergence is very complex and controversial. In general, emergence in new regions is brought about by pathogen movement due to human travel and animal trade, whereas local emergence is usually caused by a combination of environmental changes affecting vectors and reservoir hosts and social changes affecting human exposure. The effect of climate change on the emergence of vector-borne diseases has been increasingly discussed by the scientific community and while some scientific studies claim that climate change plays a primary role in the emergence of vector-borne diseases, others suggest that the effects of climate change will probably be less than those of changes in land use and social factors [14, 15].

As the emergence of zoonotic and vector-borne diseases is raising concern in Europe, the European Union has allocated financial support to several research programs, such as PREDEMICS and ANTIGONE, aiming at providing preparedness, prediction and prevention of emerging zoonotic pathogens with pandemic potential using multidisciplinary approaches. Other European projects such as EDENext and VECTORIE (Vector-borne Risks for Europe) focus their research on biology, risk assessment and control of vector-borne infections in Europe.

Nevertheless, the burden of vector-borne diseases is more significant outside Europe and arboviral diseases may often be considered as neglected tropical diseases [16]. In fact, arboviral diseases are too often neglected because they have not yet severely affected populations of developed areas. Many of these diseases remain unnoticed until outbreaks affect European or North American countries, as recently displayed in the recent surge of interest in chikungunya after outbreaks occurred in 2005-2006 in the Reunion Island, a French overseas department and major European vacation destination [17], and in Italy in 2007 [18].

The lack of research and effective diagnostic tools for arbovirus infections contributes to our rudimentary understanding of the pathogenesis of these diseases and our inability to decipher one infection from another. For example, understudied arbovirus infections such as yellow fever and chikungunya may represent a significant portion of malaria misdiagnosis causing a significant drawback to Sub-Saharan populations [19, 20]. Eventually, arboviral diseases should be considered of importance to global health as they cause long-lasting sequelae and considerably alter the quality of life of already impoverished populations [21].

INTRODUCTION - Background

Table 1: Summary of taxonomy and reported information on the ecology and human health impact of most common arboviruses. Adapted from Cleton et al., 2012 [22]

<i>Family/genus</i>	<i>Virus</i>	<i>Vector</i>	<i>Host</i>	<i>Geographical distribution</i>	<i>Occurrence</i>	<i>Symptoms</i>	<i>Incubation in days</i>	<i>Prevalence in local population</i>	<i>Considered under diagnosed</i>	<i>Ref.</i>
<i>Bunyaviridae</i>										
Nairovirus	Crimean-Congo hemorrhagic fever (CCHFV)	Tick	Domestic and wild animals, birds, small mammals	South-East and Eastern Europe, Africa, Asia	Sp and En	FD, HS, (NS)	1-9	5-13%	Yes	[23, 24]
Orthobunyavirus	Bwamba (BWAV)	Mosquito	Unknown	Sub-Saharan Africa	En	FD, AR, (NS)	1-14	2,6-80%	Yes	[25-27]
	Bunyamwera (BUNV)	Mosquito	Possibly rodents	Sub-Saharan Africa	En	FD, AR, (NS)	Unknown	Up to 100%	Yes	[27-29]
	Ilesha (ILEV)	Mosquito	Unknown	Sub-Saharan Africa	En	FD, AR, (NS, HS)	Unknown	38-54%	Yes	[27, 30]
	Ngari (NRIV)	Mosquito	Unknown	Sub-Saharan Africa	En	FD, AR, HS	Unknown	Unknown	Yes	[29, 31]
	LaCrosse (LCV)	Mosquito	Small mammals	North America	En	FD, NS	5-15	2-13%	Yes	[32, 33]
	Tahyna (TAHV)	Mosquito	Rodents, rabbits, small mammals	Europe, Asia, Africa	En	FD, AR, (NS), conjonctivitis	5-15	60-80%	Yes	[34, 35]
	Guaroa (GROV)	Mosquito	Unknown	Central and South America	En	FD, AR	Unknown	13-18%	Yes	[36, 37]
Phlebovirus	Ôropouche (OROV)	Midge	Humans, sloths	Central and South America	En	FD, AR, (NS)	4-8	15-60%	Yes	[37-39]
	Tataguine (TATV)	Mosquito	Unknown	Sub-Saharan Africa	En	FD, AR	Unknown	Estimated high	Yes	[40]
	Rift Valley Fever (RVFV)	Mosquito	Rodents, bats, cattle	Africa, Western Asia	En and Ep	FD, HS, NS, hepatitis	1-7	2-14%	No	[41, 42]
	Toscana (TOSV)	Sandfly	Humans, bats	Southern Europe	En	FD, NS, (AR)	2-14	5-51%	No	[43, 44]
	Other sandfly fever (SFV)	Sandfly	Humans, rodents	S- Europe, N-Africa, Asia	En	FD	2-14	3-36%	No	[45]

INTRODUCTION - Background

Table 1: (continued)

Family/genus	Virus	Vector	Host	Geographical distribution	Occurrence	Symptoms	Incubation period in days	Prevalence in local population	Considered under diagnosed	Ref.	
Flaviviridae											
Flavivirus	Yellow (YFV)	fever	Mosquito	Humans, Primates	Sub-Saharan Africa and South-America	En and Ep	FD, hepatitis	HS, 3-6	Estimated high	Yes	[46-48]
	Dengue (DENV)		Mosquito	Humans, Primates	South-America, Asia, Africa	En and Ep	FD, AR, HS	4-14	High	Yes	[49, 50]
	West Nile (WNV)	Nile	Mosquito	Birds	Americas, South and E-Europe, S-E Asia, Oceania	En and Ep	FD, NS, (AR)	2-14	High	No	[51-53]
	Japanese encephalitis (JEV)		Mosquito	Birds, pigs	Asia, Oceania	En and Ep	FD, NS	5-15	High	Yes	[54, 55]
	St. Louis encephalitis (SLEV)	Louis	Mosquito	Birds	Americas	En and Sp	FD, NS	5-15	3-13%	Yes	[56, 57]
	Murray Valley encephalitis (MVEV)	Valley	Mosquito	Birds	Oceania	En and Sp	FD, NS	7-28	Up to 40%	No	[58, 59]
	Tick-borne encephalitis (TBEV)		Tick	Rodents, small mammals	Northern, Eastern and Central Europe, Asia	En	FD, NS, (HS)	7-14	High	Yes	[60, 61]
	Kyasanur Forest disease (KFDV)		Tick	Humans, small mammals	South-East and Western Asia	Ep	FD, conjunctivitis, pneumonia	HS, 3-8	Unknown	No	[62, 63]
	Alkhumra hemorrhagic fever (AHFV)		Tick	Small mammals	Western Asia	Ep	FD, HS	3-12	1,3%	No	[64, 65]
	Ilheus (ILHV)		Mosquito	Birds	Central and South America	En	FD, NS	Unknown	3,4-26%	Yes	[66, 67]

INTRODUCTION - Background

Table 1: (continued)

Family/genus	Virus	Vector	Host	Geographical distribution	Occurrence	Symptoms	Incubation period in days	Prevalence in local population	Considered under diagnosed	Ref.
Reoviridae										
Coltivirus	Colorado tick fever (CTFV)	Tick	Small mammals	North America	Sp	FD, NS, AR, HS	3-6	Unknown	Yes	[68]
Seadornavirus	Banna (BANV)	Mosquito	Unknown	Asia	En	FD, NS, AR	Unknown	Unknown	Yes	[69]
Togaviridae										
Alphaviruses	Chikungunya (CHIKV)	Mosquito	Humans, Primates	Asia, Africa	En and Ep	FD, AR, (NS, HS) conjunctivitis	1-12	Up to 75%	Yes	[70-72]
	Mayaro (MAYV)	Mosquito	Birds, humans, primates	South America	En	FD, AR, (HS)	3-12	5-60%	Yes	[73, 74]
	O'Nyong-nyong (ONNV)	Mosquito	Humans, Primates	Sub-Saharan Africa	En and Ep	FD, AR	>8	31-68%	No	[75-77]
	Ross (RRV)	River Mosquito	Mammals, marsupials	Oceania	Ep	FD, AR, (HS)	3-21	8-65%	No	[78, 79]
	Barmah Forest (BFV)	Forest Mosquito	Birds, marsupials	Australia	Ep and Sp	FD, AR	2-9	High	No	[79]
	Eastern equine encephalitis (EEEV)	Equine Mosquito	Birds, small mammals	Americas	Sp	FD, NS	4-10	Unknown	No	[80, 81]
	Sindbis (SINV)	Mosquito	Birds	Europe, Asia, Africa	Ep	FD, AR	1-7	5-27%	Yes	[82, 83]
	Western equine encephalitis (WEEV)	Mosquito	Birds, small mammals	Americas	Sp and Ep	FD, NS	2-10	Unknown	No	[81]
	Venezuelan equine encephalitis (VEEV)	Mosquito	Small mammals	Americas	En and Ep	FD, NS	1-5	23-50%	Yes	[81, 84]

Sp: sporadic; En: endemic; Ep: epidemic; FD: febrile disease; AR: arthralgia, HS: hemorrhagic syndrome; NS: neurological syndrome

A.1.3 Diagnosis of arbovirus infections

Since arbovirus infections are difficult to prevent and may cause rapid and severe diseases, quick and reliable diagnosis of such infections is crucial. Unfortunately, the clinical diagnosis of arbovirus infections is particularly difficult because of the non-specificity of the clinical picture. In fact, the early symptoms caused by arboviruses, are similar to symptoms caused by a wide variety of diseases such as leptospirosis, viral hepatitis, malaria, and other hemorrhagic viral diseases. Because of these difficulties, the development of rapid identification methods and high-quality laboratory-based diagnosis is necessary for appropriate treatment and accurate assessment of the disease burden.

The choice of the most appropriate diagnostic method is based on the known characteristics specific to each virus such as its incubation period and its pattern of viremia and antibody response (Figure 2).

Laboratory diagnosis during the viremic phase of the illness is based on direct detection of the virus by detecting the virus itself, its genome or antigens. Methods available for direct detection are 1) virus isolation, 2) molecular methods detecting viral genome copies and 3) viral antigen detection methods.

Virus isolation is laborious and requires several days of cultivation. Since most arboviruses are highly pathogenic and need to be handled in appropriate bio-containment facilities, the use of virus isolation is limited to a few highly equipped laboratories.

Molecular methods include mainly polymerase chain reaction (PCR)-based methods and more particularly reverse-transcriptase (RT)-PCR as most arboviruses are RNA viruses. These methods offer a rapid and sensitive alternative for early diagnosis during the viremic phase of infection or in postmortem tissues. They also provide genetic material for further characterization by genome sequencing. Nevertheless, molecular methods have a lower sensitivity for the diagnosis of viruses such as West Nile and Toscana virus which produce short and low viremias and develop symptoms only after the viremic phase [51, 53, 85].

Antigen detection methods are poorly developed and mostly available only as in-house assays, partly due to the low commercial impact of most arboviruses. Such assays have been developed for the detection of the secretory non-structural protein 1 (NS1) of flaviviruses. NS1 detection has already been reported to be a sensitive and highly specific method for early diagnosis of dengue infections [86].

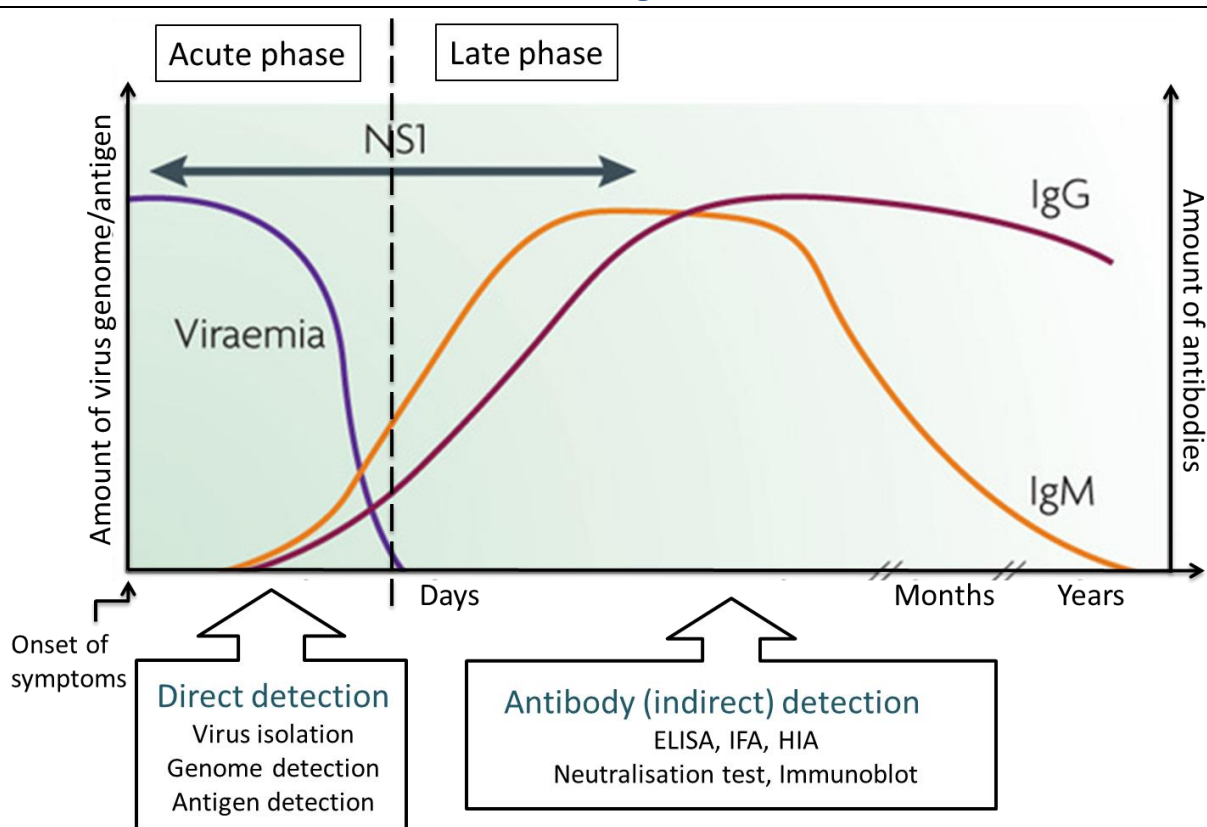


Figure 2: Main pattern of viremia and antibody response following a primary arbovirus infection and main available diagnostic methods according to the stage of infection. Adapted from Guzman et al., 2010 [87].

Once the infection enters the late phase, indirect detection methods should be used and serological detection is the most appropriate choice. Serological diagnostic methods are mainly based on haemagglutination (HIA), enzyme-linked immunosorbent (ELISA), indirect immunofluorescence (IFA) and seroneutralization (NT) assays. During arbovirosis, IgM antibodies commonly appear within a few days after infection and are usually detectable up to 3 months after infection. IgG antibodies develop several days after IgM antibodies and persist for longer periods after initial infection ranging from a few months to a life-long period. Paired sera samples collected with a 10-14 days interval are required to determine whether seroconversion occurred. A 4-fold increase in antibody titer ratio is required to confirm seroconversion, thus providing a positive diagnosis.

Nevertheless, direct methods are more specific than serological methods as IgM and IgG antibodies can cross-react within serogroups and cause false positive results when using IFA or ELISA. The flavivirus genus, in particular, reveals high levels of cross-reaction between IgG antibodies of its several serogroups [88]. Other genera are more prone to cross-reactions between IgM antibodies. Seroneutralization assays are considered the most specific serological technique. However, they are laborious and time-consuming, and only

INTRODUCTION - Background

available in laboratories with cell culture and bio-containment facilities. Table 2 summarizes the most significant characteristics of the main diagnostic techniques.

Table 2: Basic features of the main diagnostic methods for arbovirus infections

Method	Length	Sensitivity	Specificity	Simplicity
Direct detection				
Virus isolation	2-7 days	High	High	Low
PCR*	3-4 hours	High	High	Good
Real-time PCR*	2-3 hours	High	High	Low
Sequencing*	1-2 days	High	High	Low
Antigen capture ELISA	3-5 hours	Good	High	High
Indirect detection				
IgM / IgG ELISA	3-5 hours	High	Low	High
IFA	2-4 hours	Good	Good	High
NT	4-7 days	Good	High	Low
HIA	2-4 hours	Low	Good	High

*: possibility for typing

A.1.4 Prevention and treatment

There are no specific effective antiviral treatments for any of the arboviral infections. Thus only supportive care such as fluid and electrolyte management can be provided to the patient. Nevertheless, early identification of the disease allows clinicians to adjust the treatment to a variety of specific complications and substantially increase the survival rate. The lack of specific treatment is partially due to our limited understanding of virus-host interactions and the mechanisms used by hosts to restrict infection. Nevertheless, many potential molecular targets for antiviral therapeutics against arboviruses, and in particular flaviviruses are currently under exploration [89] and there is exciting potential for future success [90]. Furthermore, neutralizing monoclonal antibody (mAb)-based therapy represents a promising and safe alternative strategy, even though they are at a very early stage of development [91]. RNA interference (RNAi)-based intervention has also shown interesting results in animal models or infected cells [92] as well as the use of interferon and ribavirin [93, 94].

Vector control measures are essential to reduce the transmission of arboviruses. Habitat control involves draining swamps and removing of other pools of stagnant water that often serve as breeding grounds for mosquitoes. Insecticides can also be applied in rural and urban areas, inside houses and buildings or in outdoor environments. A more recent and

environmentally friendly method is the introduction of sterilized male mosquitoes in endemic areas in order to reduce the breeding rate of relevant mosquito species [95]. People can also reduce the risk of getting bitten by arthropods by employing personal protective measures such as sleeping under mosquito nets, wearing protective clothing, applying insect repellents and avoiding areas known to harbor high arthropod populations [96].

Vaccines are available only for Japanese encephalitis (based on inactivated or live-attenuated virus), Tick-borne encephalitis (based on inactivated virus) and yellow fever (live-attenuated strain 17D). Human vaccines for other arboviral diseases like dengue, West Nile, chikungunya and Rift Valley fever are at different stages of research [97-99].

A.2 YELLOW FEVER VIRUS

A.2.1 Introduction

Yellow fever virus (YFV) is the prototype of the genus *Flavivirus* (family *Flaviviridae*) which comprises approximately 70 viruses including other human pathogens such as dengue, West Nile, Usutu, Zika and Japanese encephalitis and tick-borne encephalitis viruses [100]. The name *Flavivirus* originated from “flavus”, the Latin word for “yellow”, jaundice being the most distinguishable symptom of yellow fever.

Yellow fever (YF) is also the original viral hemorrhagic fever and has been one of the most feared lethal diseases during the past centuries, ranking in historical impact with plague and smallpox. Unfortunately, unlike smallpox, yellow fever is a zoonotic disease and therefore cannot be eradicated.

Today, despite the availability of an effective and widely used vaccine, the World Health Organization (WHO) evaluates that the disease affects at least 200,000 persons and causes 30,000 deaths annually [101]. However, these numbers are very likely to be underestimated due to the insufficient surveillance and limited diagnostic capacities in the remote endemic areas. YF remains an important public health problem for the population of 32 African and 13 Central and South American countries, where altogether almost 900 million people are at risk (Fig. 3) [102]. YF is also considered a re-emerging disease as the number of cases has been increasing in recent years [103] and there is great concern that YF might be introduced in new areas [12]. As a recent example, the yellow fever outbreak of 2012 in Darfur has been the worst in Africa in 20 years [104, 105]. This situation can be explained by several factors such as diminishing control strategies, increasing circulation of populations and goods, anarchic urbanization and improved surveillance [106, 107].

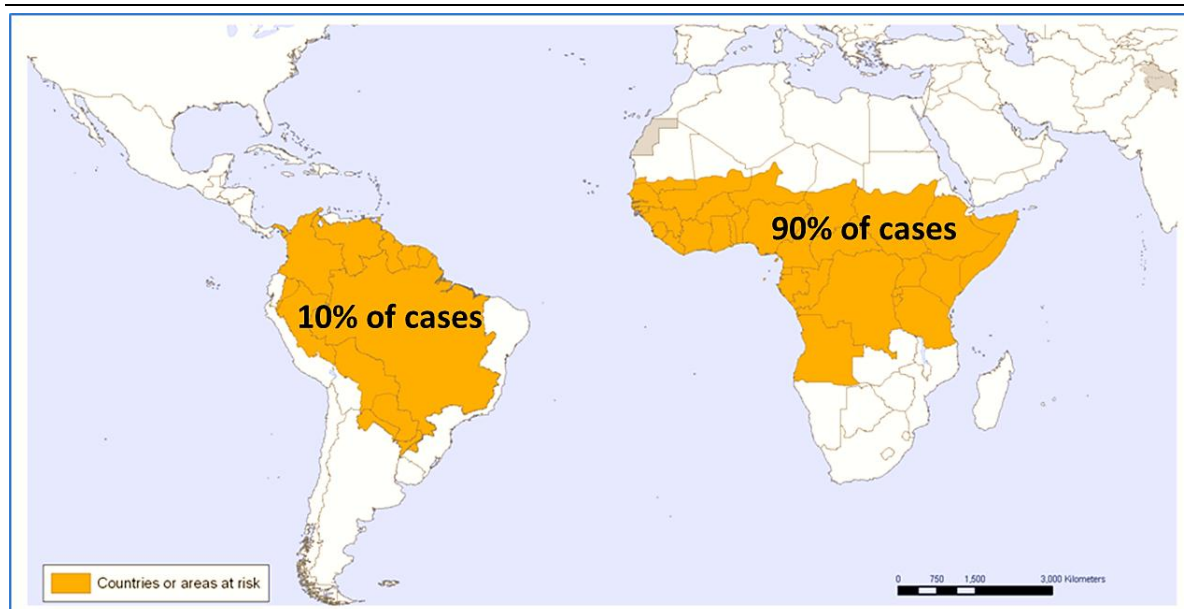


Figure 3: Countries at risk of Yellow fever infections. Source: WHO, 2008

A.2.2 Virus structure

Structural features of flaviviruses have been investigated and determined for dengue, tick-borne encephalitis (TBE), West Nile (WN), and Japanese encephalitis (JE) viruses using cryo-electron microscopy and X-ray crystallography [108-113], but no such data are yet available for YFV. However, based on the similarity of the flavivirus molecular structures and their close antigenic relationships, it is assumed that YFV particles share the same structural organization and properties than other flaviviruses.

Flavivirus virions are small enveloped viruses of approximately 500 Å in diameter composed of three structural proteins: the envelope (or E) protein, the membrane or precursor of membrane (or M/prM) protein and the capsid (or C) protein. The first assembled particles are immature virions produced in the endoplasmic reticulum covered by spiky complexes of 60 trimers of prM-E heterodimers (Fig. 4A, left). Once in the trans-Golgi network, protease furin cleaves the prM resulting in the reorganization of the E proteins and the formation of smooth-surfaced particles covered with 90 E dimers (Fig. 4A, right). Cryo-electron microscopy and image reconstruction have recently provided a wealth of information on flavivirus structure as shown in Figure 4B.

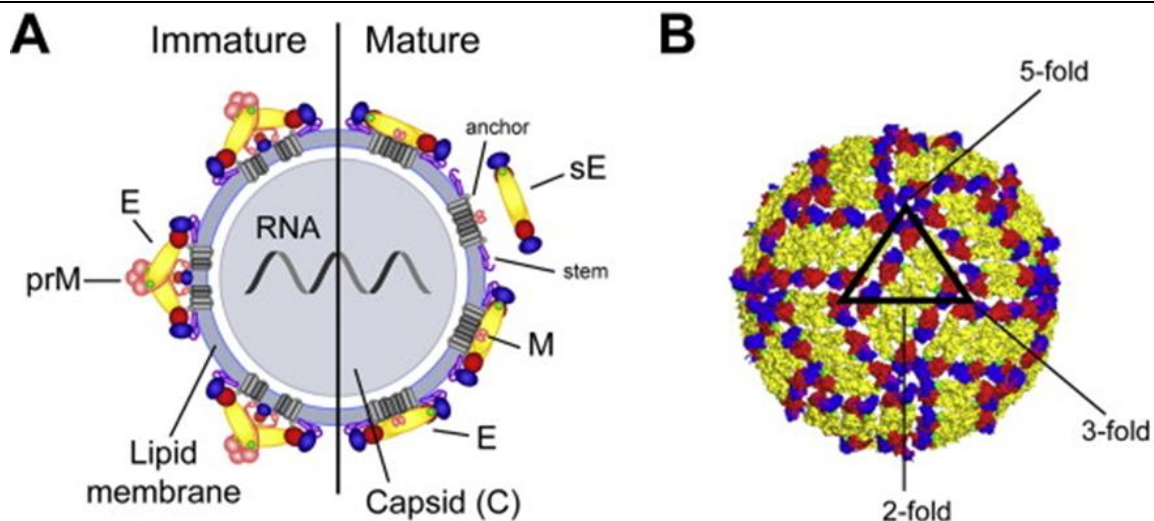


Figure 4: Flavivirus structure. **A:** Schematic representation of a flavivirus particle. Left: immature virion; Right: mature virion. sE: soluble form of E lacking the membrane anchor and an adjacent sequence element called ‘stem’. M: Membrane-associated cleavage product of prM; **B:** Herringbone-like arrangement of 90 E protein dimers at the virion surface as determined by cryo-electron microscopy. The triangle indicates 2-, 3-, and 5-fold symmetry axes. Source: Heinz et al., 2012 [114]

The YF genome is a positive-sense, single-stranded RNA which contains a single open-reading frame of 10 233 nucleotides encoding three structural and seven nonstructural (NS) proteins, flanked by short non-coding regions (Fig. 5).

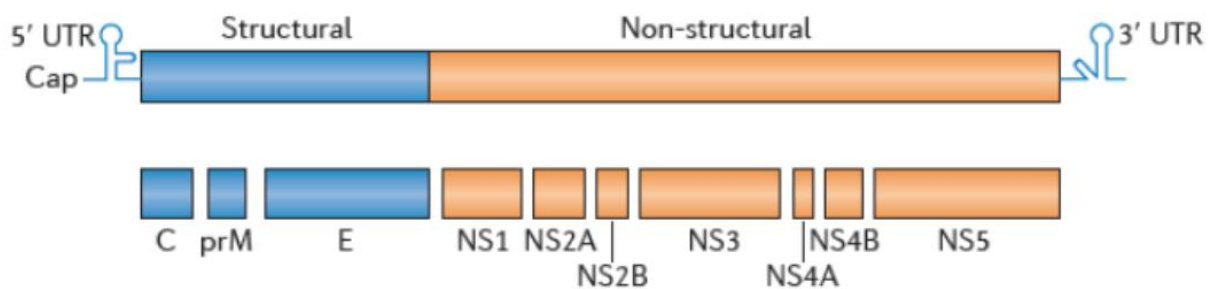


Figure 5: The genome structure of flaviviruses. Source: Beck et al., 2013 [115]

The structural proteins are incorporated in released mature virus particles, while the NS proteins responsible for replication remain in infected cells. The viral envelope consists of a lipid bilayer derived from the infected cell, with dimers of the envelope (E) protein on the surface anchored at their hydrophobic tails. The E protein is responsible for the initial phases of infection of host cells and is also a principal target for the host’s immune response. Other

INTRODUCTION - Background

viral proteins of major biological significance are NS1, NS3 and NS5. NS3 and NS5 are multifunctional proteins that contain protease (NS3) and RNA-dependent RNA polymerase (NS5) activities. NS1 is a highly conserved glycoprotein that is essential for the viability of YFV and is produced both in membrane-associated and secretory forms by the virus. It is unique in being the only glycoprotein to be exposed at the surface of flavivirus-infected cells and also secreted by the infected cells. The main characteristics of each flavivirus protein are listed in Table 3.

Table 3: List of flavivirus proteins and their respective size and functions

Protein	Size (kDa)	Function	Ref.
C	12-14	Capsid protein, RNA interaction	[116]
prM	18-19	Folding and assembly of E protein, precursor of M protein	[117]
M	7-9	Mature membrane protein	-
E	51-59	Cellular receptor-binding sites, fusion peptide, induction of neutralizing antibodies	[119]
NS1	46-55	Induction of neutralizing antibodies, RNA replication complex	[120]
NS2A	20-24	RNA replication, genome encapsidation	[121]
NS2B	14	Cofactor for capsid cleavage, RNA replication complex	
NS3	68-70	Capsid cleavage, genome encapsidation	[122]
NS4A	16	Cofactor, RNA replication complex	
NS4B	26	RNA replication complex, immunomodulation	
NS5	103-104	Methyltransferase, RNA-dependent RNA-polymerase	[123]

A.2.3 Flavivirus life cycle

Host cells targeted by flaviviruses include dendritic cells, monocytes and macrophages. Virions attach to the cell surface, mediated by the E protein, and enter the cell by receptor-mediated endocytosis (Fig. 6). Low pH in the endosomal compartment triggers trimerization of the E protein and fusion of the viral and cell membranes. Membrane fusion releases the nucleocapsid into the cytoplasm which then disassembles and releases the viral RNA. Once the genome is released into the cytoplasm, the positive-sense RNA is translated into a single polyprotein that is processed by viral and host proteases. The structural proteins, C, prM and E, are located in the N-terminal region of the polyprotein, followed by the nonstructural proteins, NS1, NS2A, NS2B, NS3, NS4A, NS4B and NS5. After appropriate cleavage and assembly of replication complexes, the genomic RNA is replicated by NS5, the viral RNA-dependent RNA polymerase, in association with other viral nonstructural and host proteins to

INTRODUCTION - Background

generate new progeny genomes. Viral RNA replication occurs in the rough endoplasmic reticulum (ER) and Golgi-derived membranes called vesicle packets [124]. The newly synthesized viral RNA is either packaged within progeny virion or used to translate additional viral proteins. Flaviviruses assemble within the ER to form immature particles that display the prM protein. Following transport through the trans-Golgi network (TGN), prM is cleaved to M by furin, resulting in mature, infectious particles. Subviral particles, which contain the surface proteins but not the capsid protein and RNA, are also cleaved by furin and released by exocytosis together with the mature virions.

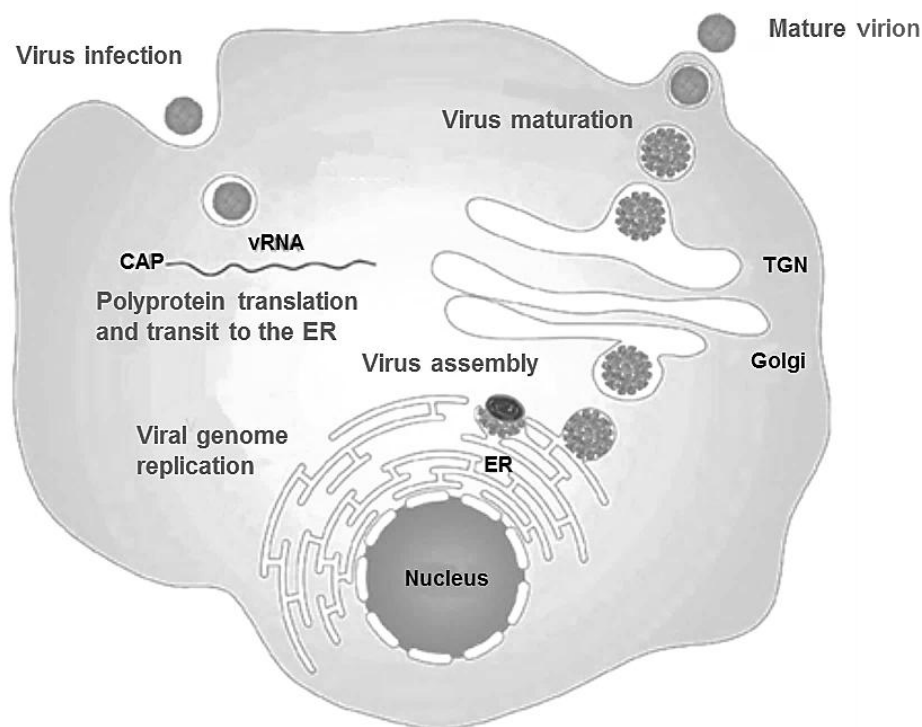


Figure 6: Life cycle of flaviviruses vRNA: viral RNA; ER: endoplasmic reticulum; TGN: trans-Golgi network. Source: Mukhopadhyay et al., 2005 [125]

A.2.4 Transmission cycle

Yellow fever virus (YFV) circulates in three ecologically distinct transmission cycles: the sylvatic or “jungle” cycle [monkey-mosquito-monkey]; the intermediate cycle [monkey-mosquito-human]; and the urban cycle [human-mosquito-human]. Each transmission cycle involves different mosquito species as vectors [100, 106]. The urban cycle involves transmission of YFV between humans by *Aedes aegypti*, a domestic vector, which breeds close to human habitation in water and scrap containers including used tires, in urban areas or dry savannah areas (Fig. 7). *Aedes aegypti* was initially considered as the only mosquito vector of YFV as this vector is the one involved in the development of outbreaks which occur

INTRODUCTION - Background

when accidentally infected humans introduce the virus in cities. This urban cycle is present in both Africa and South America although urban YF is rarely reported in South America. In Africa, two additional transmission cycles have been recognized: the jungle cycle between monkeys and the canopy-dwelling *Ae. africanus* and the intermediate or savannah cycle where the virus circulates between monkeys and/or humans and mosquitoes, including *Ae. africanus*, *Ae. fuscifer-taylori*, *Ae. luteocephalus*, and members of the *Ae. simpsoni* complex. In South America, the virus is maintained in a jungle cycle between monkeys and various species of *Haemagogus* (*Hg. janthinomys* and *Hg. leucocelaenus*) and *Sabethes chloropterus* (Fig. 8).

There are still many remaining questions on the ecology of YF, especially concerning the underlying factors that explain the cyclic appearance and disappearance of virus activity and the means by which the virus survives between epidemics. According to several studies, YFV can survive through dry season by vertical transmission from infected female mosquitoes to their eggs, as the viral particles are stable for long periods and can be reactivated when the progeny emerges under better conditions [126, 127]. This vertical transmission of YFV in the mosquito vector may contribute to virus maintenance in nature.

The incidence of yellow fever depends on the circulation of the mosquito vectors. Surprisingly, YF is present in tropical regions of the African and American continents but is absent from Asia, although the epidemic vector, *Aedes aegypti*, is present. Lower vector competence of the Asian mosquito strains and cross-protective immunity of the population due to the circulation of other flaviviruses have been advanced as hypothesis for the absence of YFV in Asia [128].



Figure 7: *Aedes aegypti*, the vector responsible for the yellow fever urban transmission cycle (Source: Wikipedia, photography by Muhammad Mahdi Karim, 2009)

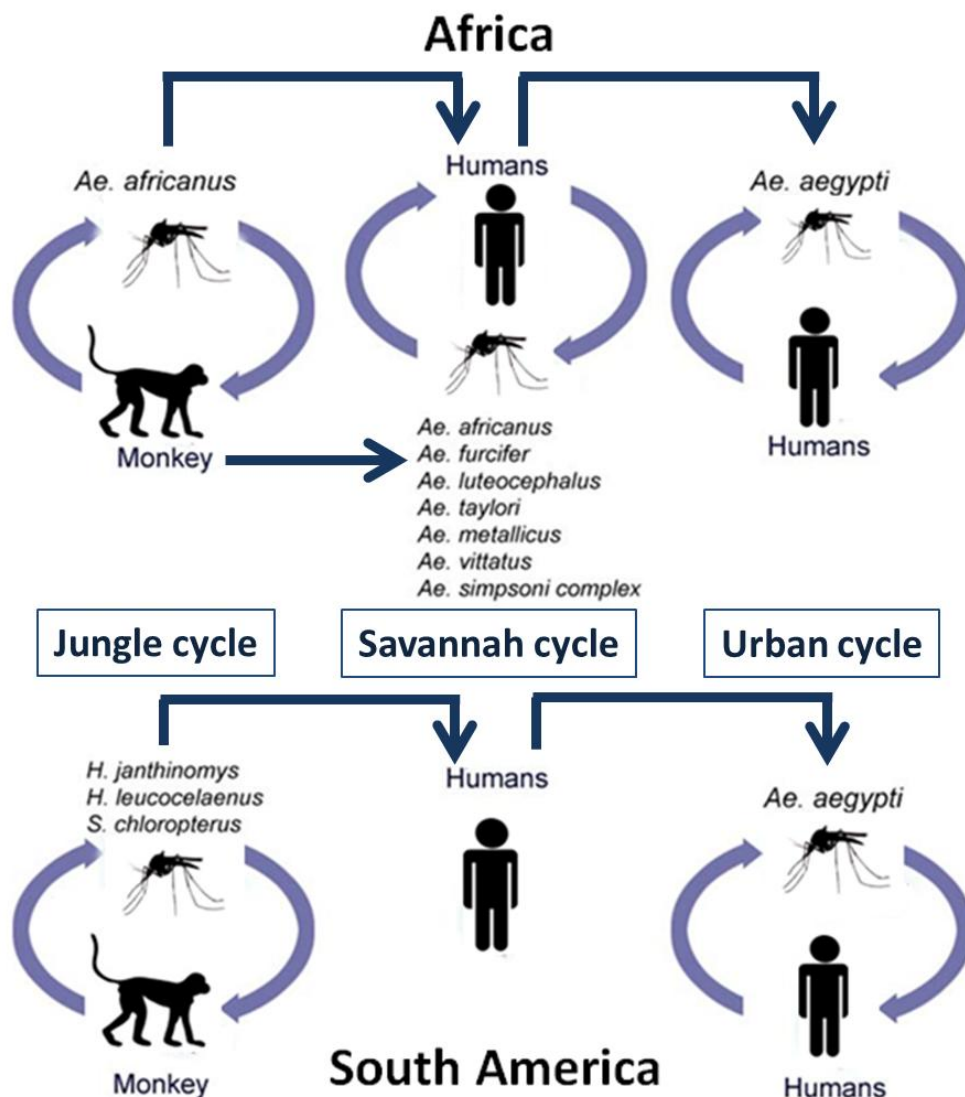


Figure 8: Transmission cycles of yellow fever in Africa and Central/South America indicating the vector species involved. Adapted from Barrett et al., 2007 [128]

A.2.5 The disease

An infected female mosquito inoculates approximately 1000 to 100,000 virus particles intradermally during blood feeding. Immediately after YFV infection, the virus first replicates in the local dendritic cells in the epidermis and spreads to regional lymph nodes. Then the virus reaches other organs via the lymph including the liver, kidneys, heart and thymus, causing lesions, either as a consequence of the cytopathic effect of the virus or due to alterations produced by the immune response of the host. The disease mechanisms are still poorly understood and the role of specific genes and molecular determinants of pathogenicity has been defined only partially. The role of the immune response to infection, particularly cellular immune response, is also poorly characterized [129].

INTRODUCTION - Background

The clinical picture varies from asymptomatic or non-specific disease, to fatal hemorrhagic fever [130]. The incubation period after the bite of an infected mosquito is 3 to 6 days. Once the incubation period is over, three stages of illness have been described in humans during a classical clinical picture of yellow fever (Fig. 9). The disease begins with an abrupt onset of fever, headache, malaise, photophobia, lower backache, myalgia, irritability, dizziness and vomiting. This acute stage lasts for 3–5 days and corresponds to the period of viremia also called period of infection [131]. During this period, the blood is infectious to biting mosquitoes as the virus is present in blood at titers up to 10^5 – 10^6 infectious particles/ml [130]. The period of infection is followed by a period of remission, which lasts approximately 12 h to 2 days, during which the virus is cleared by antibodies and the cellular immune response. During this stage, patients have a sensation of recovery and most of them abort infection presenting no further symptoms. However, about 20% of patients suddenly become severely ill with typical signs of liver and renal failure, which characterizes the third stage, the period of intoxication. During this stage, patients develop severe hemorrhagic fever and multiple organ dysfunction accompanied by jaundice, oliguria or anuria, cardiovascular instability and hemorrhagic manifestations [129, 130]. At this stage of the disease, described as the toxic phase, the fatality rate may reach 50%. The convalescent phase is characterized by prolonged weakness and fatigue lasting several weeks.

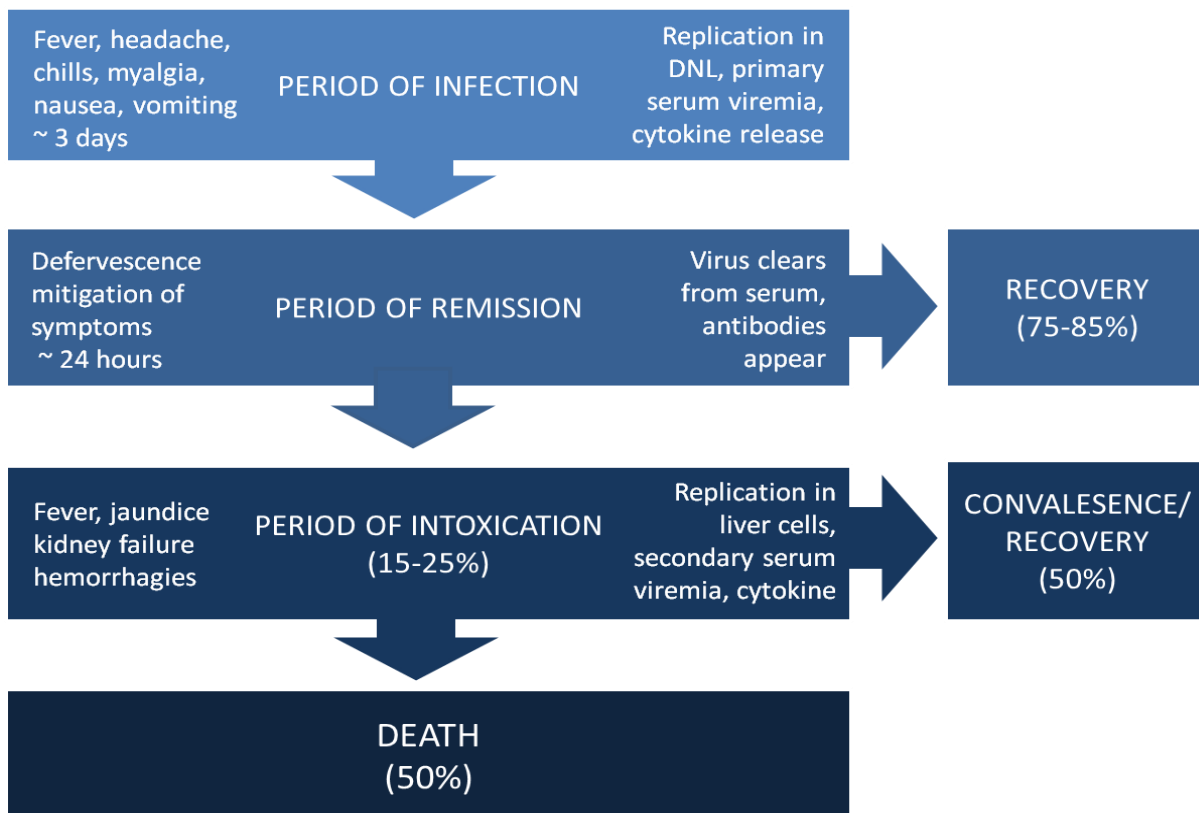


Figure 9: Phases of yellow fever disease with the corresponding clinical symptoms and pathogenesis of the infection

A.2.6 Diagnosis

Preliminary yellow fever diagnosis is based on the patient's clinical features, vaccination status, travel history, activities and epidemiological history of the location where the presumed infection occurred. However, confirmed diagnosis of YFV infection is very challenging as the early symptoms caused by YFV are similar to the ones of leptospirosis, louse-borne relapsing fever, malaria, viral hepatitis and other hemorrhagic fevers [130]. Laboratory confirmation is therefore essential for the differential diagnosis of yellow fever. Unfortunately, commercial tests are available only for testing by immunofluorescence assay (IFA) and diagnostic capabilities are restricted to reference laboratories. Also, clinical samples often reach the laboratory only once the patient has overcome the viremic phase due to limited access to diagnostic capacities in most endemic areas. Thus, serological methods are most commonly used for case confirmation as they detect the disease in the later phase. Detection of virus-specific IgM antibodies by in-house ELISA is the most frequently performed test although it has not been properly evaluated and standardized until now. Moreover, most serological diagnostic tests, including ELISA and IFA, lack specificity due to the high homology of antigenic structures among the Flavivirus group [88, 132, 133]. For this reason test confirmation is required with the plaque reduction neutralization test (PRNT), the gold standard YFV serological test. The disadvantages of PRNT are that the assay is time-consuming and requires high expertise and bio-containment facilities which are rarely available in endemic areas.

For an early diagnostic, direct diagnostic methods represent an essential tool as they are able to detect infections during the viremic phase. Early detection of cases may be crucial in order to provide efficient patient management, rapid outbreak response and emergency vaccination measures. For this reason, considerable efforts are made to develop accessible direct detection methods based on molecular detection which allow a rapid and highly sensitive detection of YFV. Several molecular methods for YFV detection based on polymerase chain reaction (PCR), such as real-time RT-PCR (qRT-PCR), have been established but these methods require the use of complex instruments and well-equipped laboratories [134-138]. The development of a portable, simple and robust method suitable for low resource settings and field diagnosis would be of great use in the case of direct detection methods for YFV, especially for outbreak investigations. For this reason, new molecular methods based on isothermal amplification have been developed for YFV detection such as real-time reverse-transcription loop-mediated isothermal amplification (RT-LAMP) [139] and helicase-dependent amplification assays (HDA) [140]. Unfortunately, direct serological methods based on antigen detection have not yet been developed for YFV.

A.2.7 Treatment and prevention

There is no specific antiviral treatment against YF. The use of ribavirin has shown to be ineffective in several studies. Passive antibody or interferons are effective only before or within hours after infection. Intensive supportive care is often the only option but it may not rescue the patient with yellow fever from the inexorable course of fatal infection. For this reason, prevention and control measures are crucial in order to prevent cases of yellow fever [141]. Such measures include vector control measures by destroying mosquito-breeding sites or using pesticides. The reduction of urban mosquito transmission may be a complementary measure. The most promising technique in this area of research is the introduction of endosymbiotic *Wolbachia spp.* bacteria, which suppress the replication of some arboviruses including YFV [142]. However, reduction or elimination of enzootic circulation is highly challenging as large scale insecticide use raises environmental concerns, vaccination of wild animals is impractical, and sylvatic foci are widespread and most often situated in remote areas.

Prevention of enzootic spillover is performed by vaccination with the YF-17D vaccine. Unfortunately, the current yellow fever vaccine production of 75 million doses per year is well below the current needs for routine immunization, preventive campaigns and outbreak control [101]. Despite the Yellow Initiative launched in 2005 by the Global Alliance for Vaccines and Immunization (GAVI), it is now evident that a larger stockpile of yellow fever vaccine is required [143]. Repeated shortages of yellow fever vaccine for travelers are also becoming more common, such as in India and in the United Kingdom in 2013. In the coming years, vaccine supply is likely to become more critical since the conditions for the re-emergence of urban yellow fever are well-established in many countries, especially in sub-Saharan Africa. In the future, the increase of urban population in Africa associated with the presence of non-immune populations and high vector density is likely to further increase the risk of large outbreaks of urban yellow fever. Political commitment to maintain a secure supply of vaccine is required in order to prevent yellow fever cases.

A.2.8 The yellow fever vaccine history

The yellow fever vaccine history begins in 1927, when the yellow fever virus was isolated from a Ghanaian patient, called Asibi [144]. An Anglo-American research group repeatedly propagated the Asibi-virus on mouse embryo tissue in order to reduce virus neurotropism. Finally, the virus was further attenuated by repeated passage on chicken embryo tissue and after 176 passages this led to the development of an immunogenic and safe Yellow Fever-17D (YF-17D) vaccine strain [145]. For supervising this work, Max Theiler

INTRODUCTION - Background

received the 1951 Nobel Prize in Physiology or Medicine, the only Nobel Prize attributed for a virus vaccine [146]. Concurrently, French researchers isolated a virus from a patient in Dakar and developed the French Neurotropic Virus (FNV).

The FNV and YF-17D strains were then both used for immunization against yellow fever. Unfortunately, several vaccination campaigns with the FNV were associated with multiple cases of encephalitis. Consequently, FNV production was discontinued in 1982. Since then, YF-17D has been the only available vaccine strain for yellow fever vaccination [147] and over 600 million doses have been administered with good results [148]. The phylogeny of the vaccine strain has been well described in a recent study [149]. Nevertheless, the mechanisms of attenuation and immunogenicity for the 17D strain are not yet known.

Protective antibody levels can be demonstrated over 35 years after vaccination [150]. For many years, WHO has recommended re-vaccination after 10 years for individuals exposed to the virus. Nevertheless, in March 2013, a WHO advisory panel confirmed that the protective effects of yellow fever vaccine are life-long, and that ten-year boosters are no longer needed to maintain immunity. The WHO Strategic Advisory Group of Experts (SAGE) remarked that out of more than 600 million doses administered, only 12 cases of yellow fever were reported in a vaccinated person. All 12 cases developed within five years after vaccination, which led the SAGE on immunization to conclude that immunity does not decrease with time and that vaccine failures are extremely rare.

The live-attenuated YF-17D virus is one of the most outstanding human vaccines ever developed as it is able to induce efficacious immune responses at a low production cost. Given the unique properties of the YF-17D virus, there has been considerable interest in exploiting the vaccine as a vector for foreign genes. In fact the virus has the potential to clone its full-length genome as cDNA into bacterial plasmids. Such plasmids can be modified, transcribed back to messenger-sense RNA and reconstitute live virions from cells transfected with the full-length RNA. With this “infectious clone” technology, the envelope genes of YF-17D have been replaced by the corresponding genes of other viruses, including Lassa virus [151], Japanese encephalitis, West Nile and dengue viruses [152, 153]. This approach holds great promise for the development of recombinant live vaccines against a variety of other viruses such as HIV [154, 155].

Interest in developing an alternative inactivated vaccine against YF has been incited by the presence of rare but serious adverse events following live virus vaccination [156-160]. A safer inactivated yellow fever vaccine could be useful for vaccinating people at higher risk of adverse events from the live vaccine, but could also have broader global health utility by lowering the risk-benefit threshold for assuring high levels of yellow fever vaccine coverage

INTRODUCTION - Background

[161]. In 2010, Monath et al. [162] described the development of an inactivated whole virion vaccine using the 17D virus inactivated with β -propiolactone and adsorbed to aluminum hydroxide [163]. However, it is unlikely that an inactivated vaccine could fully match the long-term protection provided by a single dose of live 17D.

B OBJECTIVES AND OUTLINE OF THE DISSERTATION

Vector-borne viral infections are increasingly common causes of severe febrile illness that can also progress to more acute diseases, such as encephalitis or hemorrhagic fevers, potentially resulting in early death or in long-term physical and cognitive sequelae. Vector-borne diseases can be transmitted by rodents but they are mainly transmitted by arthropods and are then referred to as arthropod-borne viruses or arboviruses. Over one hundred arboviruses are known to cause disease in humans and most of them are members of the Flaviviridae, Bunyaviridae, and Togaviridae families. Arboviruses are also considered to be emerging pathogens based on their geographic spread and their increasing impact on susceptible human and animal populations. Unfortunately, limitations in health systems in endemic areas undoubtedly lead to underestimation of arbovirus incidence and its related impact on global health. For this reason, there is an important need to improve diagnostic methods as well as our understanding of the pathogenesis of such infections in order to prevent, control and estimate more accurately the burden of arboviral infections on human and animal health.

Yellow fever virus (YFV) is the prototype of the genus *Flavivirus* (family Flaviviridae) which includes other important human vector-borne viruses such as dengue, West Nile, Japanese encephalitis and tick-borne encephalitis viruses. Compared to other flaviviruses, YFV is associated with a high human mortality due to its potential to progress in 15% to 25% of early symptomatic cases into a toxic phase which has a fatality rate from 20% up to 50%.

Despite the availability of an effective and widely used vaccine (YFV-17D), yellow fever (YF) remains an important public health problem for the African and South American population, where altogether over 900 million people are at risk. WHO evaluates that the disease affects at least 200,000 persons and causes 30,000 deaths annually. However, these numbers are very likely to be underestimated due to limitations in surveillance and diagnostic capacities in the remote endemic areas. For this reason, it is crucial to reinforce research in yellow fever pathogenesis and increase efforts in developing new diagnostic tools for an improved surveillance, treatment and control of YFV infections.

The aim of this PhD work is to develop and evaluate diagnostic methods and live-imaging tools for the study of vector-borne viral infections. The dissertation is divided into three separate chapters with the two last chapters focusing on the study of one particular vector-borne virus, the yellow fever virus (YFV).

INTRODUCTION – Objectives

The first chapter is dedicated to the establishment and evaluation of external quality assessment (EQA) studies of diagnostic methods for vector-borne viral infections. Five EQA studies have been launched, analyzed and published as part of my doctorate, targeting the following aspects: 1) serological detection of YFV, 2) molecular detection of YFV, 3) serological detection of hantavirus, 4) molecular detection of Rift Valley virus and 5) molecular detection of Crimean-Congo hemorrhagic fever virus. The methodology adopted to organize such studies will be described and results will be summarized, compared and discussed throughout this first chapter.

The second chapter of the dissertation describes the development of diagnostic methods for yellow fever infections. The first part of the chapter presents a molecular method based on isothermal amplification named recombinase polymerase amplification which can be used in low-resource settings. The second part of the chapter describes the development of a serological method for NS1 antigen detection which represents a new approach to YFV early diagnosis.

The last chapter describes a project aiming to construct infectious YFV-17D cDNA clones as tools for live-cell imaging microscopy. The vaccine strain has been used as a model system for the study of flaviviruses in order to identify and characterize components involved in viral pathogenesis, replication and virion formation. This knowledge would be very valuable as to date there is no specific therapy available against yellow fever and other main flavivirus infections. To investigate these mechanisms, several steps have been achieved towards the construction of an infectious fluorescent yellow fever-17D virus by tagging the capsid or the envelope protein with a short peptide sequence which can be recognized by a cell-permeating fluorophore named FIAsH. The genetically modified viruses will be characterized and tested for their potential as viable tools for the investigation of viral pathogenesis by live-cell imaging microscopy.

The dissertation is concluded by a general discussion on the main results of each project and an outlook on further investigations in the related topics.

CHAPTER 1 EXTERNAL QUALITY ASSESSMENT OF DIAGNOSTIC METHODS FOR VECTOR-BORNE VIRAL INFECTIONS

A INTRODUCTION

In the past two decades, emerging and re-emerging vector-borne viruses have become a threat of increasing importance to global health. Several endemic vector-borne viral diseases have increased in incidence such as dengue in South America and Crimean-Congo hemorrhagic fever in the Middle East. Concurrently, vector-borne viruses have appeared in new regions such as West Nile virus in North America in 1999, Rift Valley fever virus in the Arabian peninsula in 2000 or chikungunya virus in the Caribbean in 2013 [12-14, 164]. Similar events have been observed on the European continent, where endemic vector-borne viral diseases such as tick-borne encephalitis and hemorrhagic fever with renal syndrome (caused by hantavirus) have increased in incidence [60, 165-168]. Crimean-Congo hemorrhagic fever is also a matter of concern in Europe, as cases are reported yearly in former Soviet Union countries, Balkan countries and Turkey (with 1315 cases and 63 deaths confirmed in 2008) [169]. Additionally, epidemics of vector-borne viral diseases have been reported recently in areas of Europe which were previously clear of epidemics. As an example, outbreaks of West Nile have been occurring regularly throughout southern and south-eastern Europe since 2010 [170], pointing out the need to implant appropriate safety measures concerning blood transfusions and organ transplants [171, 172]. In 2007, the first outbreak of chikungunya on the European continent occurred in Italy [173] and in the following years, outbreaks of autochthonous dengue fever were reported in Madeira (Portugal), in Pelješac peninsula (Croatia) and twice in the south of France [174-176]. These events indicate that diseases transmitted by the *Aedes albopictus* mosquito, also known as the Tiger mosquito, are becoming a real threat to public health in Europe. Such occurrences also remind us that severe viral diseases can be imported from endemic countries and quickly spread in formerly virus-free areas.

In response to the (re-)emergence of vector-borne viral diseases, collaborative efforts to support EU member states in strengthening preparedness and response activities have been intensified in recent years. Preparedness activities include enhancing surveillance (reporting of human cases, vector and animal surveillance, monitoring of ecological determinants) and reinforcing diagnostic proficiency and capacity (development of tests and quality assurance).

CHAPTER 1 – Introduction

In this framework, the European Network for Diagnostics of “Imported” Viral Diseases (ENIVD) was established in 1998 as one of the epidemic preparedness and surveillance networks on infectious diseases funded by the European Commission. Since 2008, the ENIVD is part of the “Outbreak Assistance Laboratory Network” of the European Centre for Disease Prevention and Control (ECDC). To date, it comprises 57 expert laboratories as permanent members located in all 28 European Union (EU) member states and 7 non-EU countries. The purpose of the ENIVD is to establish a network of expert European laboratories in order to ensure surveillance activities and control measures of imported and emerging viral infections which comprise mainly vector-borne viral diseases. The activities are divided into four work packages: coordination, epidemic intelligence, outbreak laboratory response and external quality assurance.

As stated in the introduction at §A.1.3, the quality of vector-borne virus diagnostics is very important as most symptoms caused by vector-borne viral diseases are non-specific and similar to the symptoms of many other diseases. In such context, the availability of high-quality laboratory-based diagnostic techniques is crucial in order to provide appropriate treatment and assessment of case fatalities and disease burden. Nevertheless, vector-borne virus diagnostics still represent a challenge to expert laboratories involved in public health and clinical microbiology. In fact, as vector-borne viral diseases are mostly a burden to developing countries, research in such topics often mobilizes limited resources and laboratory capacities. Therefore, the development of vector-borne virus diagnostics is relatively restricted compared to other viruses such as HIV, influenza or gastrointestinal viruses, and EQA programs cannot be organized on a regular basis for technical and economic reasons.

For this reason, the ENIVD has reinforced preparedness activities by launching the periodical organization of external quality assurance (EQA) programs in order to assess and improve the performance of laboratory diagnostics of vector-borne viruses and other imported viral pathogens. The network prepares 2-3 EQA studies per year on viral pathogens prioritized by the network members. An EQA study may evaluate serological methods based on immunoassays and detection of antibodies and/or molecular methods based on detection and amplification of genetic material.

During my PhD, I launched, analyzed and published several EQA studies within the context of the ENIVD activities. This chapter first describes the methodology applied to perform an EQA and then summarizes and discusses the data generated by the EQA studies launched from 2011 to 2013 which included:

- an EQA study for the serological detection of yellow fever virus [177]
- an EQA study for the molecular detection of yellow fever virus [177]

- an EQA study for the serological detection of Hantavirus [178]
- an EQA study for the molecular detection of Crimean-Congo hemorrhagic fever virus [179]
- an EQA study for the molecular detection of Rift Valley fever [180]

B METHODS

B.1 PLANNING

The EQA studies provided by the ENIVD follow the workflow illustrated in Figure 10 where the successive steps are divided into a pre- and a post-analytical phase. As a first step, the upcoming EQA studies are agreed upon during the yearly network meeting based on current needs and up-to-date knowledge.

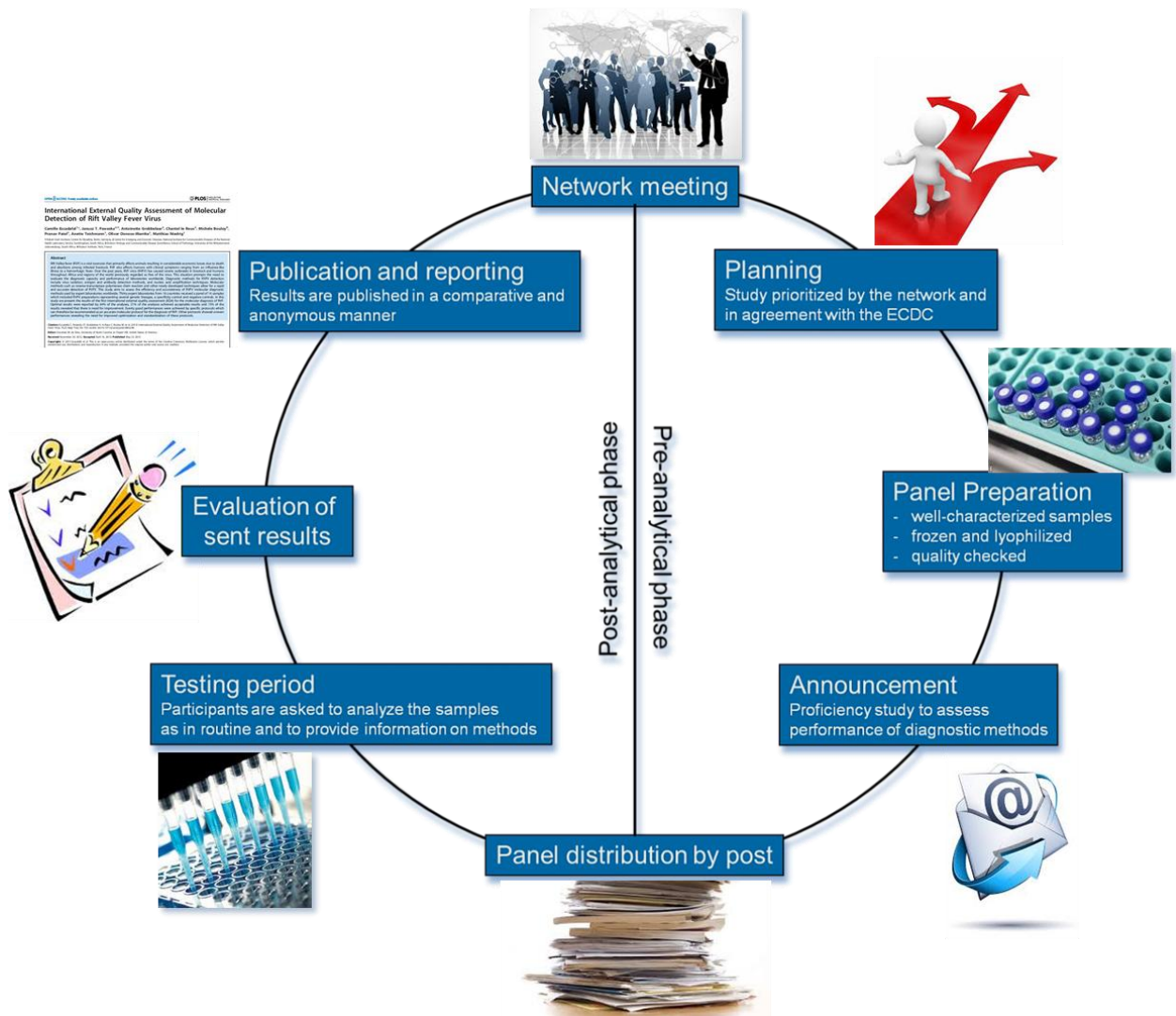


Figure 10: Workflow of EQA programs provided by the ENIVD. Adapted from a figure shared by Dr. Oliver Donoso-Mantke

B.2 PANEL PREPARATION AND DISTRIBUTION

Panels included 12 to 20 number-coded samples and sample preparation was similar for serological and molecular EQA panels.

Serological EQA panels were prepared with well-characterized human sera from clinical cases collected by the laboratories of the network or collaboration partners. The proficiency test panels were obtained by diluting the initial sera containing IgM and/or IgG antibodies with fresh-frozen human plasma. After dilution, the serum samples were frozen in 100 µl-aliquots, freeze dried for 24 h and stored at 4°C until distribution. Each panel also included sera reactive to heterologous viruses as specificity controls, and at least two confirmed seronegative samples as negative controls.

Molecular diagnostic EQA panels were prepared with human plasma samples spiked with virus strains obtained from cell culture supernatants of different viral genetic lineages and origin. All viral preparations were heat inactivated at 60°C and gamma irradiated (25 kilogray) to guarantee their non-infectivity. Aliquots of 100 µl were number-coded, freeze dried for 24 h and stored at 4°C until dispatched. In order to assess the specificity of each method, EQA panels included two negative controls and at least one control containing RNA of a virus genetically closely related to the target virus. Panels also included serial dilutions of one or two specific RNA samples in order to assess the sensitivity of each assay.

Before dispatching to the participants, the EQA panels were tested by at least two different ENIVD expert laboratories as internal reference to control the quality of samples after preparation. Once the quality of the proficiency test panel was confirmed, all set of samples were sent out by regular mail at ambient temperature.

B.3 ANNOUNCEMENT

The studies are announced as EQA studies aimed to assess the analytical sensitivity and specificity of laboratory diagnostic methods of a target virus. Participation to a study is open and free of charge and includes the publication of the results in a comparative and anonymous manner. Invited participating expert laboratories were selected based on the register of ENIVD members, on their literature contributions to the relevant viral agents, or with support of collaborating organizations such as the European Centre for Disease Prevention and Control (ECDC), the World Health Organization (WHO), the World Organization for Animal Health (OIE), the Pan American Health Organization (PAHO), the EpiSouth network, the ArboZoonet project, or the Quality Control for Molecular Diagnostics (QCMD) organization.

Laboratories willing to participate are asked to analyze the panel samples using their routine diagnostic procedures for detection of the targeted virus and to report their test

results in a standardized evaluation form provided. All samples from the proficiency test panel must be handled and tested as patient samples taking into consideration the required safety conditions. Participating laboratories were also required to specify technical details about the type of diagnostic test, laboratory equipment and reference protocols used during testing. Specification of the strain type and determination of the viral load of positive samples was requested when available to the participants in order to evaluate experience in strain typing and viral load determination.

B.4 EVALUATION OF RESULTS

Regarding the evaluation of results, a scoring system has been put in place in order to compare performances for each technique. For all EQAs, we assigned one point for correct positive or negative result whereas false- negatives/-positives results were not scored. For serological detection methods, borderline or indeterminate results were taken out of the evaluation. Regarding molecular techniques, borderline results were classified as incorrect results. This distinction is explained by the fact that nucleic acid amplification involves determined cut-off values and should always provide a clear positive or negative result.

Results were classified as:

- **Optimal** when all results were correct
- **Acceptable** when all results were correct except for one false-negative result (i.e correct in the clinical sense)
- **Need for improvement** when one or more false-positives and/or several false-negative results were reported

After reception and evaluation of all datasets, we provide all participants with a full overview of the EQA results and individual performance reports by e-mail. To guarantee anonymous participation, an individual numerical identification code was assigned to each laboratory followed by letter code in case the laboratory reported several sets of results. The reports can benefit the participants by identifying the weaknesses in their own procedures and by providing information on the overall performance and the laboratory techniques and protocols employed by the other participants. The interactions between the EQA provider (RKI) and the participating laboratories during the whole study period are illustrated in Figure 11. In order to value their participation to a proficiency test, laboratories should always take the appropriate corrective measures based on the performance report they received at the end of the proficiency testing.

Additionally, such EQA studies provide an overview of the state-of-the-art of diagnostic methods for each targeted virus.

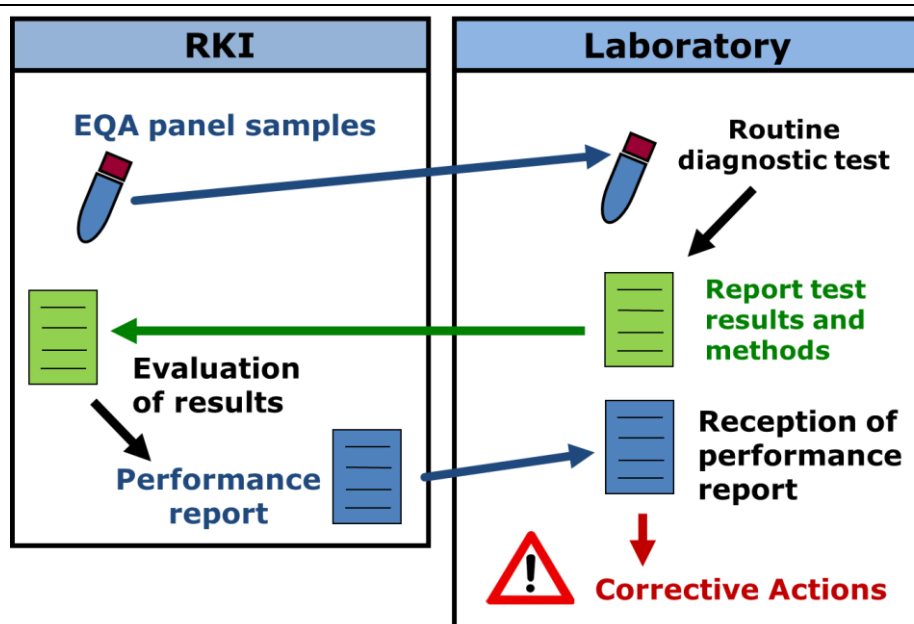


Figure 11: Interactions between RKI and the participating laboratories during an EQA study

C RESULTS

C.1 SUMMARY

In the period from 2011 to 2013, five EQA studies were launched, analyzed and published in order to evaluate the performance of serological and/or molecular diagnostic methods used by expert laboratories for the detection of vector-borne viral infections. In total over 80 laboratories from 44 different countries combined (27 EU member states and 17 non-EU member states including Middle Eastern, African, Asian, and American countries) participated in at least one of these EQA studies. The response rate was above 90% for all studies demonstrating that laboratories are highly interested in assessing the quality of their diagnostic methods.

A brief description and main results of each study are summarized in Table 4. Based on the evaluation criteria mentioned above, if a laboratory obtains optimal or acceptable results, it is considered to have a good overall proficiency and the participant fulfills the minimum requirements for successful participation in the study. It is important to note that the number of data sets received was always superior to the number of participants as some laboratories tested the samples with several methods and thus provided double, triple, quadruple or even quintuple data sets.

The complete result tables featuring all laboratories, assay specifications and performances can be consulted for each EQA in the corresponding publications referenced

CHAPTER 1 – Results

in Table 4. The next two paragraphs will summarize the EQA results for molecular and serological detection methods separately.

Table 4: Summary of the 5 EQA studies

Target virus	Yellow fever virus	Yellow fever virus	Hantavirus	CCHF virus	Rift Valley virus
Date of publication	2012	2012	2011	2012	2013
Type of detection	Molecular	Serology	Serology	Molecular	Molecular
Participating laboratories	28	28	27	44	30
EU participating laboratories	22	20	27	32	22
Number of countries	20	22	20	29	16
Positive / negative samples	10 / 4	9 / 4	11 / 3	13 / 2	11 / 3
Labs with good overall proficiency	5 (18%)	9 (32%)	15 (56%)	27 (61%)	25 (83%)
Reference	[177]	[177]	[178]	[179]	[180]

C.2 MOLECULAR ASSAYS

EQA studies assessing the quality of molecular detection methods were launched for YFV, RVFV and CCHFV. A variety of techniques for the detection of viral genome were used by the participants. As shown in Figure 12, the most performed technique was real-time RT-PCR representing 63% of assays used for YFV molecular diagnostic, 73% for CCHF molecular diagnostic and 83% for RVFV. Some methods were only performed for one virus such as isothermal amplification methods which were only available for testing of RVFV or hemi-nested RT-PCR which was only performed for YFV.

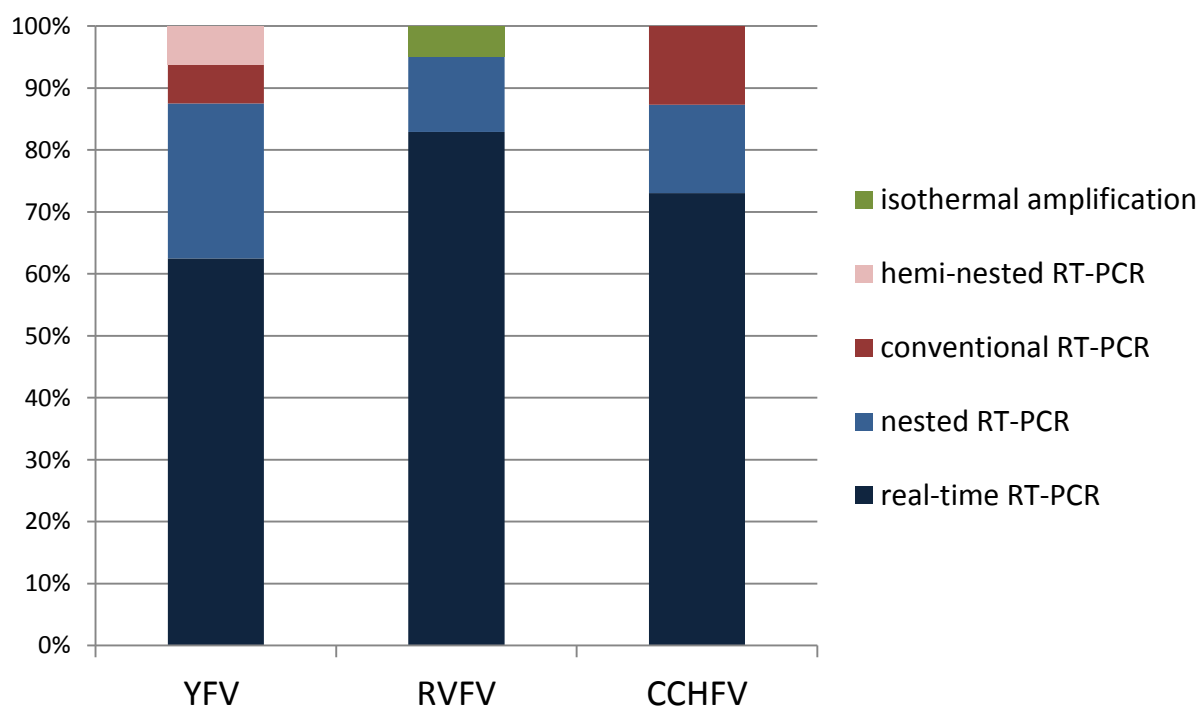


Figure 12: Repartition of the type of technique used for the molecular based EQA studies

Performance comparisons between each type of assay are limited as some techniques were not sufficiently represented such as hemi-nested RT-PCR and isothermal amplification assays. For this reason statistical analysis could not always reach any significant conclusion except for the CCHFV EQA. In this study, it could be shown that assay performance is significantly associated to the type of method used, as the p-value was inferior to 0.0001 (Table 5). Real-time RT-PCR has been chosen as the reference method for the analysis. The confidence intervals indicate that nested RT-PCR and conventional RT-PCR are significantly worst performing than real-time RT-PCR as their odd ratios are inferior to 1 and not included in the confidence interval.

Table 5: Odd ratios obtained for each method for the molecular detection of CCHFV [179]

Method	Proportion of correct results		OR (95% CI)	P-value
	Number	%		
Real-time RT-PCR	398/468	85.0%	1.00 (reference)	<0.0001
Conventional RT-PCR	43/65	66.2%	0.34 (0.19-0.61)	
Nested RT-PCR	12/26	46.2%	0.15 (0.07-0.34)	

OR: odd ratio; **CI:** confidence interval

CHAPTER 1 – Results

Apart from this statistical analysis, some general observations could be clearly delineated from the results of all three EQA studies combined.

Further information on the protocol applied for each diagnostic test was requested from the participants. In all studies, laboratories performing a same technique most often referred to different protocols, each of them most often sourced from publications. The variety of protocols used for each technique rarely revealed higher performances for specific protocols. In fact, laboratories using the same protocol differed in their performance, indicating variations in individual operational procedures rather than limitations of the technique itself.

In all three molecular EQAs combined, 94% of the assays used were commercial. Nevertheless the few in-house protocols provided performances as good as the commercial assays.

In order to assess the sensitivity of each method and estimate the effect of virus concentration on the test performance, serial dilutions of one or two specific RNA samples were used in each EQA. The percentage of correct results was calculated for each sample and compared between samples of the same serial dilution. As expected, we observe a clear correlation between increased dilution of the sample and low sensitivity in RNA detection. This decreased sensitivity was the main reason for reporting false negative results in the CCHFV EQA but not in the YFV and RVFV EQAs. In the YFV EQA, false negatives were also observed for particular virus strains thus suggesting that they were not only due to a lack of test sensitivity but also to a lack of specificity. In the RVFV EQA, false negative results were distributed equivalently among samples and thus cannot be attributed to sensitivity nor specificity issues but rather to the lack of reproducibility and consistency of the employed test procedure.

In order to assess the specificity of each method, each EQA panel included at least three different strain types of the target virus. When comparing test results obtained from the different strain types, we observed even performances indicating the detection methods can detect all strains of the target virus except for the YFV EQA as stated in the previous paragraph. In fact, the overall performance for YFV testing was significantly higher for the detection of the YFV-17D vaccine strain than for the two wild strains isolated in Ivory Coast (strain accession n°AY603338.1) and Brazil (strain accession n°AF094612.1). Two real-time RT-PCR protocols [138, 181] and one RT-PCR protocol [182] exclusively detected the YFV-17D vaccine strain.

In order to further assess the specificity of each method, each EQA panel included two negative controls and at least one specificity control containing RNA of a virus genetically closely related to the target virus. The RVFV EQA specificity control containing sandfly fever virus revealed a good specificity of the molecular detection methods. The YFV EQA included

two specificity controls, one with a mixture of RNA from West Nile, Japanese encephalitis, tick-borne encephalitis and St Louis encephalitis viruses, and one with RNA of the four dengue virus serotypes. Both controls revealed an overall lack of specificity, in particular the control with dengue RNA which resulted in 75% of false positive results while detecting YFV RNA. Such lack of specificity for the genome detection of flaviviruses was previously described in other EQA studies including a dengue EQA [183].

The percentage of false positive results in the negative controls ranged from 8 to 14% depending on the EQA study. These incorrect results were not attributed to a particular method except in the RVFV EQA where 2 out of 3 false results were obtained with nested RT-PCR methods.

In order to evaluate experience in viral load determination, participants were requested to provide the number of genome copies in each positive sample. This information is only available while testing with real-time RT-PCR assays. Considering all three studies, as much as 39% of the set of results which mentioned the use of real-time-based procedures (37 out of 94) did not provide any information on the viral load although the use of such method could provide quantitative or semi-quantitative results. The majority of the reports which provided quantitative results provided their measures only as Ct values even though such data is insufficient to estimate accurately the viral load.

In order to estimate practice in strain typing and sequencing, specification of the viral strain detected in each sample was requested to the participants of the CCHFV and RVFV EQAs. Only 16% (12 out of 74) of the laboratories participating to these two studies reported complete or partial specifications on the strain type.

C.3 SEROLOGICAL ASSAYS

EQA studies assessing the quality of serological detection methods were conducted for YFV and hantavirus infections. A variety of techniques were used by the participants for the detection of IgM and IgG antibodies. As shown in Figure 13, the type of technique used was highly dependent on the type of target virus. For YF serology, IFA was the method most commonly performed, representing 65% of all YFV tests, while EIA represented 58% of all tests used for hantavirus serology. Laboratories testing for YF antibodies used also seroneutralization and hemagglutination tests while such methods were not performed for hantavirus serology. On the other hand, immunoblot assays (IBAs) represented 15% of the tests used for hantavirus antibody detection while they were not used for YF serology. These differences are explained by the fact that some techniques are better developed and

CHAPTER 1 – Results

sometimes only available for some specific virus such as IBAs which are commercially available for hantavirus and not for YFV serology.

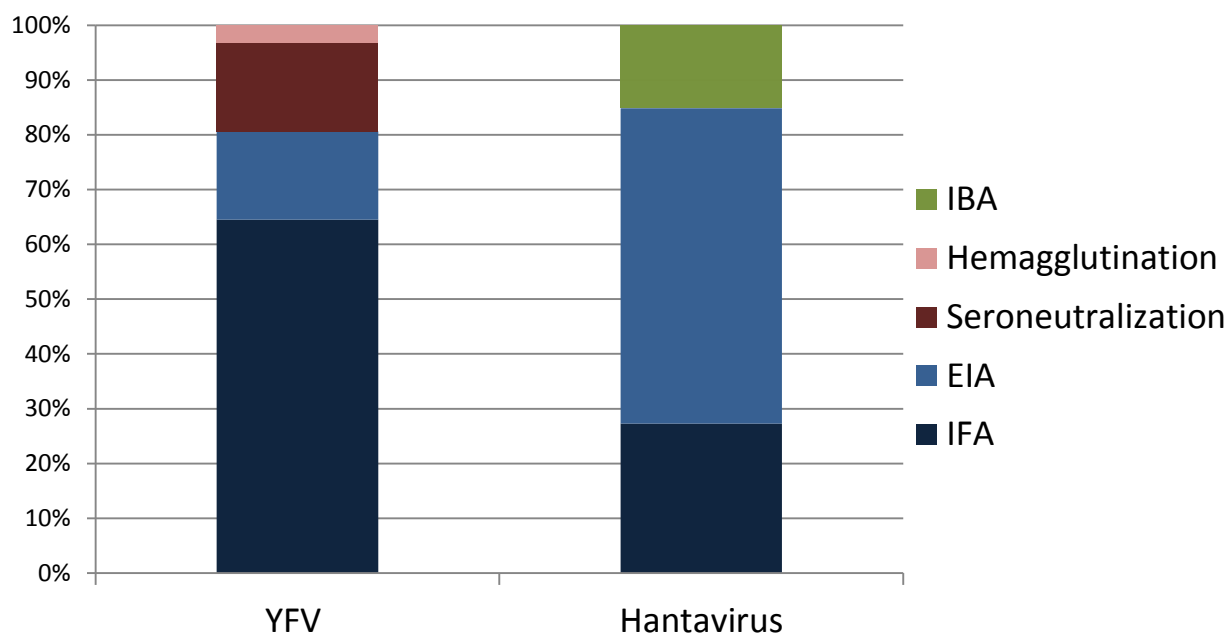


Figure 13: Repartition of the type of methods used for the serology based EQA studies

Performances of both EQAs varied greatly, depending on the type of method used, the subclass of antibodies to be detected but also depending on each performing laboratory.

Although participants were requested to test the panel samples for the presence of both IgG and IgM, not all of them provided results for both antibody subtypes. All participants of the hantavirus EQA included IgG testing results but 6% of laboratories did not test for IgM antibodies. On the other hand, participants of the YFV EQA used techniques such as seroneutralization and hemagglutination tests which cannot distinguish between IgG or IgM antibodies. Among the YFV EQA reports using IFA and EIA, 16% did not include results for IgM testing and 12% did not include results for IgG testing.

The result reports revealed very disparate data as the techniques used for both EQAs were different, some result reports combined several techniques and some reported only partial results. This heterogeneity of results does not allow us to summarize the overall performances in terms of sensitivity and specificity for each separate technique. Nevertheless general observations can be made for both EQAs.

Two thirds of the assays used were commercial and one third was in-house. Overall, the performance of in-house methods was equal to that of commercial tests for both IgM and IgG detection.

CHAPTER 1 – Results

Nevertheless while comparing performances for hantavirus IgG detection, it appeared that commercial IBAs (from Mikrogen, Neuried and Euroimmun, Lübeck) provided very good performances in terms of sensitivity and specificity. A previous EQA on hantavirus serology demonstrated similar good performances for commercial IBAs [184]. IFA demonstrated lower performances concerning sensitivity of IgG detection (56% of false negative results), and EIA showed the lowest performances in this regard revealing 73% of false negative results for IgG detection.

Results of the YFV EQA revealed that 48% of the test results for IgM detection did not report the presence of IgM antibodies in any of the positive samples for YFV-17D IgM antibodies. This lack of sensitivity observed for YFV-17D IgM antibodies was not observed in serum infected with wild type YFV strains from West Africa and South America. Regarding YFV IgG detection, best performances appear to be achieved by laboratories using IFA or seroneutralization test as they obtained the highest scores in the evaluation.

In the hantavirus EQA panel, the positive controls included sera positive for Puumala virus (PUUV) and Dobrava-Belgrade virus (DOBV) from different origins in order to test the specificity of each technique. By comparing the IgM and IgG results obtained for the DOBV positive samples, we observe that IgM were detected more accurately than IgG antibodies as 6% of methods failed to detect IgM while 42% failed to detect IgG antibodies against DOBV. Such difference was not observed for PUUV positive samples. Comparing results of the positive samples by country of origin (Finland, Sweden and Slovenia), no main differences were observed for IgG or IgM antibody detection. Furthermore, out of the 33 data sets obtained, 48% did not report virus type specific results as they only tested for the presence of hantavirus and not DOBV or PUUV antibodies.

The hantavirus negative controls revealed more false positive results for IgG (8% of all results) than for IgM detection (3% of all results). IgG false positive results were all obtained by commercial IFA or EIA.

The specificity controls for the YFV panel included positive sera for dengue and West Nile virus IgG and IgM. Very few false positives were reported for these samples demonstrating a low cross-reactivity between flavivirus antibodies. In addition, these false positive results were not attributed to any particular technique suggesting a problem in the operational procedures rather than a lack of specificity of the method itself. False positive results in the negative controls were reported for EIA, IFA as well as for seroneutralization tests which raises the question of whether the positive results of seroneutralization tests are rather due to a high sensitivity or to a strong background.

D DISCUSSION

Vector-borne infections, and more particularly YF, CCHF, RVF and hantavirus infections, represent a constant threat to animal and human public health and have widely spread all over the globe during the recent years. Therefore, improved diagnostics and enhanced disease monitoring are important for early and effective response strategies of such infections. Since laboratory diagnostic for rare, imported or emerging viral infections are not properly standardized and often based on in-house assays, it is of utmost importance to assure the quality of diagnostic methods currently in use. For this purpose, EQA programs provide comparative testing of multiple number-coded samples which allow participating laboratories to evaluate their routine tests and identify the corrective measures to apply in order to improve their performance.

As part of the ENIVD activities and my PhD work, five EQA studies were launched, analyzed and published by the RKI from 2011 to 2013. Most reference laboratories responded keenly to the EQA announcements as response rates for all studies were over 90%. Nevertheless, it is crucial to further encourage laboratories situated in endemic countries to participate in quality assurance programs.

By summarizing all EQA results, it was demonstrated that commercial and in-house assays revealed similar overall performances. It could also be concluded that differences in laboratory diagnostic performance depend not only on the type of method used but also on the type of strain tested, the concentration of the sample tested and the individual laboratory applying to the test. In fact, from the results of the five EQAs, it appears clearly that performance is mostly linked to the reporting laboratories and their use of the different protocols since their performance differ greatly even when using the same technique. Unfortunately, such studies cannot designate precisely the best method in use since several factors including reagents, instruments and reaction conditions, all have an influence on test performance. The impact of these variations is difficult to assess but it can be minimized by including adequate controls, revising and standardizing protocols, and optimizing testing conditions.

Nonetheless, it appeared from all molecular EQA results that real-time RT-PCR performed better than conventional or nested RT-PCR. Real-time is also the only method which enables to quantify directly the number of genome copies in each sample. However, the major limitation of implementing such techniques in endemic areas is the cost of thermocyclers and reagents. Among the methods used in the RVFV EQA, it was interesting to notice the appearance of newly developed technologies, such as LAMP (loop-mediated amplification) and RPA (recombinase polymerase amplification). No general conclusion can

be made concerning their performance as each technique was only performed by one laboratory. However, RPA has shown optimal results with comparable sensitivity and specificity than real-time RT-PCR, thus representing an interesting alternative for sensitive molecular detection in field settings.

The main weakness revealed by the EQA of YFV molecular testing was the inability of 25% of the reported techniques to detect YFV RNA of wild-type strains. Three published protocols [138, 181, 182] could only detect the YFV-17D vaccine strain and therefore are not recommended for the identification of suspected YFV infections with wild type strains.

For EQAs of molecular detection methods, information on the viral load was requested as it can be very useful to monitor progress of symptoms, predict disease outcome and study virus pathogenesis. Interestingly, only 61% of the laboratories performing real-time RT-PCR assays have reported quantified or partially quantified results. This indicates that most laboratories do not include standards in their real-time RT-PCR procedures although their use would allow them to quantify instantly the viral load of each sample. According to these results as well as results from previous EQA studies, there is still room for improvement concerning viral load determination [183]. This issue is mainly due to the lack of international standards for molecular testing. Standards for nucleic acid amplification techniques can be provided by organizations such as the National Institute for Biological Standards and Controls (NIBSC) but only for a small list of viruses including influenza virus and Norovirus. Therefore there is a crucial need to develop and provide such reference material for vector-borne viruses in order to enable standardized quantification of genome copies for all laboratories performing molecular testing of vector-borne viral infections.

Summarizing the results of both EQAs of serological detection methods, one of the main observations is that 10% of participating laboratories did not include IgM detection in their diagnostic routine procedures. Moreover, result reports from laboratories testing for the presence of IgM antibodies revealed a low sensitivity for IgM positive samples. This was specially observed for the detection of YFV-17D IgM antibodies as over half of the YFV EQA participants did not detect them. This observation should be taken into account when assessing the protection provided by YFV vaccination by measuring IgM levels. Moreover, the proportion of samples correctly diagnosed for IgM in the hantavirus EQA (62%) was much lower than the proportion of correctly diagnosed IgG samples (88%). These deficiencies in IgM detection indicate a considerable risk of overlooking acute infections in hantavirus or YFV infected patients. In fact, regarding serological diagnosis, it is preferable to test for the presence of IgM antibodies which appears shortly after infection, thus confirming a recent contact with the virus. IgG testing requires analysis of two consecutive serum samples as the sole presence of IgG antibodies in a patients' serum only indicates previous

contact with the virus and not recent exposure. For this reason, reliable assays for IgM detection are crucial for the diagnosis of recent infections in humans and thus their development is first priority in order to strengthen laboratory diagnostic capacity. Differences in test sensitivity based on the antibody subtype were already reported in a previous hantavirus EQA [184] as well as in EQA studies for the serological diagnostic of other viruses [183, 185, 186].

Although no particular serological method clearly provided better performances than others, it can be noted that commercial IBAs provided very good results for hantavirus serology and seemed to be slightly more sensitive than EIA and IFA. These results were further confirmed by EQAs organized by INSTAND e.V. in their final report of External Quality Assessment Scheme (EQAS) for anti-hantavirus IgG and IgM launched in 2013 [187].

Cross-reactivity among flaviviruses was expected for the detection of IgG antibodies. However, no significant cross-reactions were observed in the YFV serology EQA. Surprisingly, lack of specificity was observed to a greater extent in the EQA for YFV RNA detection where dengue positive RNA samples were incorrectly tested positive for YFV by 75% of the methods.

Strain typing was requested in the hantavirus and RVFV EQA studies revealing that less than half of participants provided information on the type of strain detected in positive samples. However, correct positive results without any strain specification are satisfactory in the context of laboratory diagnosis. Strain typing represents relevant information for surveillance activities in order to monitor which strains are circulating in endemic areas and what type of clinical picture are associated with each strain type.

The pathogens covered by the presented EQA studies have a rather low incidence but the disease they cause can be very severe and even fatal. Therefore, the sensitivity of a diagnostic method used for the detection of such infections is of utmost importance. Reporting false negative results should be considered more critical than false positive results as positive results are likely to be submitted to further testing for confirmation. In other words, in case of low disease prevalence, the predictive value of a negative test should be higher than the predictive value of a positive test.

The percentage of laboratories with overall good proficiency for each study revealed that the results of the molecular EQA studies were overall better than the results from serology EQAs (Table 5). However, the scoring and classification system was put in place in order to allow performance comparisons between laboratories within a same study and not to compare the overall scores of each study. In fact, comparison between studies should be avoided since the sample composition of each EQA panel varied from one study to another,

CHAPTER 1 – Discussion

including different sources, different viral strains, different controls and in different concentrations. Additionally, it should be recognized that the evaluation of EQA studies for serological diagnosis is more complex than for molecular diagnosis due to the higher variety of serological methods used, the presence of borderline results and the different subclasses of antibodies tested.

In all EQA studies presented, variations of performance among participating laboratories clearly demonstrate the need to improve serological and molecular diagnostic techniques and to provide standardized protocols and further quality assessment programs. Performing EQAs on a regular basis enables to ensure reliability of diagnostic results, to guarantee a regular quality of existing methods and eventually further improve them. Given the demand for biological preparedness, regular participation in EQA programs will become increasingly important for laboratories worldwide. In this process, ENIVD's role is essential as it provides international EQA programs for a number of rare, imported or emerging viral agents that are usually not addressed by commercial organizations. This is mainly due to the difficulty of providing the required reference material in sufficient amount and quality. The ENIVD recognizes that the current configuration of EQA programs need further development and require wider proficiency panels but at present, financial and technical limitations are impeding preparation and analysis of wider panels.

CHAPTER 2 DEVELOPMENT OF DIAGNOSTIC METHODS FOR YELLOW FEVER INFECTIONS

A RECOMBINASE POLYMERASE AMPLIFICATION

A.1 INTRODUCTION

Recently the interest for point of care diagnostics (POCs) and the need to develop simple, reliable, accessible and robust diagnostic tests has been increasingly acknowledged. The development of POCs can provide quick turnaround time, lower cost and sample-in-result-out capability to specialized techniques which were not formerly accessible to most diagnostic laboratories. Such developments are currently being made for molecular detection of infectious diseases by nucleic acid amplification techniques. Currently, quantitative polymerase chain reaction (qPCR) is the new gold standard method used for nucleic acid detection but the testing procedures require complex temperature cycling and expensive instruments. For this reason, isothermal amplification methods have been considered an interesting alternative for molecular POCs. The advantages of isothermal amplification include high sensibility, rapid result (as low as 5 minutes for high genome copy numbers), portability and robustness which makes it suitable for POCs as well as for field diagnostics and limited resource settings. Moreover, the device required for isothermal amplification is smaller, lighter, cheaper, and has less power consumption than qPCR devices which require temperature cycling.

Many isothermal amplification technologies have been developed in the past years and they can be categorized into:

- **Strand displacement** methods such as strand displacement amplification (SDA), multiple displacement amplification (MDA), loop-mediated isothermal amplification (LAMP), cross-priming amplification (CPA), smart amplification (SmartAmp), genome exponential amplification reaction (GEAR)
- **T7 promoter-activated** methods such as nucleic acid sequence-based amplification (NASBA), transcription mediated amplification (TMA) and single primer isothermal amplification (SPIA)
- **Helicase-dependent amplification** (HDA) methods
- **Rolling circle amplification** (RCA) methods
- **Recombinase polymerase amplification** (RPA) methods

Some methods were at first designed to target DNA (SDA, RCA, RPA, LAMP, and HDA) and were later adapted to detect RNA whereas other techniques were purposely

designed for direct RNA amplification (SPIA, TMA, and NASBA). Real-time detection has been developed for isothermal amplification techniques by using fluorescent primers or nonspecific intercalating fluorophores for RCA, SDA, LAMP and HDA methods or specific detection probes for HDA, RCA, NASBA and RPA methods.

The advantages of one technique over another depend on the application of interest. While large number of primers will increase test specificity, they will also complicate primer design. Also, the use of more than one enzyme may increase the costs. Time to result and operating temperature might be taken into account as well in order to choose the most appropriate technique.

Among the novel isothermal amplification methods, recombinase polymerase amplification (RPA) is certainly among the best alternatives. RPA is an exponential polymerase amplification achieved by the binding of opposing oligonucleotide primers to template DNA and their extension by a DNA polymerase. In contrast to PCR, RPA does not rely on global melting of the template to allow primers to bind to their complementary target sequences. Alternatively, RPA employs the phage recombinase *UvsX* and its co-factor *UvsY*, which combine with the oligonucleotide primers forming a nucleoprotein complex able to scan double-stranded DNA and recognize specific homologous sequences. The displaced single-strand templates are stabilized by gp32 proteins thus preventing primers from being removed by branch migration. Recombinase disassembly leaves the 3'- end of the oligonucleotide accessible to a strand displacing DNA polymerase generating dsDNA amplicons by primer elongation (Fig. 14).

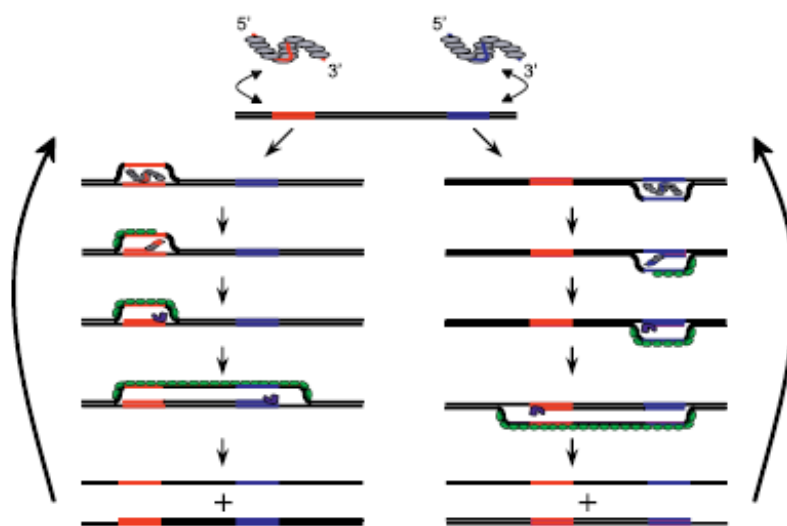


Figure 14: Schematic of the RPA process. Recombinase/primer filaments scan template DNA for homologous sequences (red/blue). Following strand exchange, the displaced strand is bound by gp32 (green) and primers are extended by the polymerase (blue). Source: Piepenburg et al. 2006 [188]

Repetition of this reaction leads to an exponential DNA amplification. In order to repeat the cycle, recombinase/primer filaments must disassemble and reassemble. This process is accomplished by the *UvsX* recombinase which binds to oligonucleotides in the presence of ATP. Upon ATP hydrolysis, the nucleoprotein complex disassembles and *UvsX* can be replaced by gp32 stabilizing proteins (Fig.15). This reaction is supported by the presence of *UvsY* co-factor and a particular crowding agent (Carbowax20M) which shifts the equilibrium in favor of recombinase loading.

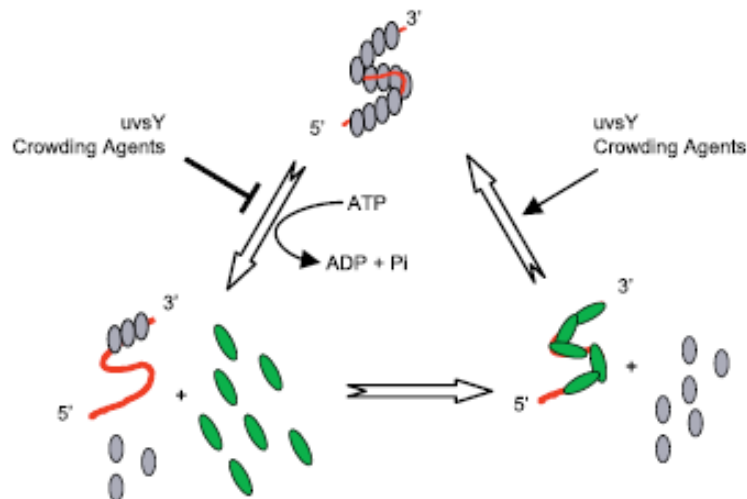


Figure 15: Assembly and disassembly of recombinase/primer filaments. In the presence of ATP, *UvsX* recombinase (gray) binds to oligonucleotides (red)(top image). The nucleoprotein complex then disassembles (left image), releasing ATP and *UvsX* can be replaced by gp32 (green) (right image). Source: Piepenburg et al. 2006 [188]

RPA technology is now commercially available and manufactured by TwistDx (Cambridge, United Kingdom). According to the manufacturers' guidelines [189], RPA TwistAmp kits are configured to operate optimally in a temperature range of 37°C to 42°C. Amplicon may be detected either in real-time with a computer or by lateral flow strip. Real-time detection of the amplification can be achieved by using TwistAmp™_{exo} probes. These synthetic oligonucleotides carry internal fluorophore and quencher linked to thymine bases and separated by an abasic site mimic (tetrahydrofuran) localized approximately 15 nucleotides upstream from the 3'end of the probe (45-55 nucleotides). Once the probe hybridizes to its target sequence the abasic site is recognized and cleaved by an exonuclease. The probe section carrying the quencher is then released which results in a fluorescent signal. The intensity of the detected fluorescence at a time point is proportional to the level of RPA mediated amplification (Fig.16).

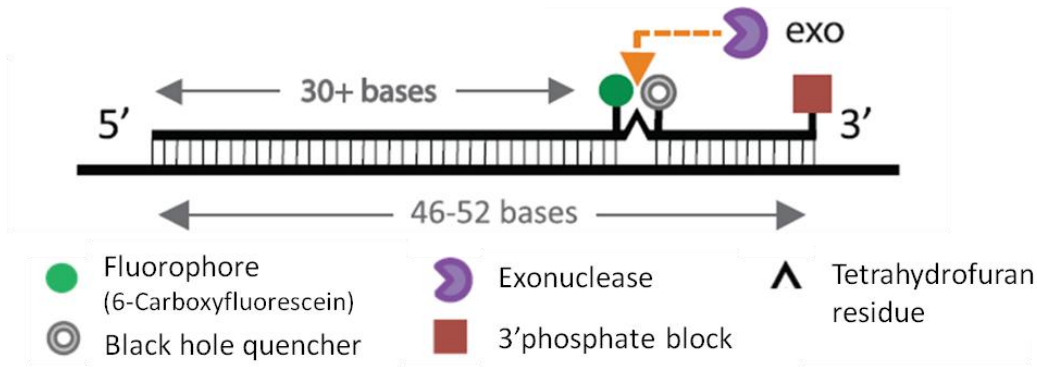


Figure 16: Structure of an annealed TwistAmp™ exo probe. The tetrahydrofuran residue is cleaved by the exonuclease once the probe is bound to the target sequence. The fluorophore and quencher are then separated and a fluorescent signal is generated. Adapted from TwistDx website: <http://www.twistdx.co.uk/>

The fluorescence signal can be detected by a mobile ESEquant Tube Scanner device (Qiagen, Hilden, Germany). This portable device collects fluorescence signals over time allowing real-time detection of accumulating fluorescence signals in 8 tubes simultaneously (Fig. 17). The output data is visualized as fluorescence intensity in mV in function of time in minutes and not number of cycles like for PCR. Results are available within 10 to 20 minutes. Measurement devices with higher throughput are now being available (i.e. the new Generation ESEQuant System from Qiagen).



Figure 17: ESEquant Tube Scanner. Source: Qiagen website www.qiagen.com

Detection by lateral flow strip (LFS) can be used as an alternative to real time detection by using the TwistAmp™ nfo kit (Cambridge, United Kingdom). Along with the basic amplification reagents, it includes an enzyme (nfo) which recognizes and cuts the abasic site (THF) in the probe only once it has bound to the complementary strand. By cleaving the abasic site, the blocked end of the probe is released and the probe can act as a primer, thereby generating a product that can be captured by a LFS. TwistAmp™ nfo probes are similar to TwistAmp™ exo probes (Fig.16) except for the absence of quencher and the displacement of the fluorophore at the 5' end. The LFS reverse primer should also include an additional biotinylation at the 5' end as the LFS only detects biotin labeled amplicons. Once amplified, the genetic material can then be detected in instrument-free formats such as LFS. Figure 18 describes the principle on which a LFS performs.

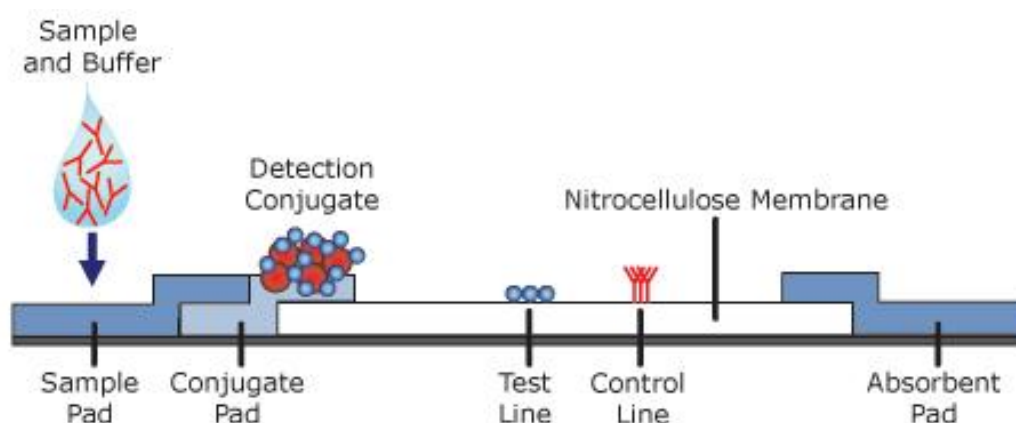


Figure 18: Operating diagram of a lateral flow strip. The sample is placed on the sample pad. Detector molecules solubilize and mix with the analyte in the sample if the analyte is present. The mixture migrates by capillary action until it reaches the analyte capture molecule which will then capture the complex if it is positive for the target analyte. Excess of solution is absorbed by an absorbent pad at the end of the strip. Source: PATH website <http://sites.path.org/dx/rapid-dx/technologies/lateral-flow/>

RPA has already been developed for some vector-borne viruses such as RVFV [190] and it has shown optimal performances comparable to those of qPCR during the first international EQA of molecular detection of RVFV described in Chapter 1. What is more, RPA demonstrated a better sensitivity than RT-LAMP [180].

The objective of this project was to apply the RPA technology to the molecular detection of YFV. Diagnosis of YFV infection is very challenging as the early symptoms caused by YFV are similar the ones of leptospirosis, malaria, viral hepatitis and other hemorrhagic fevers. For this reason early laboratory confirmation of suspected cases is crucial in order to provide efficient patient management, rapid outbreak response and

emergency vaccination measures. Direct diagnostic methods represent an essential tool for early diagnostic as they are able to detect infections during the viremic phase. For this reason, considerable efforts are made to develop accessible direct detection methods based on molecular detection which allow a rapid and highly sensitive detection of YFV. Several molecular methods for YFV detection based on polymerase chain reaction (PCR), such as real-time RT-PCR (qRT-PCR), have been established [134-138]. These methods have proven to provide optimal performances, as shown is the EQA for molecular detection of YFV described in Chapter 1 [177]. However, they require the use of well-equipped laboratories and complex instruments. Therefore, such techniques are not suitable in low resource settings and field outbreak investigations, where portable, simple and robust diagnostic methods are needed. For this reason, new molecular methods based on isothermal amplification have been developed for YFV detection such as real-time reverse-transcription loop-mediated isothermal amplification (RT-LAMP) [139] and helicase-dependent amplification assays (HDA) [140].

This chapter describes the development of an RPA assay which can be performed with a small portable instrument and easy-to-use lyophilized reagents. The assay was developed in real-time format with the ESEquant Tube Scanner and in lateral-flow strip format. Analytical specificity and sensitivity were evaluated for each format with a wide panel of viruses and serial dilutions of YFV RNA. Spiked human plasma samples were also used as a model for clinical samples and mosquito pools were tested as well for assay validation.

The development of this method is described in an article of the journal PLoS Neglected Tropical Diseases of March 2014 [191].

A.2 METHODS

A.2.1 Viruses and mosquito pools

All flavivirus and non-flavivirus strains used were derived from cell culture and provided by the Robert Koch Institute in Berlin, the Bernard-Nocht Institute in Hamburg, Germany and the Pasteur Institute of Dakar in Senegal. All virus preparations used in this study were inactivated and stabilized.

Pools of mosquitoes infected or not with YFV were provided by the Pasteur Institute of Dakar. The mosquito sampling protocol was extensively described by Diallo and colleagues [192]. Briefly, the mosquitoes were collected during the period of activity of the *Aedes* vectors in different landscapes of Kedougou in South Eastern Senegal. Mosquitoes were sorted into monospecific pools of a maximum of 50 mosquitoes and then frozen in liquid nitrogen. Before viral detection processing, each mosquito pool was homogenized in 2.5 ml of

Leibovitz 15 cell culture medium containing 20 % fetal bovine serum and centrifuged for 20 min at 10,000 x g at 4° C.

A.2.2 RNA extraction and sample preparation

Viral RNA was isolated from 140 µl aliquots of cell culture supernatants or 100 µl aliquots of mosquito pools, using the QIAamp Viral Mini Kit (Qiagen, Hilden, Germany) according to the manufacturer's instructions. RNA was eluted in 100 µl of nuclease-free water and stored at -80°C until further use.

RNA extracts for sensitivity testing were prepared by extraction of 10-fold serially diluted YFV preparation. Human plasma samples spiked with low concentrations of YFV were used as a model for assay validation with clinical samples.

A.2.3 Primer and probe design for RPA

Primers and probes for RT-RPA were designed by Dr Pranav Patel from ZBS1 at Robert Koch Institute of Berlin. All YFV full-length sequences from the NCBI database covering the 5'-UTR region were aligned using Geneious 5.0 software. Based on the alignment, degenerate generic primers representing all 79 sequence variants were designed for amplification of all YFV strains. According to recommendations of Piepenburg and colleagues [188] and the guidelines from TwistDx (Cambridge, United Kingdom) [189], primers should be 30 to 35 nucleotides long. RPA exo probe for fluorogenic detection and RPA nfo probe for detection of dual-labeled amplicon were designed according to the TwistDX guidelines [189] and synthesized by TIB MOLBIOL, Berlin. The primer set YFV RF2/RR2 was selected to amplify YFV RNA with the nfo probe in LFS RT-RPA and with the exo probe in real-time RT-RPA.

A.2.4 Real-time RT-PCR

Real-time PCR allows both amplification and quantification of specific DNA target sequences in real-time. Real-time PCR can be performed with fluorescent reporter probes which detect only the DNA sequence containing the target sequence. Therefore, use of a reporter probe significantly increases specificity, and enables quantification even in the presence of non-specific DNA amplification. This method relies on a DNA-based probe with a fluorescent reporter at one end and a quencher of fluorescence at the opposite end. The cleavage of the probe by the 5' to 3' exonuclease activity of the Taq polymerase breaks the reporter-quencher proximity allowing emission of fluorescence which can be detected. An increase in the quantity of DNA targeted by the reporter probe at each PCR cycle therefore causes a proportional increase in fluorescence due to the breakdown of the probe and release of the reporter.

CHAPTER 2 – Yellow fever virus RPA - Methods

The method described requires the use of DNA templates, so that for the detection of viral RNA, a first cDNA synthesis must be performed. Several commercial kits propose a one-step approach by including a reverse transcriptase enzyme, so that the entire reaction from cDNA synthesis to PCR amplification occurs in a single tube.

Real-time RT-PCR testing was performed with the YFV-specific primers YFV FP/RP and probe YFV LNA2 in order to detect and quantify genomic RNA of YFV by using in-vitro transcribed RNA standards as described by Weidmann and colleagues [134]. The assay was performed in one-step format using the QuantiTect Virus Kit (Qiagen) and the ABI 7500 thermocycler with reaction mixture and conditions as listed in Table 6.

Table 6: Mix composition and reaction conditions for one real-time PCR reaction

Reagents	Volume (µL)	Time (sec)	T (°C)	Nb. of cycles
5 x QuantiTect Virus Master Mix	5			
RT-mix	0.25	1200	50	45
YFV FP [10 µM]	0.25	300	95	
YFV RP [10 µM]	1	15	95	
YFV LNA2 probe [10 µM]	1	45	60	
Nuclease-free water	12.5			
Volume of master mix	20			
RNA Template	5			
End volume	25			

A.2.5 Real-time RT-RPA

Real-time RT-RPA assay was performed using the TwistAmp exo RT kit according to the manufacturer's instruction (TwistDx, Cambridge, United Kingdom). The TwistAmp exo RT kit contains an additional RT-enzyme enabling the direct amplification of RNA targets. The composition of the reaction mixture and the conditions required for the reaction are listed in Table 7. For each reaction sample, rehydration solution was first mixed with primers and probes. Then 5 µl of RNA template was added to the 42.5 µl master mix. The template/master mix solution was added to the dry reagent pellet and mixed by pipetting up and down. Finally, the reaction was triggered by adding the magnesium acetate (Mg(OAc)₂, 280 mM) solution to the reaction mix. The reaction tubes were vortexed, centrifuged and then placed in the ESEQuant Tube Scanner for real-time monitoring of fluorescence. Reaction was performed at 39°C for 20 min, with brief mixing and centrifugation of reaction tubes after 3 minutes of reaction. This reaction temperature was determined optimal in terms of sensitivity.

Table 7: Mix composition and reaction conditions for one (real-time or LFS) RPA reaction

Reagents	Volume (µL)	Time	T (°C)	Nb. of cycles
RPA rehydration buffer	37.7	20 min	39	None
YFV RF2 [10 µM]	2.1			
YFV RR2(-Bio)[10 µM]	2.1			
YFV Rprobe exo/nfo [10 µM]	0.6			
Volume of master mix	42.5			
RNA template	5			
Mg(OAc) ₂	3.5			
End volume	51			

The resulting curves were analyzed by ESEQuant Tube Scanner software Version 1.0 and threshold values were determined by slope validation. In other words, slope (mV/min) values were compared in order to distinguish positive results from negative results. This real-time RPA protocol could be developed based on previous studies performed by collaborators from the Department of Virology in Göttingen, UMG [193, 194].

A.2.6 Lateral-flow strip RT-RPA assay

LFS-RPA assay was performed using the TwistAmp™ nfo RT kit from TwistDx (Cambridge, United Kingdom) according to the manufacturer's instructions. The reaction composition and conditions are listed in Table 7. LFS RPA protocol is the same than for real-time RPA (§A.2.5) except that it requires the reverse primer YFV RR2-Bio and the probe YFV Rprobe nfo. After amplification at 39°C for 20 min, 2 µl of amplification product was diluted in 100 µl of PBST buffer, and 10 µl of diluted amplicon was dropped on the sample pad of a HybriDetect lateral flow strip (LFS) (Milenia Biotec, Giessen). Strips were then placed into tubes containing 100 µl of PBST buffer for proper migration of the sample along the strip. The final result was interpreted visually after 5 min of incubation. A test was considered positive when the detection line as well as the control line was visible. A test was considered negative when only the control line was visible. The control line should always show as a visible line, otherwise the test is invalid and must be repeated.

A.2.7 Analytical specificity of real-time and LFS RT-RPA

To test whether our assay is able to detect a wide variety of YFV strains, we utilized a panel of 20 different YFV strains from different origins and lineages (Table 8). The analytical specificity was also tested with a panel of 13 arboviruses and hemorrhagic fever viruses of which 9 are flaviviruses genetically related to YFV (Table 9).

Table 8: Yellow fever viral strains used for analytical specificity testing

Virus description	Accession No.	Origin	Date	Lineage	Real-time RT-PCR	RT-RPA	
						real-time	LFS
YFV virus strains					Cycle threshold	Time threshold [min]	
ArD 24553	–	Senegal	1976	–	24.6	3.3	not determined
ArD 408/78	–	Burkina Faso	1978	–	23.9	3.0	not determined
HD 117294	JX898868	Senegal	1995	6	16.5	2.3	not determined
ArD 114891	–	Senegal	1995	6	16.0	1.6	not determined
ArD 99740	–	Senegal	1993	3	25.0	5.1	not determined
ArD 114991	–	Senegal	1995	–	24.3	3.4	not determined
HD 122030	–	Senegal	1996	6	19.4	2.4	not determined
ArD 122522	–	Senegal	1996	6	21.3	3.3	not determined
HA 016/97	–	Liberia	1997	–	20.0	1.6	not determined
HD 47471	–	Mauritania	1987	–	28.5	5.9	not determined
ArD D X	–	Senegal	2000	5	21.4	2.4	not determined
Asibi	AY640589.1	Ghana	1927	–	20.6	3.2	positive
ArD 114896	JX898871	Senegal	1995	3	20.3	3.1	positive
ArD 156468	JX898876	Senegal	2001	4	16.8	2.4	positive
DakArAmt7	JX898869	Ivory Coast	1973	1	15.4	2.1	positive
ArD 121040	JX898870	Senegal	1996	6	16.4	2.3	positive
ArD 149214	JX898873	Senegal	2000	5	15.5	2.2	positive
Ivory C 1999	AY603338.1	Ivory Coast	1999	6	19.1	2.5	positive
Trinidad 79A 788379	AF094612.1	Brazil	1979	3	20.1	2.5	positive
17D RKI #142/94/1	Vaccine strain	RKI	–	–	20.0	2.1	positive

Table 9: Viral strains other than YFV used for analytical specificity testing

Virus family	Virus specie	Virus strain	Real-time RT-PCR		RT-RPA result
			reference	result (Ct)	real-time / LFS
<i>Flaviviridae</i> <i>other than YFV</i>	Dengue virus serotype 1	VR344 (Thai 1958 strain)	in-house assay [183]	15.9	negative
	Dengue virus serotype 2	VR345 (TH-36 strain)		18.8	negative
	Dengue virus serotype 3	VR216 (H87 strain)		20.3	negative
	Dengue virus serotype 4	VR217 (H241 strain)		16.2	negative
	West Nile virus lineage 1	Israel	[195]	19.9	negative
	West Nile virus lineage 2	Uganda		26.8	negative
	Tick-borne Encephalitis virus	K23 strain	[196]	16.3	negative
	Russian Spring Summer Encephalitis virus	Far eastern subtype		24.2	negative
	Japanese Encephalitis virus	ATCC SA14-14-2	[197]	19.4	negative
<i>Bunyaviridae</i>	Rift Valley Fever virus	strain ZH548	[198]	26.2	negative
<i>Filoviridae</i>	Ebola virus	Zaire strain	[199]	24.7	negative
	Marburg virus	Musoke strain		24.4	negative
<i>Alphaviridae</i>	Chikungunya virus	African isolate	in-house assay	17.5	negative

Table 10: List of primers and probe for the lateral-flow stripe and real-time RPA assay based on the YFV strain accession n° NC00203

Assay format	Oligo name	Sequence 5' → 3'	Direction	Position
Lateral-flow strip RT-RPA	YFV RF2	AAATCCTGTGTGCTAATTGAGGTGYATTGG	sense	4 to 33
	YFV RR2-Bio	Biotin- ACATDWTCTGGTCARTTCTCTGCTAATCGC	antisense	93 to 122
	YFV Rprobe nfo	FAM- CTGCAAATCGAGTTGCTAGGCAATAAACAC- [THF] TTTGGATT-AATTTTRATCGTT- Ph	sense	35 to 86
Real-time RT-RPA	YFV RF2	AAATCCTGKGTGCTAATTGAGGTGYATTGG	sense	4 to 33
	YFV RR2	ACATDWTCTGGTCARTTCTCTGCTAATCGC	antisense	93 to 122
	YFV Rprobe exo	gCAAATCgAgTTgCTAggCAATAAACACATT [BHQdT]g[THF]A[FAMdT] TAATTTTRATCgTTC- Ph	sense	37 to 87

FAM: 6-Carboxyfluorescein; **THF:** tetrahydrofuran; **Ph:** 3'phosphate to block elongation; **BHQ:** black hole quencher

A.2.8 Analytical sensitivity of real-time and LFS RT-RPA

RT-RPA sensitivity was evaluated by testing RNA extracts from 10-fold serial dilutions of YFV preparations and by comparing RT-RPA results with results obtained with the reference method, real-time RT-PCR. RNA was extracted from the YFV Asibi strain and RNA concentrations ranged from $2 \cdot 10^5$ to 8 genome equivalent copies per reaction (Geq/rxn). Testing for each diluted sample was performed 10 times with real-time RT-RPA and 5 times with LFS RT-RPA as LFS represent an extra cost.

A.2.9 Testing of mosquito pools with real-time RT-RPA and RT-PCR

Thirty-four samples of monospecific pools of wild-caught mosquitoes collected from Kedougou in southern Senegal were included in this study. The RNA extracts from these samples were tested in parallel with real-time RT-PCR and RT-RPA. All the mosquito samples as well as the majority of the YFV strains listed in Table 8 were tested in March 2013 in the laboratory of the WHO Collaborating Centre for arboviruses and viral hemorrhagic fevers at the Pasteur Institute of Dakar in Senegal. Primers and probes for real-time PCR and RPA were lyophilized and transported at room temperature from Berlin to Dakar as well as the TwistAmp exo RT kits. The Tube Scanner device and a laptop were also transported for data analysis. All material necessary for real-time RPA testing was easily transportable in a small suitcase.

A.3 RESULTS

A.3.1 Analytical specificity of real-time and LFS RT-RPA

The analytical specificity testing revealed that all YFV strains tested were detected by real-time RT-RPA (all 20 YFV strains tested) and by LFS assays (only 9 YFV strains tested) (Table 8). The testing results of the panel of 13 viruses other than YFV showed no cross-reactions, as all results were negative for both assays (Table 9). However, the LFS RT-RPA assay revealed a faint band in the negative controls when running time exceeded 10 minutes. Hence, the test potentially generates false-positive results which reveal great concerns regarding the analytical specificity of the LFS format (Fig.19).






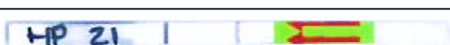

	Real-time RT-PCR		Real-time RT-RPA			Lateral-flow stripe RT-RPA		
	Ct value	GC/rxn	Pos. results/ No. of runs	% correct results	mean Tt (min)	Pos. results/ No. of runs	% correct results	Stripe scanned 5 min after run
Asibi-infected cell supernatant	29.2	8915	5/5	100	5.5	5/5	100	
	32.9	386	10/10	100	5.5	5/5	100	
	35.5	44	10/10	100	5.9	5/5	100	
	37.4	8	2/10	20	6.0	0/5	0	
Asibi-spiked human plasma	34.8	74	3/3	100	5.7	3/3	100	
	36.3	21	3/3	100	6.2	3/3	100	
Neg. control	Undet.	0	0/10	100	Undet.	0/5	100	

Figure 19: Sensitivity testing of the real-time and LFS RT-RPA with YFV cell supernatant and human plasma spiked with YFV in comparison with real-time RT-PCR results. **Ct:** cycle threshold; **Tt:** time threshold; **Neg.:** Negative; **Pos.:** Positive; **Undet.:** Undetermined

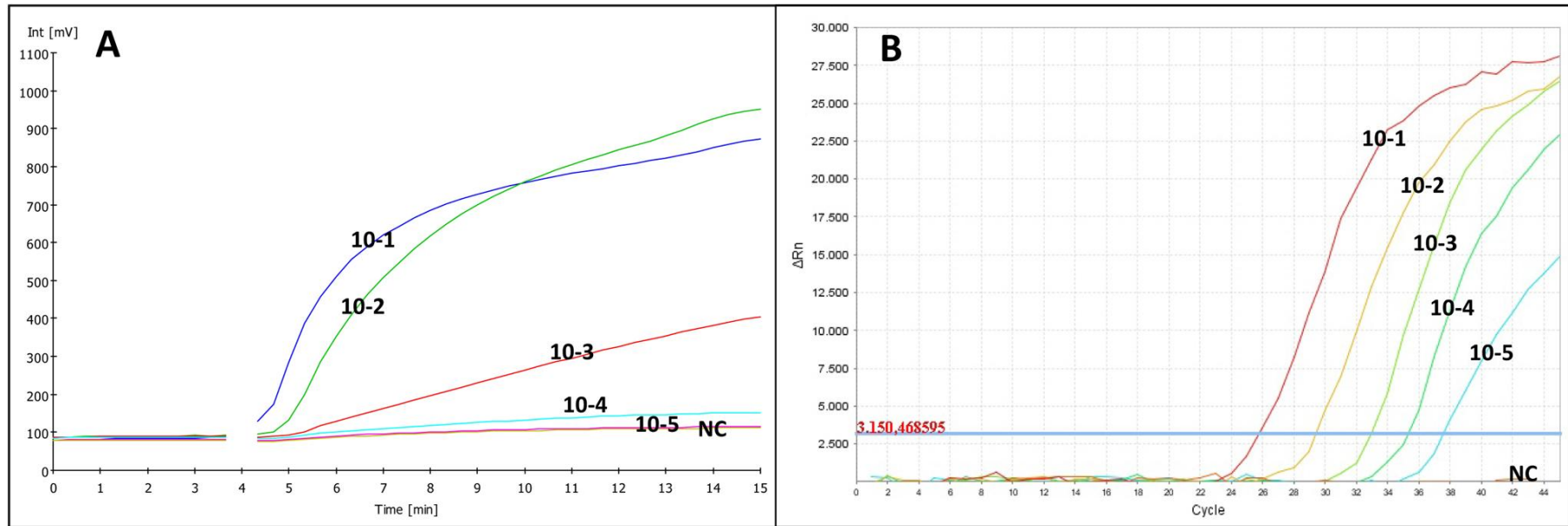


Figure 20: Amplification plots of real-time measurements for extracted RNA from 10-fold serial dilutions of YFV;
A: RT-RPA results; **B:** RT-PCR results

A.3.2 Analytical sensitivity of real-time and LFS RT-RPA

The analytical sensitivity of RT-RPA assays was evaluated by testing the RNA extracts from 10-fold serial dilutions of YFV preparations and by comparing RT-RPA results to the reference real-time RT-PCR results. The real-time RT-PCR showed linear results for the quantification of RNA standards over a range from 10 to 10⁶ genome copies. Real-time RT-PCR detected as low as 8 Geq/rxn while both RT-RPA assays could detect as low as 44 Geq/rxn in YFV RNA extracts and 21 Geq/rxn for the testing of YFV-spiked human plasma samples (Fig. 19). Amplification plots of real-time measurements by RT-RPA and RT-PCR of the extracted YFV RNA from 10-fold serial dilutions are shown in Figure 20.

A.3.3 Testing of mosquito pools with real-time RT-RPA

RNA extracts from the 34 mosquito pools samples were tested in parallel with real-time RT-PCR and RT-RPA. Fourteen mosquito samples out of 34 (41.2 %) resulted negative in real-time RT-PCR and 20 were positive (58.8 %) with Ct values ranging from 24.65 to 35.51 (data not shown). Based on these results, we calculated the sensitivity and specificity of real-time RT-RPA compared to the reference test real-time RT-PCR. Of the 20 samples detected positive in real-time RT-PCR, 16 were tested positive by real-time RT-RPA assay, providing a sensitivity of 80 % (95 % CI: 56.3 % to 94.1 %). Of the 14 samples tested negative in real-time RT-PCR, all were also tested negative by real-time RT-RPA assay, providing a specificity of 100 % (95% CI: 76.7 % to 100 %). The overall agreement between the two assays was 88.4 % (30/34).

A.4 DISCUSSION

Yellow fever remains a medically neglected disease and several endemic countries are regularly experiencing YF outbreaks despite the organization of preventive vaccination campaigns. Although vaccination should remain the foremost policy for YF control, a complementary approach, based on the early detection of cases followed by vaccination campaigns and vector control, would reduce significantly the disease burden. For this purpose, there is a need for reliable, rapid, specific, simple, robust and portable diagnostic methods which can be performed and/or transported to the field for surveillance or in outbreaks.

In this chapter, the development of a RT-RPA assay was described for YFV detection which can be performed without complex equipment in an elementary laboratory setting, a rural health care center or an outbreak field investigation. A real-time methodology was developed including the design of a set of primers and probe which enables to detect down

to 21 Geq/rxn. This detection limit is slightly higher than the 8 Geq/rxn detected by real-time PCR [134]. Nonetheless, this level of sensitivity is sufficient to detect wild-type YFV in natural infections or serious adverse events (SAEs) following YFV immunization which produce viremia levels up to 10^8 PFU/ml [148, 159, 200].

The RPA in LFS format experienced problems of specificity, as a faint nonspecific band appeared in the negative controls when running time exceeded 10 minutes. Such appearance was not observed neither for the very low dilutions of YFV RNA nor for testing of other viruses. Therefore, these false-positive results are not due to contamination but rather to undesired primer interactions. Such interactions can be intramolecular (hairpins, etc.) or result from primer dimer formation, both between identical or different oligonucleotides. Unequivocal interpretation of LFS may be provided by an ESEQuant Lateral Flow Reader (Qiagen, Hilden, Germany). However, at this point, we recommend particular caution during LFS interpretation and further optimization of the assay before use under field conditions.

Real-time RT-RPA assays performed at the WHO Collaborating Centre for arboviruses and viral hemorrhagic fevers in Dakar demonstrated optimal testing results with all RNA extracts from YFV strains and mosquito pools. Testing results of the mosquito pools demonstrated an analytical sensitivity of 80% and a specificity of 100%.

Test results for spiked human plasma samples indicated that serum does not affect the analytical sensitivity of the assay. Therefore, we can assume that the test can be applied for laboratory case confirmation of suspected YFV cases. However, the assay will need to be further validated with YF clinical samples from various endemic countries and from patients with different clinical pictures. This is currently performed at the laboratory of the WHO Collaborating Centre for arboviruses and viral hemorrhagic fevers at the Pasteur Institute of Dakar. The laboratory is now equipped with all the material necessary to perform real-time RPA for YFV diagnostic and they can test clinical samples from West African patients as soon as these are received at the laboratory.

An external quality assessment study on diagnostic methods for YFV infections launched in 2011 revealed that the main weakness observed for molecular methods was the inability of some assays to detect the YFV genome of wild-type strains, whereas the vaccine strain was always detected [177]. This specificity problem has not been observed for the YFV RT-RPA assay, as all YFV strains were detected. Furthermore, our assay revealed no cross-reactions with other closely related viruses.

Recently, another isothermal amplification method for YFV detection was developed based on reverse transcription loop-mediated isothermal amplification (RT-LAMP) technology [139]. In contrast to RPA, LAMP requires a larger set of six primers, a higher temperature (62°C) and a longer run time. Sensitivity is not comparable, as results of RT-

LAMP were expressed as PFU instead of Geq detected, but RT-LAMP usually presents equal or lower sensitivity than RPA [180, 201].

In summary, a rapid and sensitive isothermal RPA assay in real-time and lateral-flow strip format for the detection of YFV could be developed. However, the LFS format needs further optimization to exclude all risks of false-positive results. The real-time RT-RPA assay using the transportable Tube Scanner device was later performed by German and Senegalese colleagues in field conditions in Senegal. Real-time RT-RPA was combined with a RNA extraction method based on magnetic beads and energy supply was provided by a battery charged by solar panels in order to implement an energy self-sufficient system. The use of identical positive controls enabled to demonstrate that RPA testing in field conditions provided as good performances as in laboratory conditions. These results allow us to confirm that the real-time RT-RPA assay for YFV detection is a suitable technique which performs under field conditions with the same accuracy and efficiency to that of cutting-edge laboratory settings.

B DETECTION OF YELLOW FEVER VIRUS NS1 ANTIGEN

B.1 INTRODUCTION

The flavivirus non-structural protein 1 (NS1) was first reported in 1970 as a viral antigen circulating in the sera of dengue-infected patients [202]. However, its structure and functions have remained unclear ever since. Amino acid sequences of the NS1 protein share a high degree of homology among flaviviruses, encoding a 352-amino-acid polypeptide with a molecular weight of 45 to 55 kDa. NS1 is a multi-functional glycoprotein synthesized as a monomer which dimerizes after post-translational modification in a cell membrane-associated form and which also exists as a soluble secreted hexamer with a lipid core [120]. Intracellular NS1 is found together with other components of the viral replication complex and plays an essential role in virus replication as demonstrated by several studies showing that flaviviruses containing deletions in NS1 are not able to replicate efficiently [203-205]. However, the precise function of NS1 during replication has not been elucidated and it is still unclear whether NS1 can be used as a target for viral inhibition.

Recently, the potential use of NS1 as a diagnostic marker has been investigated and NS1 detection has already been reported to be a sensitive and specific method for diagnosis of dengue infections. An antigen capture ELISA for dengue NS1 was first developed in 2000 [206] and its early assessment [207] led to the commercial development of ELISA kits by companies such as Panbio and Biorad. Later on, dipsticks were developed for point-of care diagnosis and dengue kits based on this technology have been successfully developed and implemented, in particular in India [86, 208]. Each kit comprises rapid tests for simultaneous detection of dengue NS1, anti-dengue IgM and IgG thus offering an affordable, accurate and easy-to-use full diagnosis of dengue infections [209]. As a result of these developments, NS1 detection has now become an essential diagnostic tool for dengue diagnosis.

Studies based on dengue NS1 detection methods indicated NS1 is found circulating in the blood of infected individuals very early in infection, from the first day after the onset of symptoms and up to 9 days [207]. Moreover, NS1 is detected before the appearance of an antibody response and as early as viral genome indicating that NS1 detection can be considered as an alternative marker for dengue viremia [210] (Fig. 21). Such early diagnosis is crucial since the risk of shock and hemorrhage appears before any antibodies against dengue can be detected. Moreover, serology is not always definitive on a single specimen in order to determine whether the infection is recent. Studies on dengue infections could also reveal a correlation between high levels of NS1 and onset of severe disease which indicates NS1 could be used as an early biomarker of severe disease [211]. It is now considered

CHAPTER 2 – Yellow fever virus NS1 Detection - Introduction

whether NS1 detection can be applied to the diagnosis of other flavivirus infections such as West Nile, Japanese encephalitis or yellow fever infections [212].

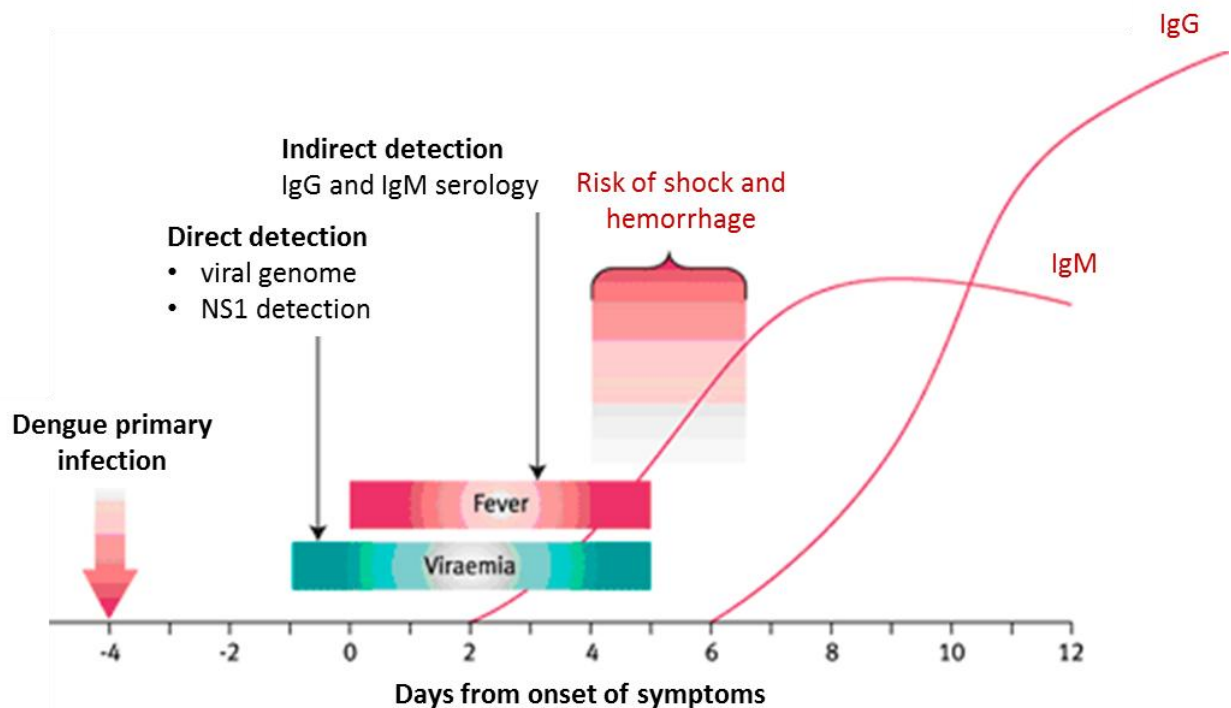


Figure 21: Typical primary dengue infection with timing of diagnostic tests. Adapted from <http://www.health.qld.gov.au/cdcg/index/dengue.asp>

The objective of this research project was to develop specific tools for the detection and identification of YFV NS1 protein for research purposes and to investigate their potential use for yellow fever virus diagnostics. An affordable and efficient method for producing such tools is the production of polyclonal antibodies by immunizing animals with synthetic peptides used as immunogens. This method has been developed since the 1980s when it was demonstrated that peptide immunogens are able to induce antibodies specific for intact viral particles and can be of considerable value in the production of serological reagents for the detection of pathogens such as flaviviruses [213, 214]. Therefore, synthetic peptide immunogens homologous to regions of the YFV NS1 protein were identified and evaluated for their ability to produce polyclonal antisera specific for YFV NS1 protein.

This project was initiated prior to this PhD work by Dr Nina Stock during her PhD thesis in Prof. Niedrigs' research group at the Robert Koch Institute [215]. In 2011, a polyclonal antibody against the YFV NS1 protein had been produced by immunizing rabbits with a synthetic peptide. The obtained polyclonal antiserum was able to detect specifically the YFV NS1 protein by western blot (WB) and immunofluorescence assays (IFA).

As part of this PhD project, the objective of this chapter was to produce additional YFV-specific polyclonal antisera for NS1 detection by immunization with other peptide immunogens in order to provide further tools for NS1 detection during YFV infections. The newly produced polyclonal antisera were then characterized by WB, IFA and neutralization test and their potential use in ELISA was investigated in combination with the already available rabbit polyclonal antiserum.

B.2 METHODS

B.2.1 Peptide immunogen design

In order to provide further tools for NS1 detection, it was decided to produce additional YFV-specific polyclonal antisera for NS1 detection by immunization of guinea pigs with other synthetic peptides than P1, previously used to immunize a rabbit (see peptide sequence in Table 13).

For the production of further NS1 polyclonal antisera, two peptide immunogens were selected *in silico* by using the Lasergene SeqMan Pro (Version 8.1.5, DNASTAR inc.) and Geneious software (Version 6.1.6, Biomatters LTD). The following guidelines were applied in order to select the most efficient peptide immunogens:

1. The appropriate virus strains and protein sequences were identified. The peptide sequence should be conserved in all variants of the target protein and also be specific to the target protein.
2. Peptide immunogens should be selected from an accessible region of the native protein. Most often, such regions are exposed on the surface of the protein in contact with the hydrophilic environment. Computer programs can be used which assign a "hydrophilic index" to each amino acid in a protein and then plot a profile displaying the regions of hydrophilicity or hydrophobicity.
3. Long chains of hydrophobic residues and complex regions such as alpha helices or beta sheets should be avoided.
4. The addition of a terminal cysteine residue to the peptide sequence allows conjugation of the peptide to carrier proteins, such as keyhole limpet hemocyanin (KLH) or bovine serum albumin (BSA).

More specifically, NS1 peptide sequences from 16 different YFV strains were aligned in order to identify conserved regions among all YFV NS1 peptide sequences. Description and accession numbers of all vaccine and wild YFV strains used for the sequence analysis are listed in Table 0-10 in the list of material. Then the generated consensus sequence was

subsequently aligned to the NS1 protein sequences of other closely related flaviviruses (WNV, JEV, TBEV and dengue 1, 2, 3, 4) in order to verify that the regions selected for our peptide design were not conserved regions in other flavivirus sequences. Comparison with other flavivirus sequences was performed in order to guarantee a better specificity of the produced anti-YFV NS1 sera which should not cross-react with other flaviviruses. Description and accession numbers of all flavivirus sequences used for this analysis are listed in Table 0-10 in the list of material. The Lasergene SeqMan Pro software was then used to determine the antigenic potential of preselected sequences according to the guidelines listed in the previous paragraph. The final length of the selected peptide regions should be between 10 and 20 amino acids.

Finally, the choice of two peptide immunogens was made in agreement with the peptide design service of the Eurogentec (Seraing, Belgium) which later produced the polyclonal antisera. A terminal cysteine residue was added to the peptide sequence, when it was not already present, in order to allow the conjugation of the carrier protein, KLH.

B.2.2 Production of polyclonal antisera

Polyclonal antisera were produced by immunizing another species than rabbit in order to avoid non-specific binding in case both antisera were to be used in the same diagnostic assay, e.g. a sandwich ELISA. Immunization of three guinea pigs was performed by Eurogentec, an international biotechnology supplier based in Belgium. A classic polyclonal antibody protocol has been chosen which ordinarily provides high titer antibodies with excellent affinity within 3 months. A single peptide strategy is best suited for reproducing a successful polyclonal production with a known peptide sequence. For the first-time generation of antibodies against a particular antigen, it is recommended to design two peptides from the same antigen and immunize the animal hosts with both peptides as co-immunization more closely mimics the protein than a single peptide strategy. To increase chances of producing high affinity antibodies, it was decided to immunize one guinea pig with both synthetic peptides and two other guinea pigs with only one of each peptide. Final bleed was performed on day 87 after first immunization. The polyclonal antisera were provided without any additional purification step as the previously produced polyclonal antiserum, the rabbit anti-P1, provided satisfying results as a non-purified serum.

B.2.3 Indirect immunofluorescence assay

For the characterization of the polyclonal antisera produced, immunofluorescence assay (IFA) was performed with a commercial slide from EUROIMMUN AG in which cover glasses coated with YFV-infected Vero cells are cut into millimeter-sized fragments and fixed on a BIOCHIP. If the sample is positive against the YFV antigens presented by the infected

cells, specific antibodies in the diluted serum sample will attach to the antigens coupled to the solid surface. In a second step, the attached antibodies are stained with fluorescein-labeled anti-guinea pig (or anti-rabbit) antibodies and visualized with the fluorescence microscope (Fig. 22).

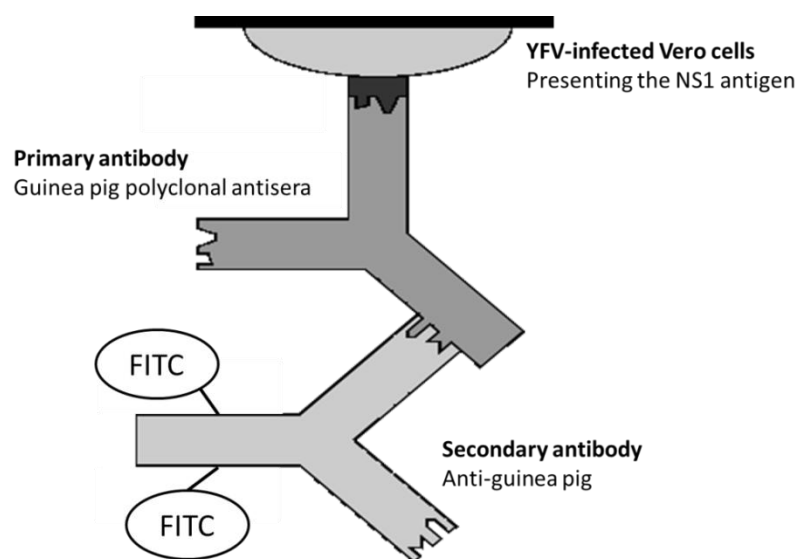


Figure 22: Schematic description of the antigen/antibody interactions in an IFA YFV slide for detection of NS1 antigen with the guinea-pig polyclonal antisera

To detect antibodies against YFV NS1, the EUROIMMUN slide was incubated for 45 minutes at room temperature (RT) with the polyclonal anti-NS1 antisera and primary antibodies diluted at 1:25, 1:50, 1:100 and 1:200 in 1x PBS with 0,1% Tween (PBST). MAB6330 (a mouse anti-YFV antibody [216]) was tested at a 1:100 dilution as a positive control. After washing with TBST, the EUROIMMUN slide was then incubated for 45 minutes at room temperature in the dark with FITC labeled anti-guinea pig (or anti-mouse for the positive control) secondary antibodies diluted at 1:200 in 1x PBST in order to detect primary antibodies. After washing with TBST, the slide was covered with mounting medium composed of glycerol only, for a standard observation or glycerol containing DAPI, a fluorescent dye staining the DNA content and nuclei, for simultaneous observation of the cell nucleus. The slide was then mounted with a cover slip and observed with a fluorescence microscope with the appropriate color filters to analyze the immunofluorescence of the secondary antibodies (FITC - green channel) and cell nucleus (DAPI - blue channel).

“Flavivirus Profile 2” IFA slides from EUROIMMUN were used for cross-reactivity testing. Flavivirus profile slides from EUROIMMUN are designed for flavivirus serological diagnosis and allow reliable differential diagnosis in infections with similar or unclear symptoms (Fig. 23).

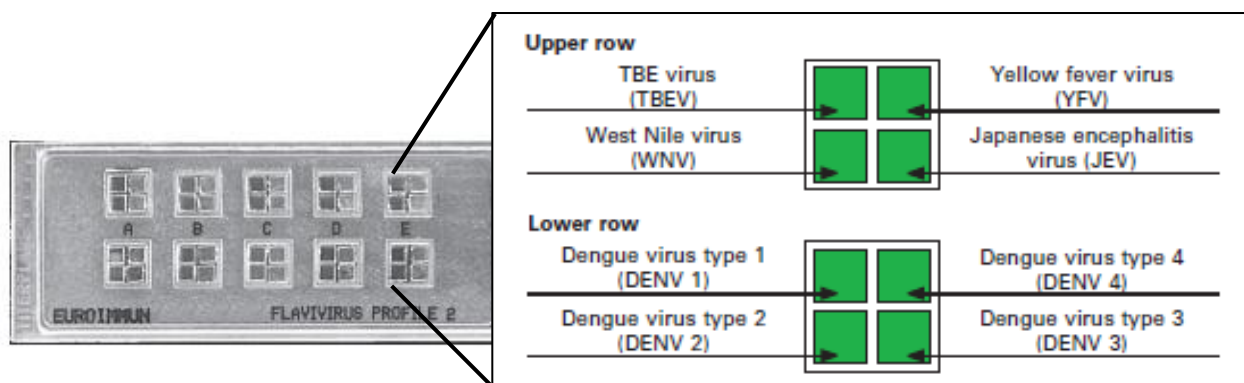


Figure 23: Picture of an IFA slide “Flavivirus Profile 2” from EUROIMMUN and disposition of the cover glass squares coated with flavivirus-infected cells on the biochip. Source: EUROIMMUN website http://www.euroimmun.ch/uploads/media/FI_2600_I_UK_B06.pdf

The protocol applied using the “Flavivirus Profile 2” slide was similar to the one used for the YFV EUROIMMUN slide. The anti-guinea pig (or rabbit) antisera were diluted at 1:20 and used as primary antibody. Negative and positive controls were used from the kit. Anti-guinea pig (or rabbit)-FITC at 1:200 dilution were used as secondary antibody. The slide was then mounted with glycerol and a cover slip for observation with a fluorescence microscope.

B.2.4 Cultivation of adherent cells

Vero E6 cells (ATCC CRL-1586) and Pig kidney epithelial (PS) cells were used for YFV-17D cultivation. The *Vero* lineage was isolated from kidney epithelial cells extracted from an African green monkey. Vero E6 cells show some contact inhibition so are suitable for propagating viruses that replicate slowly such as YFV. PS cells have been identified since the 1970s as a perfect tool for the study of flaviviruses and some other arboviruses [217].

Vero E6 cells were cultivated in D-MEM medium with 10% FBS (fetal bovine serum), 1% penicillin, 1% streptomycin and 1% glutamine and incubated at 37°C with 5 % CO₂. PS cells were cultivated in L15 medium supplemented with 10% FBS, 1% penicillin, 1% streptomycin and 1% glutamine and incubated at 37°C without CO₂. When the cell monolayer became confluent, the media was removed from the culture flask and cells were washed with PBS. Trypsin was added in order to detach the cells from each other and from the flask surface. Excess trypsin was removed and the flask incubated at 37°C until complete dissociation of the cells from the flask surface. Fresh medium was then added to the cells and cells resuspended by up and down pipetting. Cells were inoculated in new flasks at an appropriate density depending on the time of further use required.

B.2.5 Plaque Reduction Neutralization Test

The plaque reduction neutralization test (PRNT) is used to quantify in a serum the titer of neutralizing antibodies against a specific virus. The serum sample or solution of antibody to be tested is mixed with a viral suspension of known titer and incubated to allow the antibody to react with the virus. This mixture is poured over a confluent monolayer of host cells. After infection, the surface of the cell layer is covered with a layer of carboxymethyl cellulose (CMC) to stop the virus from spreading further to other cells by dissemination in the medium. For YFV, plaque forming units (PFU) can be counted by naked eye four days after infection (Fig. 24).

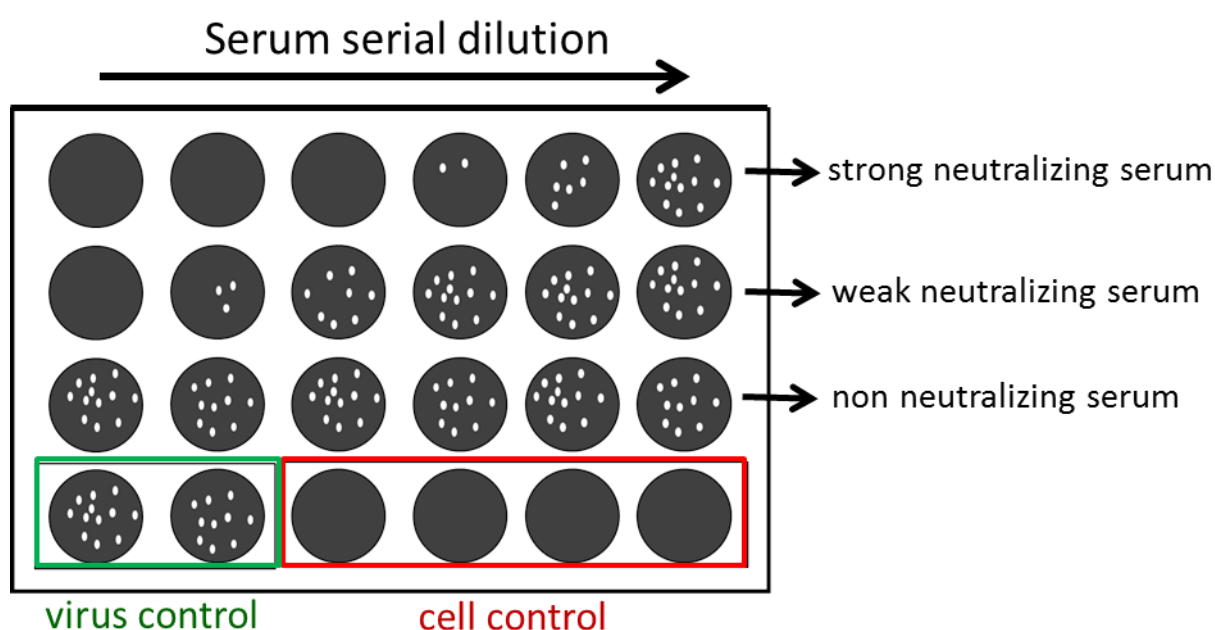


Figure 24: Diagram of a standard neutralization test performed in a 24-well plate

In this study, YFV-17D solutions were prepared with the Reference charge 354/1 at a titer of 200 PFU/ml and mixed with the antiserum in a 1:1 ratio and heated at 37°C for 1h. PS cells were prepared in suspension and $1.2 \cdot 10^5$ cells in a volume of 200 μ l per well were seeded in a 24-well plate. The virus/serum dilutions were then added to each well and the plate was incubated 4h at 37°C without CO₂. An overlay of CMC media (1.6% CMC in cell culture media) was then added to each well. After 4 days of incubation at 37°C, the media was removed from the wells and cells were fixed with 3.7% formaldehyde for at least 15 min. This step also inactivates viruses. Fixed cells in each well were then stained with Naphthalene black solution for at least 30 min and washed with tap water. Once the plate was dry, plaques were counted by naked eye.

One of the possible methods to measure the neutralizing effect of the serum is the determination of the dilution of serum to reduce the number of plaques by 50% compared to the serum free virus. The corresponding dilution factor is represented by the PRNT₅₀ value.

B.2.6 Preparation of cell culture supernatants positive for YFV NS1 protein

Cell supernatant from YFV-infected Vero cells was used as a positive control and source of YFV NS1 protein in further Western blot and ELISA experiments for characterization of the newly produced antisera. In fact, until now, YFV NS1 protein is not available as a recombinant protein unlike NS1 proteins of other viruses such as dengue which are available commercially.

Vero E6 cells (ATCC CRL-1586) confluent at 80% were infected with the vaccine strain YFV-17D (RKI Reference charge 354/1) with an MOI of 0.01 for 1 h and then washed 2 times with PBS before fresh medium was added. One culture flask of infected Vero E6 cells was prepared for each daily harvest and cultivation was pursued until 10 days after infection. Cell supernatant from non-infected Vero E6 cells was cultivated in parallel and sampled as negative control. Cells were incubated at 37°C and supplied with 5% CO₂. For each daily harvest, the culture supernatant of one flask was collected and stored in aliquots at -80°C until further use for detection of NS1 protein by Western blot or ELISA.

B.2.7 Western blot

Western blot (WB), also called protein immunoblot, is the most widely used analytical technique to detect specific proteins. Western blotting identifies with specific antibodies, proteins that have been separated from one another according to their size by SDS-gel electrophoresis. The blot is most commonly a membrane of nitrocellulose or polyvinylidene fluoride (PVDF). After protein separation, the gel is placed next to the membrane and application of an electrical current induces the proteins in the gel to move towards the membrane to which they bind. The membrane is then a replica of the protein pattern of the gel and is subsequently stained with antibodies specific to the target protein.

This technique was used to test the immunogenicity of the newly produced polyclonal antisera against the YFV NS1 protein. Cell supernatant from YFV-infected Vero cells, prepared as described in the previous paragraph (§B.2.6), were used as a source of YFV NS1 protein during detection by the produced antisera.

All the steps required to perform a WB for YFV NS1 detection are presented in Figure 25 as well as the final protein construction for the chemiluminescent detection of anti-YFV NS1 polyclonal antibodies.

CHAPTER 2 – Yellow fever virus NS1 Detection - Methods

Sample preparation of denatured proteins was done by treating protein samples (cell supernatant) with the Lane Marker Reducing Sample Buffer (Thermo Scientific Pierce) and heated 5 min at 95°C. PageRuler Prestained Protein Ladder (10-170 kDa) was used as protein ladder. Electrophoresis was performed with ready-to-use gels from Pierce (8-16% Precise Tris-HEPES at 4% polyacrylamide) or self-made gels including a separating gel and a stacking gel (Table 11). Tris-HEPES-SDS buffer was used as running buffer and electrophoresis ran at 150V for approximately 45 min. All materials for blotting were saturated in transfer buffer (25mM Tris, 150mM glycine, 10% methanol) before usage. PVDF membranes were additionally activated for 15 sec in methanol and rinsed with distilled H₂O before equilibration in transfer buffer.

Table 11: Composition of the separating and stacking gel

Component	Separating gel	Stacking gel
H2O dest.	3.755 ml	3.5 ml
2M Tris (pH 8,8)	2.1 ml	-
0,5M Tris (pH 6,8)	-	1 ml
20% SDS	50 µl	37.5 µl
PAA	3.96 ml (12%)	1.25 ml (5%)
60% sucrose	-	1.75 ml
10% APS	120 µl	62.5 µl
Temed	15 µl	6.25 µl

Semi-dry blotting was prepared by placing the filter paper sheets, membrane and gel as pictured in Figure 25.B. Semi-dry blotting was performed for 1h 30 min at 230 mA with low voltage. After blotting, the membrane was dyed for 5 minutes with Ponceau S for rapid reversible detection of protein bands in order to be able to cut the membrane in stripes which can then be used for incubation with different antibodies. The membrane was then blocked with Tris-buffered saline + 0.05% Tween 20 (TBST) with 5% milk during 1h at room temperature. Primary antibodies (polyclonal rabbit or guinea-pig antisera) were diluted in 0.75% milk TBST and incubated overnight at 4°C. After washing, the secondary antibody (anti-rabbit poly-HRP or anti-guinea pig poly-HRP) was added and the membrane incubated for 1h. ECL Western blotting substrate (Thermo Scientific Pierce) was added directly onto the membrane and incubated for 3 minutes. Finally, the blot was exposed against a Thermo Scientific CL-XPosure film for 1 minute and developed in a dark room.

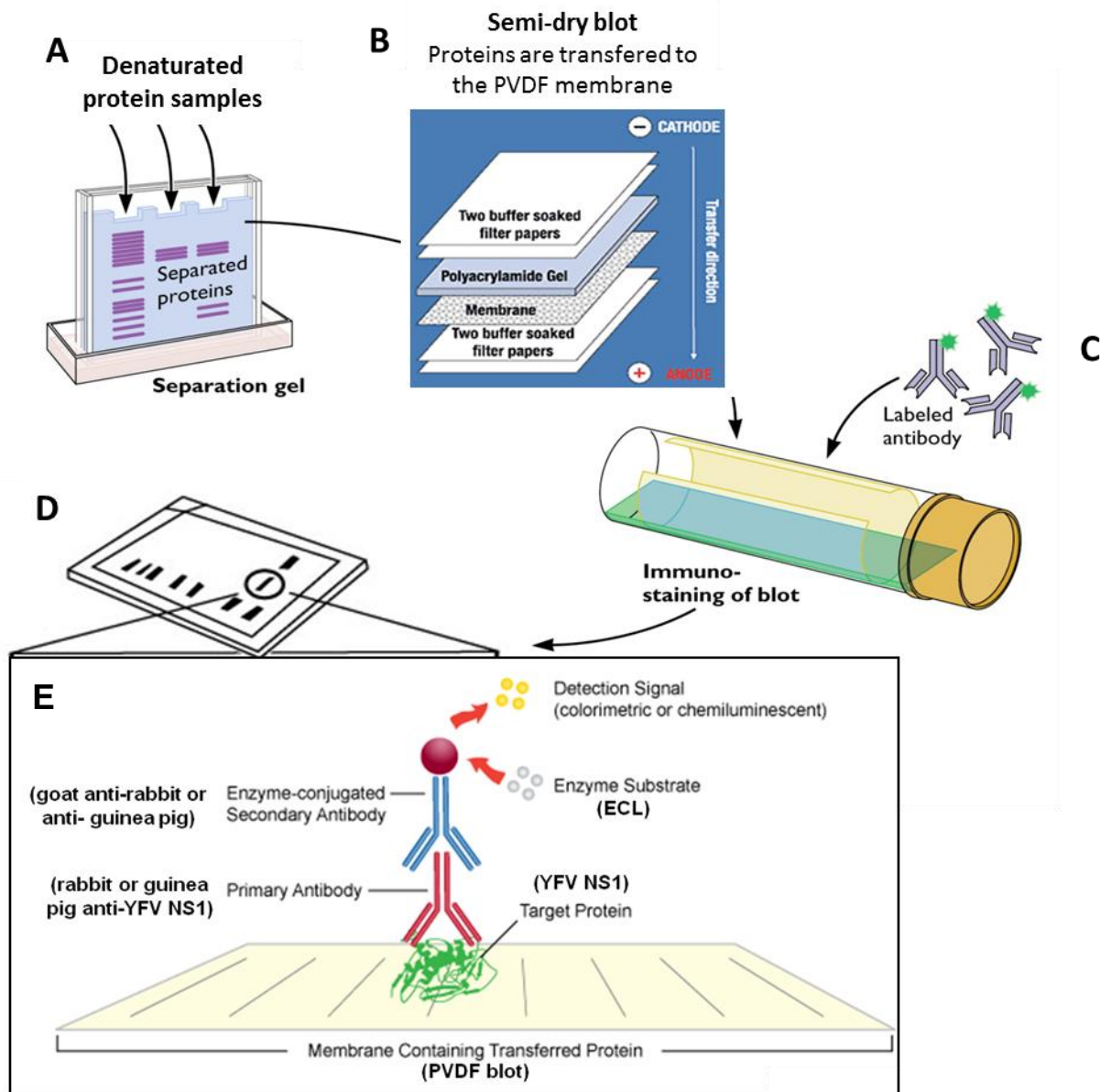


Figure 25: The different steps of a Western blotting procedure for (YFV NS1) protein detection. **A:** Denatured protein samples are separated using SDS-gel electrophoresis. **B:** The separated molecules are blotted on a nitrocellulose or PVDF membrane by semi-dry blotting. The picture shows the layout of the WB sandwich for semi-dry blotting. **C:** The transferred protein is detected by specific antibodies which are then detected by labeled antibodies for chemiluminescent detection. **D:** A chemiluminescent substrate is added to the enzyme and together they produce light as a byproduct. **E:** In this study, YFV NS1 was our target protein. The primary antibody, the polyclonal rabbit or guinea pig anti-NS1, binds to the NS1 protein and is detected by the secondary antibodies coupled with horseradish peroxidase (HRP). In contact with HRP, the ECL substrate produces a chemiluminescent signal. Adapted from the Leinco Technologies website http://www.leinco.com/general_wb and the Virology Blog <http://www.virology.ws/2010/07/07/virology-toolbox-the-western-blot/>

B.2.8 ELISA

The enzyme-linked immunosorbent assay (ELISA) is a powerful method for detection and quantification of a specific protein in a complex mixture. ELISAs are most commonly constructed in an indirect format of which there are two main variations of this method: an antigen is coated on the plate in order to determine the quantity of a specific antibody in a sample (Fig. 26.A), or antibodies are coated on the plate to determine the quantity of a specific antigen bounding to an antibody (Fig. 26.B).

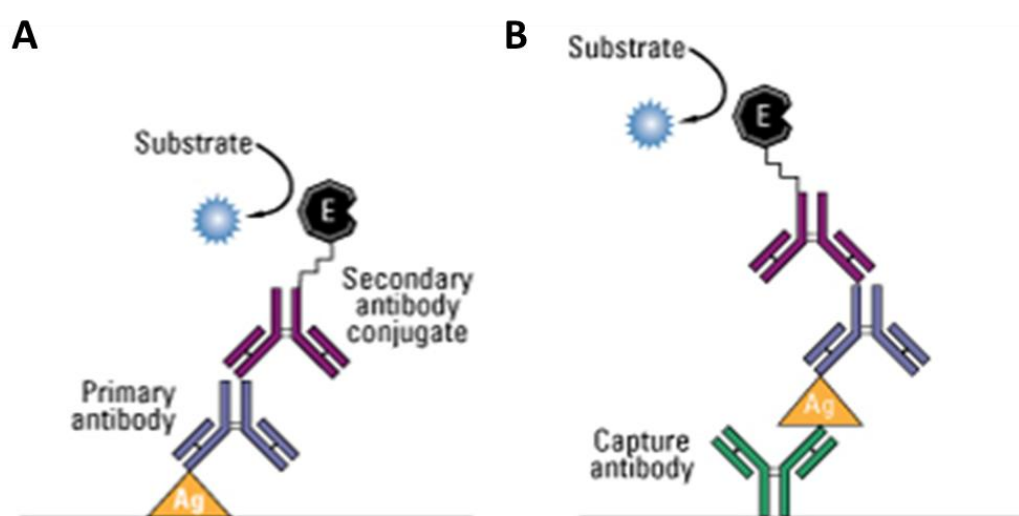


Figure 26: Main indirect ELISA formats. (A): coating with antigen (Ag) (in yellow); (B) coating with capture antibody. The detection antibody can be detected by a secondary antibody that is linked to an enzyme (E) through bioconjugation. An enzymatic substrate is then added and the produced chemiluminescent signal is proportional to the amount of antigen in the sample. Adapted from the Thermo Scientific website <http://www.piercenet.com/method/overview-elisa>

For all ELISA testing in this study, Maxisorp 96-well plates (Nunc) were coated with the synthetic peptides or with the polyclonal antisera by dilution in 0.1M carbonate buffer (pH 9.6) and incubation at 4°C overnight. After coating, plates were incubated for 2 hours with a blocking solution containing 3% fetal bovine serum (FBS) to cover all unsaturated surface-binding sites. Antibody solutions were prepared with a dilution buffer consisting of 2xPBS+ 0.05% Tween +1% FBS. Washing steps were performed at least 3 times with 2xPBS + 0.05% Tween to ensure that only specific binding events are maintained to cause signal at the final step. All reagents were added in a volume of 100 µl per well and washing steps were performed with a volume of 200 µl per well. After final washing step, the TMB substrate was used to detect horseradish peroxidase (HRP) activity, yielding a blue color that changes to yellow ($\lambda_{max} = 450\text{nm}$) upon addition of a sulphuric acid (H_2SO_4) stop solution. Once

CHAPTER 2 – Yellow fever virus NS1 Detection - Methods

TMB was added, the reaction was stopped after 15 minutes of incubation in the dark with a 1M solution of H₂SO₄. An ELISA microplate reader from Tecan was used to measure the optical density (OD) at 450 nm with 620 nm as reference wavelength.

Preliminary ELISA tests based on the format of Figure 26.A were performed in order to determine whether the antisera were able to bind to their corresponding peptide immunogen. Peptide solutions were coated on the plates with serial dilutions ranging from 50 to 500 ng/ml. After washing, anti-YFV NS1 antisera were added to the plate at a 1:200, 1:500 or 1:1000 dilution and incubated for 2h at room temperature. After washing, the detection antibody (goat anti-guinea pig IgG-HRP or goat anti-rabbit IgG-poly HRP) was added at a 1:10000 or 1:20000 dilution.

Subsequent ELISA experiments were performed with peptide P2 and P3 coated simultaneously and individually on a microplate at a concentration of 50 ng/ml. In order to test the effect of antiserum dilution, P2 and P3 were detected with serial dilutions (from 1:200 to 1:3200) of anti-P2, anti-P3 or anti-P2/3. Anti-P2 was used to detect P2, anti-P3 to detect P3 and anti-P2/3 to detect both P2 and P3. Goat anti-guinea pig IgG-HRP was used as secondary antibody at a dilution of 1:5000.

After this preliminary ELISA testing for peptide recognition with each antiserum, it was investigated whether a sandwich ELISA based on the format of Figure 26.B could be developed using the rabbit and guinea pig polyclonal antisera. Next ELISAs were performed with cell supernatant tested positive for NS1 in WB as a positive control for NS1 detection. Dilution buffer and cell supernatant of non-infected cells were used as negative controls.

Several ELISA constructions were tested with different combinations of antisera for capture and detection of NS1 and are listed in Table 12. For all ELISA constructions, polyclonal antisera were used at a 1:200 dilution and secondary antibodies were used at a 1:10000 dilution. Incubations with all antibodies were performed 2h at room temperature. Test n°1, 2 and 3 were performed with anti-P1 as capture antibody and the three different guinea pig antisera (anti-P2, -P3 and -P2/3) as detection antibodies. Inversely, test n°4, 5 and 6 were performed with the guinea pig antisera for capture and the rabbit anti-P1 antiserum for detection. The last three ELISAs (n°7, 8 and 9) were performed by direct coating of YFV-infected cell supernatant and detection was performed with anti-NS1 antisera from guinea pig as primary antibody and anti-guinea pig IgG-HRP as secondary antibody.

For all test listed in Table 12, cell supernatants (positive and negative controls) were tested without any denaturing treatment and also with denaturing treatment in order to unfold the NS1 protein and potentially allow better access to binding sites. Denaturing treatment included heating at 60°C or 95°C for 30 min and addition of detergent (1% SDS or 0.1% Tween20).

Table 12: List of ELISA constructions performed with the newly produced guinea antisera

	Coating	Primary antibody	Secondary antibody
1	Anti-P1 (1:200)	Anti-P2	goat anti-guinea pig IgG-HRP
2	Anti-P1 (1:200)	Anti-P3	goat anti-guinea pig IgG-HRP
3	Anti-P1 (1:200)	Anti-P2/3	goat anti-guinea pig IgG-HRP
4	Anti-P2 (1:200)	Anti-P1	goat anti-rabbit IgG-poly HRP
5	Anti-P3 (1:200)	Anti-P1	goat anti-rabbit IgG-poly HRP
6	Anti-P2/3 (1:200)	Anti-P1	goat anti-rabbit IgG-poly HRP
7	Cell supernatant (1:5)	Anti-P2	goat anti-guinea pig IgG-HRP
8	Cell supernatant (1:5)	Anti-P3	goat anti-guinea pig IgG-HRP
9	Cell supernatant (1:5)	Anti-P2/3	goat anti-guinea pig IgG-HRP

B.3 RESULTS

B.3.1 Peptide immunogen design and production of polyclonal antisera

Based on the peptide immunogen guidelines described in the introduction chapter, peptides P2 and P3 were selected to immunize the guinea pigs (Table 13). Three anti-YFV NS1 antisera were obtained by immunization of three guinea pigs with peptide P2 and P3 as described in Figure 27. P1, the synthetic peptide previously used for immunization of a rabbit is also listed in Table 12 and the production of the corresponding anti-P1 serum is illustrated in Figure 27 to provide an overview of all available tools for YFV NS1 detection.

Table 13: Sequence and position of peptides for immunization and antibody production

Peptide	Position in YFV-polyprotein	Target protein	Peptide sequence
P1	908-922	YFV NS1	QDP KNV YQR GTH PFS-C
P2	945-960	YFV NS1	RKN GSF IID GKS RKE C
P3	985-1000	YFV NS1	VNG KKS AHG SPT FWM-C

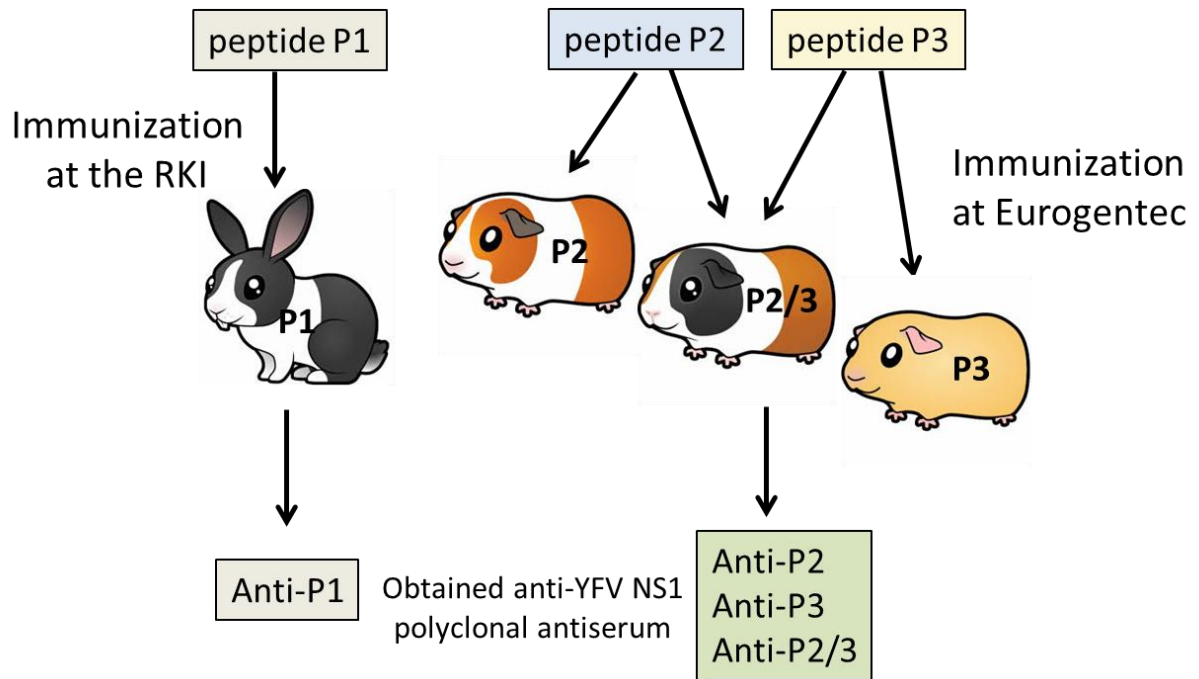


Figure 27: Diagram of the procedure followed for the production of polyclonal antisera. The rabbit was immunized previously at the RKI with peptide P1 and the three guinea pigs were immunized by Eurogentec with peptides P2 and P3.

B.3.2 Indirect immunofluorescence assay

Reactivity of all polyclonal anti-NS1 sera was tested by indirect immunofluorescence assay using EUROIMMUN YFV slides described in §B.2.3. The rabbit anti-P1 serum produced and characterized in a previous work [215] was used in all assays as a comparison with the newly produced antisera from guinea pigs. A rabbit monoclonal antibody against the YFV-E protein, MAB6630 [216], was used as a positive control in the IFA experiments. IFA results demonstrated uneven results for the newly produced guinea pig antisera. The anti-P2 antiserum provided good results and its reactivity was comparable to the one of the anti-P1 rabbit antiserum (Fig. 28). The anti-P3 guinea pig antiserum demonstrated a very weak fluorescent signal. Anti-P2/3, the antiserum obtained from double peptide immunization, demonstrated a slightly weaker signal than the anti-P2 antiserum obtained by single peptide immunization (Fig. 28).

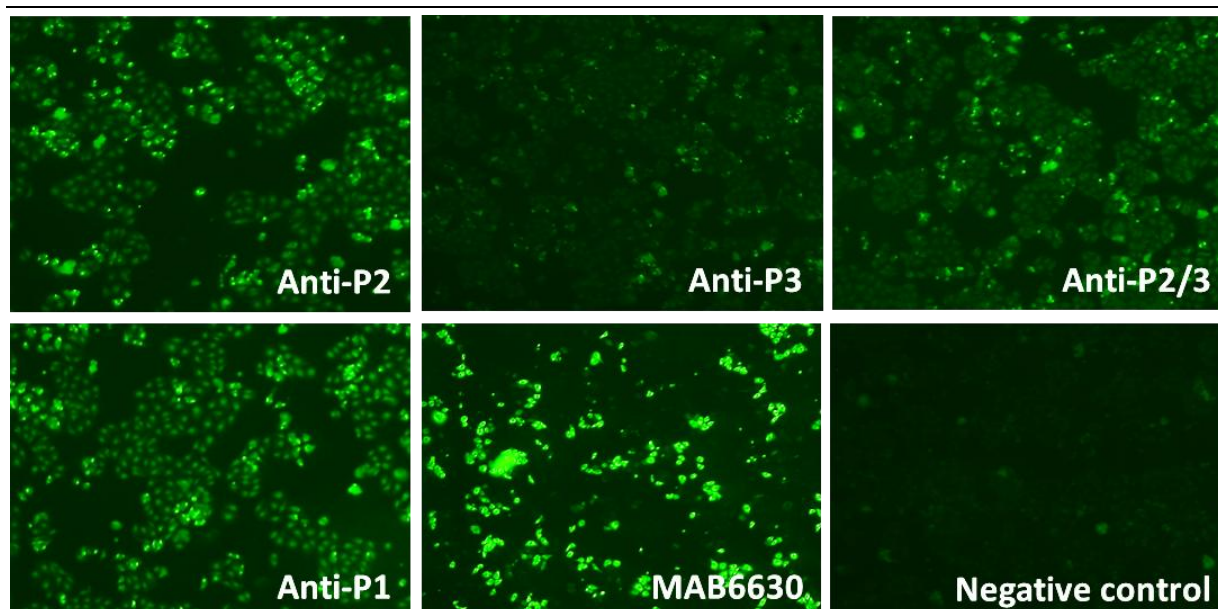


Figure 28: IFA for the detection of YF-specific antibodies. Incubation occurred with primary antibodies diluted at 1:100 including MAB6630 and anti-P1, used as positive controls. Negative controls included non-infected cells incubated with each antiserum as well as infected cells incubated with only secondary antibody, anti-rabbit (or guinea pig)-FITC (1:200). All negative controls demonstrated the same appearance as the one presented in the figure which corresponded to the negative control provided in the EUROIMMUN IFA kit. Image magnification: X10

EUROIMMUN “Flavivirus Profile 2” slides were used for cross-reactivity testing of the newly produced antisera with other closely related flaviviruses. Fluorescence microscopy results for anti-P2 are shown in Figure 29 and IFA demonstrated reactivity of the sera against YFV and not against any other flaviviruses. Anti-P3 and anti-P2/3 demonstrated similar results although results for anti-P3 are difficult to interpret as the antiserum reactivity with YFV is very weak (data not shown). IFA results for all YFV-antisera demonstrated no cross-reactivity with other flaviviruses. Cross-reactivity testing of anti-P1 was also performed as a control and demonstrated no cross-reactivity as described in Nina Stocks’ PhD dissertation [215].

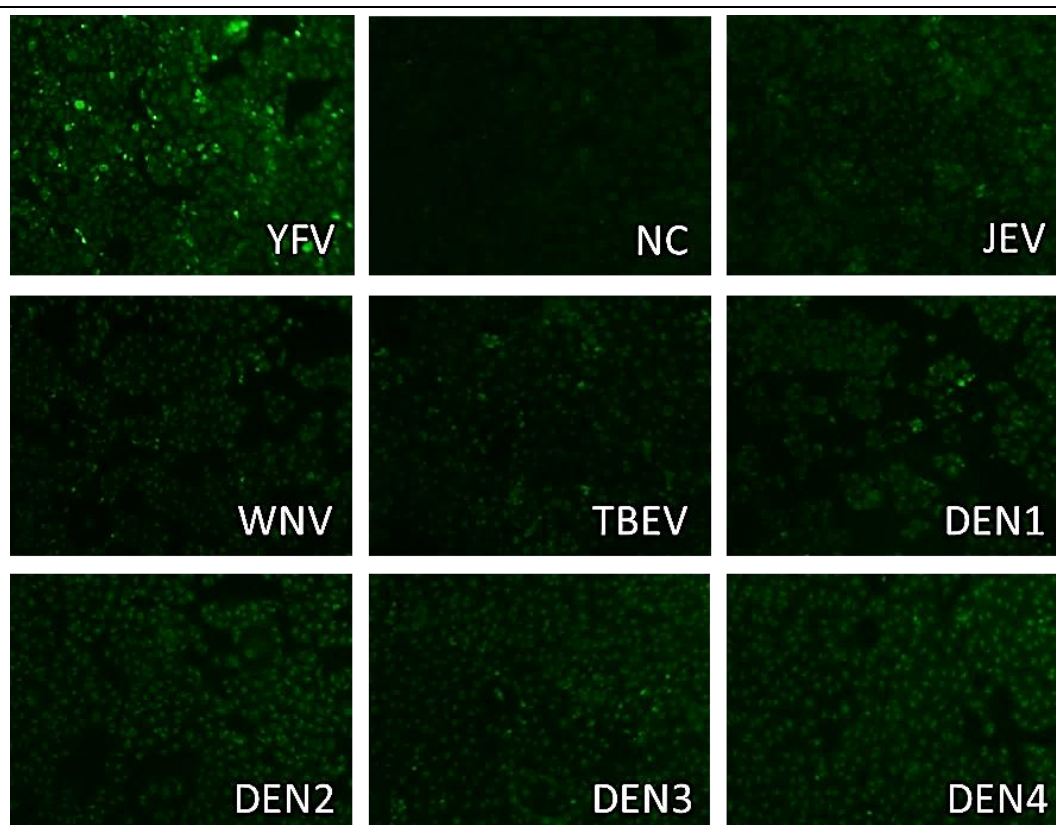


Figure 29: IFA images obtained with a EUROIMMUN Flavivirus Profile 2 slide for the guinea pig anti-P2 antiserum diluted at 1:20. **NC:** negative control was included in the EUROIMMUN IFA kit; **JEV:** Japanese encephalitis virus; **WNV:** West Nile virus; **TBEV:** Tick-borne encephalitis virus; **DEN 1/2/3/4:** Dengue serotype 1/2/3/4. Image magnification: X10

B.3.3 Plaque reduction neutralization test

The neutralization effect of each anti-YFV NS1 antiserum was tested by plaque reduction neutralization test. The titer of neutralizing antibodies is expected to be low for NS1 antisera. For this reason, undiluted serum and low dilutions of antiserum were tested (1:3, 1:6, 1:12 and 1:24 dilutions).

Results of the plaque reduction neutralization test for the guinea pig antisera anti-P2 and anti-P3 are shown in Figure 30. All antisera demonstrated the same results in plaque reduction neutralization test and indicated a very low neutralizing effect against YF-17D virus as the PRNT50 values were situated between 3 and 6, which is below the diagnostic threshold of 10.

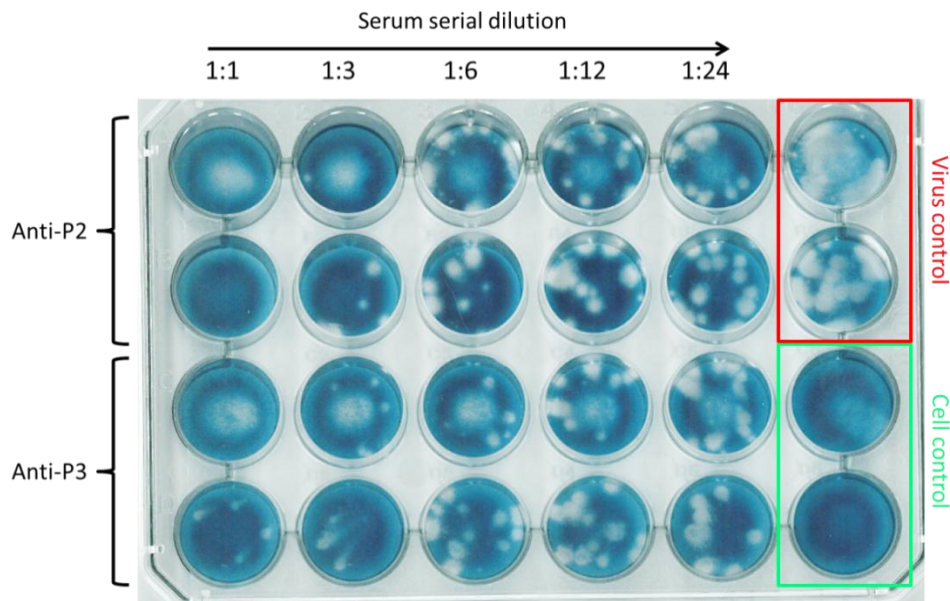


Figure 30: Results of the plaque reduction neutralization test for the guinea pig antisera anti-P2 and anti-P3 including the virus and cell control. All samples were tested in duplicate.

B.3.4 Western blot

A first Western blot was performed with all samples from the cultivation of Vero E6 cells infected with YFV-17D performed as described in §B.2.6 previously in this chapter. NS1 detection was performed with the already characterized anti-P1 rabbit antiserum as a control method in order to determine the presence of NS1 protein in each sample of the cell cultivation. All samples were tested in WB in denatured conditions as described in the methods part of this chapter (§B.2.7). The results from this WB are pictured in Figure 31.A, each lane corresponding to a daily sample of cell supernatant, day 0 being the day of infection with YFV-17D. A band of approximately 45 kDa corresponding to the size of NS1 monomer was detected from day 4 after infection. The intensity of the band increased until the end of the kinetic at day 9 after infection.

Once the YFV-17D kinetic samples were tested for NS1 detection with the already characterized anti-P1 rabbit antiserum, the same WB experiment was performed by using the newly produced anti-P2 guinea pig antiserum as primary antibody. Results of this WB (Fig. 31.B) showed similar results than for NS1 detection with the rabbit antiserum (Fig. 31.A), confirming the appearance of NS1 protein at day 4 after infection and NS1 concentration increased until day 9. Based on these results, a stock of supernatant from day 9 after infection was further used as a positive control for NS1 detection in WB and ELISA experiments.

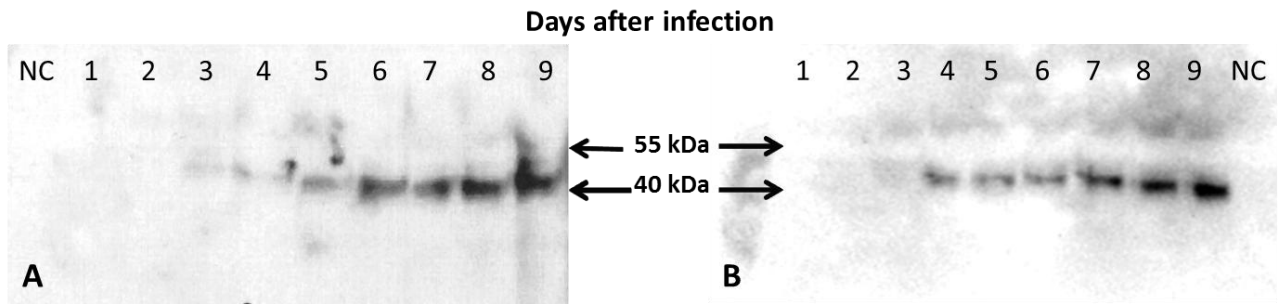


Figure 31: WB results from the kinetic of NS1 production during YFV-17D infection of Vero E6 cells (MOI=0.01). Blotting membrane: PVDF 0.45 μ m. NC: negative control. Secondary antibody: anti-rabbit (or anti-guinea pig) poly-HRP diluted at 1:50000. **A:** Primary antibody anti-P1 rabbit antiserum diluted at 1:500; **B:** primary antibody anti-P2 guinea pig antiserum at 1:500.

In order to test the functionality of all produced antisera, a WB was performed with all anti-NS1 antisera as primary antibodies and cell supernatant from day 9 of the YFV-17D kinetics, positive for NS1, as target protein. Results demonstrated a clearly positive signal for NS1 detection with anti-P1, anti-P2, anti-P2/3 and a weak signal with anti-P3 (Fig. 32). NS1 detection with anti-P2/3 did not provide better results than with anti-P2.

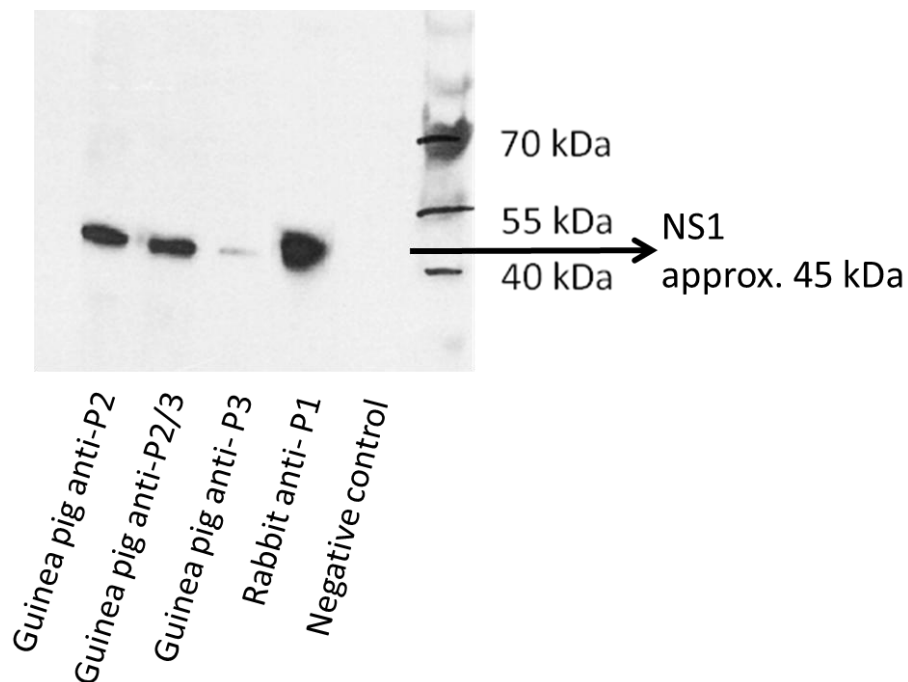


Figure 32: WB results from detection of positive NS1 cell supernatant with all anti-NS1 antisera. Proteins from cell supernatant were tested in denatured conditions. Primary antibody diluted at 1:500. Secondary antibody: anti-rabbit (or anti-guinea pig) poly-HRP diluted at 1:50000.

B.3.5 ELISA

A first ELISA test was performed by coating the P1 peptide on the microplate at different dilutions to test whether the anti-P1 rabbit antiserum could detect the coated peptide. Peptide concentration ranged from 50 to 500 ng/ml, primary antibody was diluted at 1:500 and 1:1000 and secondary antibody (goat anti-rabbit IgG-poly HRP) was added at a 1:10000 or 1:20000 dilution. Absorbance measurements were optimal for primary antibody at a 1:500 dilution and secondary antibody at a 1:10000 dilution providing OD values between 2 and 2.5 with a peptide concentration of 50 ng/ml. Testing results of the negative control with only carbonate buffer and no peptide provided negative results.

Based on these preliminary results, a similar ELISA was performed with peptide P2 and P3 coated separately on a microplate at a concentration of 50 ng/ml. Detection of each peptide was performed separately with each guinea pig antiserum (anti-P2, anti-P3 and anti-P2/3) diluted at 1:200. The mean of absorbance values obtained are summarized in Figure 33 for coating with P2, P3 and only carbonate buffer as a negative control. Overall, the absorbance measurements provided coherent results as anti-P2 detected only P2, anti-P3 detected only P3 and anti-P2/3 detected both P2 and P3. However, absorbance values for wells coated with P3 were lower than with P2 and absorbance values for P2 and P3 detection with anti-P2/3 were lower than with the respective single peptide antiserum.

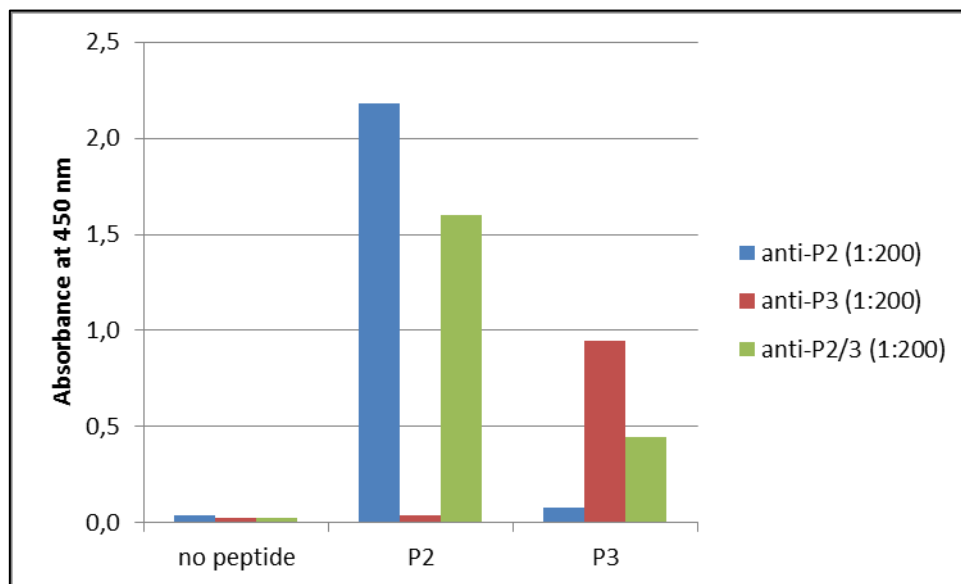


Figure 33: ELISA results for coating with P2 and P3 (50 ng/ml) and only carbonate buffer as negative control. Primary antibody was anti-P2, anti-P3 or anti-P2/3 guinea pig antiserum. Secondary antibody: goat anti-guinea pig IgG-HRP at 1:5000.

CHAPTER 2 – Yellow fever virus NS1 Detection - Results

In order to test the effect of antiserum dilution, further ELISA experiments were performed with peptide P2 and P3 coated simultaneously and individually on a microplate at 50 ng/ml. Peptides P2 and P3 were detected with serial dilutions (from 1:200 to 1:3200) of anti-P2, anti-P3 or anti-P2/3. Absorbance values from this testing are plotted for each peptide/antiserum couple in Figure 34. Values for P3 detection are lower than with P2 as observed in the previous experiment (Fig. 33). For an antiserum dilution of 1:200, absorbance values obtained for all three antisera were ranging from 2.8 to 3.5 but absorbance values decreased at a different rate for each serum as serum dilution increased. For the highest antiserum dilution (1:3200), absorbance values for detection with anti-P3 were lower than 1, for detection with anti-P2/3 values dropped under 0.5 while for detection with anti-P2, absorbance values remained close to 2. For P2 detection results, a linear relationship could be observed between absorbance value and anti-P2 concentration for absorbance values below 3.

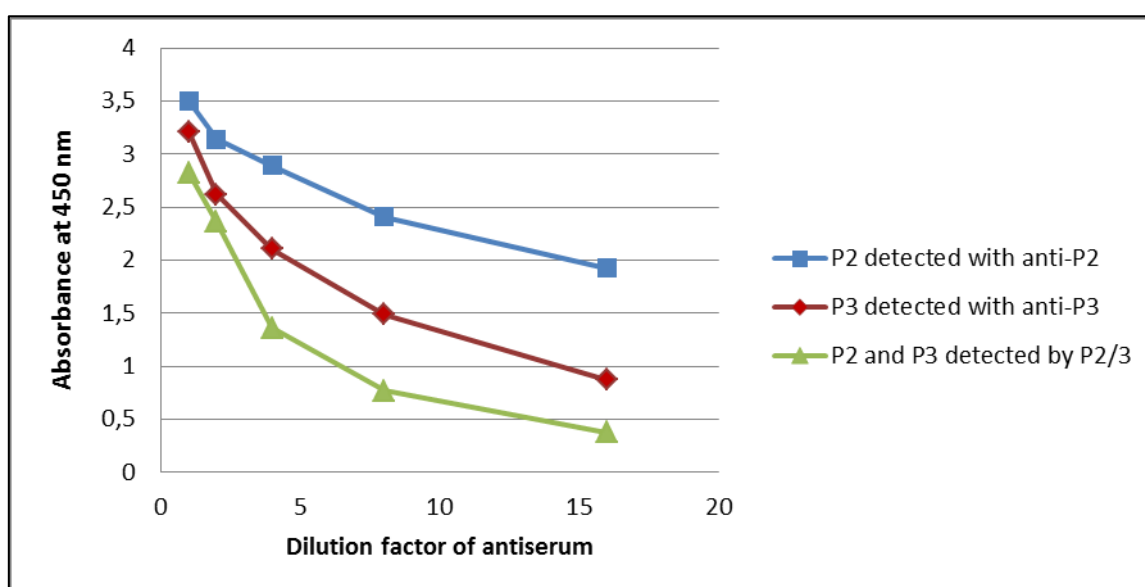


Figure 34: ELISA results for coating with peptide at 50 ng/ml and peptide detection with serial dilutions of antiserum. Dilution factors of the antisera were considered starting from a dilution of 1:200. Anti-P2 was used to detect P2, anti-P3 to detect P3 and anti-P2/3 to detect both P2 and P3. Secondary antibody: goat anti-guinea pig IgG-HRP at 1:5000.

After characterization of the newly produced antisera in IFA, WB and preliminary ELISA for peptide recognition, it was investigated whether an anti-NS1 ELISA could be developed using the rabbit and guinea pig polyclonal antisera. Next ELISAs were performed with cell supernatant tested positive for NS1 in WB as a positive control for NS1 detection. For all ELISAs, NS1 positive and negative samples were tested with and without denaturing treatment in order to test whether the anti-NS1 sera detected more effectively the NS1

CHAPTER 2 – Yellow fever virus NS1 Detection - Results

protein in a native or unfolded conformation. Denaturation was performed by heating at 60°C or 95°C for 30 minutes or addition of detergent (1% SDS or 0.1% Tween).

Several ELISA constructions for NS1 detection were tested with different combinations of antiserum as listed in Table 12 (§B.2.8 of this chapter). The absorbance results for test n°1, 2 and 3 are pictured in Figure 35 in graphs 1), 2) and 3) respectively. These three sandwich ELISAs were performed with anti-P1 as capture antibody and the three different guinea pig antisera as detection antibodies. Results from the three ELISAs provided false positive results with all antiserum combinations as absorbance values were positive for both the positive control (NS1 positive cell supernatant) and negative controls (negative cell supernatant and dilution buffer). False positive results were observed with all samples regardless of sample preparation. Results for samples denatured with heating at 60°C or addition of 1% SDS or 0.1% Tween are presented separately in each graph of Figure 35. Additional testing was performed with heating at 95°C for 30 minutes with and without detergent denaturation. Like the previous testing results, these additional tests provided false positive results regardless of the sample preparation (data not shown).

False positive results were already observed with ELISA tests using the rabbit antiserum for both capture and detection. To avoid such false positive results, the guinea pig antiserum was therefore used for detection and the rabbit antiserum for capture. Moreover, a pre-absorbed goat anti-guinea pig antibody was used to reduce the risk of unspecific binding between secondary antibodies and capture antiserum. Despite these precautions, false positive results and unspecific binding of antibodies could not be avoided.

Therefore, an ELISA was performed to check for the presence of unspecific binding between the pre-absorbed anti-guinea pig secondary antibody and the rabbit antiserum. Results from this test revealed that the anti-guinea pig antibody does bind to the rabbit antiserum although it is pre-absorbed (data not shown).

In order to bypass unspecific binding between secondary and capture antibodies, ELISA plates were coated directly with YFV-infected cell supernatant and detection was performed with anti-NS1 antisera as primary antibody and anti-guinea pig IgG-HRP as secondary antibody (test n°7, 8 and 9 of Table 12 in §B.2.8). Test n°7 corresponds to the detection of NS1 with the anti-P2 antiserum and results of this test are pictured in graph 4) of Figure 35. Absorbance values were all negative for positive and negative cell supernatants regardless of the sample preparation (denatured or not). The same negative results were observed for test n°8 and 9 for NS1 detection with anti-P3 and anti-P2/3 respectively.

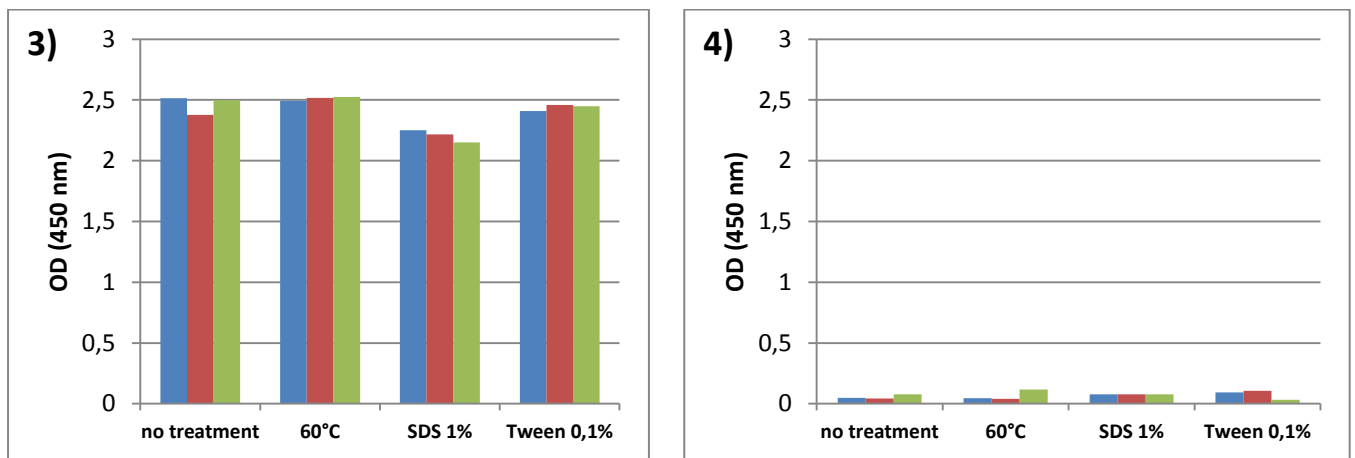
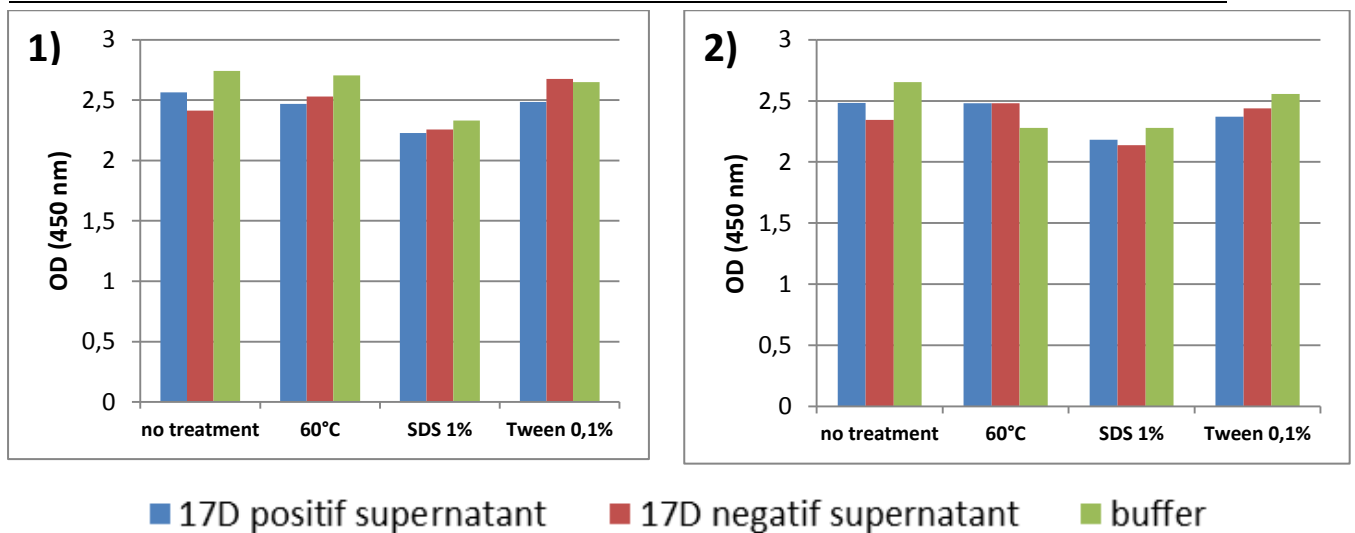


Figure 35: Absorbance results obtained for four different ELISA constructions all performed without treatment and with denaturing treatment (heating at 60°C, addition of 1%SDS or 0.1% Tween) of the tested samples which included NS1 positive cell supernatant (blue) as positive control and negative cell supernatant (red) and dilution buffer (green) as negative controls; Graphs 1) 2) and 3) correspond to the results of the sandwich ELISA tests n°1, 2 and 3 respectively (Table 12 in §B.2.8 of this chapter); Graph 4) corresponds to the results of ELISA test n°7 (Table 12 in §B.2.8 of this chapter) with direct coating of cell supernatant and detection of NS1 with anti-P2.

B.4 DISCUSSION

Serological methods are affordable diagnostic techniques that can easily be implemented in low-resource settings. However, accurate serological diagnosis of a flavivirus infection can be challenging, particularly in regions of the world in which several flavivirus co-circulate. Serological approaches, mostly based on IgM capture ELISA, are confronted to a high level of antigenic cross-reactivity among flaviviruses. Furthermore, they are not applicable during the early course of the disease as such indirect diagnostic methods detect

the immune response of the patient to infection and not the infectious agent itself. As the NS1 protein is secreted from flavivirus-infected cells, it was reasoned that this viral protein would be a suitable early diagnostic marker for flavivirus infections in patients and the use of the NS1 protein as a biomarker has been investigated for several flavivirus infections [120, 218-220]. Presently, NS1 detection has already proved to be a very useful tool for the diagnosis of acute dengue infections by providing a cheap and accurate diagnostic method in combination with detection of IgG and IgM antibodies [221, 222]. The possibility of using NS1 detection for the diagnosis of yellow fever infections has not been investigated yet. For this reason, this research project aimed to develop and characterize YFV-specific polyclonal antisera against the NS1 protein and to investigate the possibility of these antisera for diagnostic purposes for YFV NS1 detection.

The project was initiated by Nina Stock with the production of a polyclonal antibody against the YFV NS1 protein by immunizing rabbits with a peptide immunogen identified from the YFV NS1 protein. The obtained polyclonal antiserum, here referred as anti-P1, was able to detect specifically the YFV NS1 protein by Western blot and immunofluorescence assay [215].

A first experiment to test the use of the rabbit antiserum in ELISA was performed by coating the peptide P1 at several concentrations and test peptide recognition with anti-P1. Absorbance results indicated that the antiserum could detect less than 50ng/ml of peptide and that the antiserum could be used at a 1:500 dilution in further ELISA experiments. A further test using the rabbit antiserum as both capture and detection antibody revealed positive results for the NS1 positive cell supernatant but also for the negative cell supernatant. In this case the secondary antibody, a goat anti-rabbit IgG-HRP, was suspected to detect both the capture and detection antibody thus providing false positive results.

In order to avoid such false positive results, further polyclonal antisera against YFV NS1 protein were produced by immunization of guinea pigs with selected synthetic peptides (§B.3.1). Three different antisera (anti-P2,-P,-P2/3) were obtained and were characterized by testing in IFA (§B.3.2) and Western blot (§B.3.4).

IFA results demonstrated a good reactivity of the guinea pig anti-P2 and anti-P2/3 sera for the specific detection of Vero E6 cells infected with YFV-17D. Both antisera demonstrated a fluorescence comparable to the one observed for the rabbit antiserum (anti-P1) even though the double immunized antiserum (anti-P2/3) revealed a slightly weaker specific signal. The third guinea pig antiserum, anti-P3, provided the least satisfying result, showing a very weak specific signal for the detection of YFV NS1 protein. Such differences of reactivity among the produced antisera can be explained by several factors including differences of immunogenicity of the selected peptides; differences in accessibility of the NS1 protein

binding sites for the produced antisera; differences of binding affinity and/or differences in the immune response of the immunized animals.

IFA tests were also performed with all antisera to test for cross-reactivity with other flaviviruses including all four dengue serotypes, West Nile, Japanese encephalitis and tick-borne encephalitis viruses. These tests revealed no cross-reactivity of the produced antisera with any other of the tested flaviviruses which is a prerequisite for any application in diagnostics. However cross-reactive reactions in other types of tests cannot be excluded as the reactivity of the antisera can differ from one application to the other.

All antisera indicated a low neutralizing effect against YF-17D virus which remained under the diagnostic threshold of 1:10 (§B.3.3). A neutralizing effect of NS1 antibodies is not necessarily expected as NS1 is not a component of the virion and antibodies against NS1 cannot neutralize the virion itself. Nevertheless, several studies on flaviviruses demonstrated that anti-NS1 monoclonal antibodies were able to provide protection to mice against a lethal viral challenge [223, 224]. The observed mechanism of protection was shown to involve the complement mediated lysis of infected cells through the binding of cell surface-bound NS1 [225, 226]. However, further studies indicated that protection did not always correlate with the ability of the Mab to fix complement [227, 228] and studies on West Nile virus demonstrated that antibody recognition of cell surface-associated NS1 triggers Fc- γ receptor-mediated phagocytosis and clearance of infected cells [229]. The neutralizing effect of an anti-NS1 antibody obtained by peptide immunization may be dependent on whether the immunogen peptide is localized in a region of the NS1 protein which induces such Fc- γ receptor or complement-mediated lysis of infected cells.

To characterize the newly produced antisera in Western blot and ELISA, a positive control for YFV NS1 protein was required. For this purpose, a stock of protein solution was produced from supernatant of Vero cells infected with YFV-17D which was confirmed positive for the presence of YFV NS1 protein by WB with the already characterized rabbit anti-NS1 sera.

All antisera produced in guinea pigs were able to detect YFV NS1 protein in WB after protein separation under denaturing conditions revealing a positive signal at circa 45 kDa corresponding to the size of the NS1 protein [120] (§B.3.4). Comparing the reactivity of each antiserum, similar variations of signal intensity were observed than during characterization of the antisera in IFA. The guinea pig anti-P2 serum demonstrated a clear signal comparable to the one observed with the rabbit anti-P1 antiserum while the anti-P3 antiserum provided a very weak signal. Interestingly, the anti-P2/3 serum obtained by double immunization, demonstrated a slightly weaker signal than the anti-P2 serum obtained with a single peptide immunization. Immunization with two peptides simultaneously is expected to produce an

antiserum more reactive against the whole antigen than with single peptide immunization. Nevertheless this increased signal intensity was observed neither by IFA nor by WB testing. This might be explained by the very weak reactivity produced by the immunization with P3 which may have impaired the overall immune response of the guinea pig after double immunization or by the fact that the immune system of the two guinea pigs used for single or double immunization responded differently.

A kinetic of the daily production of NS1 protein in the cell supernatant of YFV-infected cells over a period of 10 days was performed by using anti-P1 and anti-P2 for NS1 detection in WB as these two antisera performed the best in previous IFA and WB testing. Results of the both WB experiments revealed that NS1 protein appeared at day 4 after infection and then constantly increased until the end of the kinetic (Fig. 31.A and B). The appearance of NS1 at the fourth day after infection correlates with previous findings on West Nile infections [212]. Nevertheless, secretion of the NS1 protein could probably be detected earlier with ELISA techniques as the detection limit of ELISA is lower than for WB as described in studies on NS1 detection by ELISA during dengue, West Nile or Japanese encephalitis infections which revealed a detection limit of circa 1 ng/ml [207, 212, 220]. Concerning the duration and the quantification of NS1 secretion, no conclusion can be reached based on our findings as the amount of NS1 protein was accumulating in the cell supernatant. Moreover, at this stage, it is not possible to differentiate between the secreted hexameric form of NS1 and the intracellular form of NS1 released from infected cells undergoing lysis. However, this experiment demonstrates the secretion of NS1 protein from YFV-infected Vero cells in an early stage of infection. Hence, it would be of great interest to conduct animal experiments in order to investigate the kinetic of NS1 secretion in YFV-infected animals and thus confirm the potential of NS1 detection as a diagnostic tool.

Preliminary ELISA results proved that all anti-NS1 sera at a 1:500 dilution could detect their respective peptide immunogen coated on a microplate at a concentration of 50 ng/ml. Absorbance values decreased at different rates for each antiserum as the antiserum concentration decreased starting from a dilution of 1:200 (Fig. 34). Detection with anti-P2 serum revealed a lower decrease of absorbance values as the serum concentration decreased than detection with anti-P3 and anti-P2/3. Moreover, detection with anti-P2 serum demonstrated a linear relationship between absorbance value and anti-P2 concentration. Therefore, preliminary ELISA results revealed that the anti-P2 serum is the most suited of the guinea pig serum for further development of a quantitative detection method for YFV NS1. Lower absorbance values observed with anti-P3 may be explained by a lower quality of the lyophilized P3 peptide or a lower affinity and/or accessibility of the antisera to peptide P3. These results are in accordance with the WB and IFA results as the anti-P2 antiserum also provided the most satisfying results in these tests.

CHAPTER 2 – Yellow fever virus NS1 Detection - Discussion

Further ELISA testing based on the sandwich ELISA format (Fig. 26.B) was performed with rabbit or guinea pig antiserum coated on the plates as capture antibody and cell supernatant positive for NS1 used as target protein. Rabbit antiserum was used as detection antibody when guinea pig antiserum was used for capture and vice versa. ELISA results with the several combinations of capture and detection anti-NS1 antiserum all provided false positive results revealing absorbance values over 2 for NS1-positive cell supernatant and also for the negative controls which included negative cell supernatant and dilution buffer. All samples tested for NS1 detection were tested in parallel with and without denaturing treatment in order to test whether the antisera detected more effectively the NS1 protein in a native or unfolded conformation. Denaturing treatment included heating at 60°C or 95°C for 30 minutes and addition of detergent (1% SDS or 0.1% Tween). These additional denaturation steps performed on the samples before testing in ELISA did not provide improved results compared to testing in native conditions (Fig 35. Graphs 1, 2 and 3).

The use of antisera of two distinct species (rabbit and guinea pig) for capture and detection of the NS1 protein did not prevent the appearance of false positive results. The use of pre-absorbed secondary antibodies to avoid unspecific binding between capture and secondary antibodies could neither avoid the appearance of false positive results. A specificity test could reveal that the anti-guinea pig secondary antibody was binding to the rabbit antiserum even though the secondary antibody had been cross adsorbed using rabbit immunosorbents to remove cross reactive antibodies.

To avoid binding of secondary antibodies to the capture antiserum, direct detection of NS1 protein was tested with each anti-NS1 sera by coating YFV-infected cell supernatant directly on the ELISA plates. All test results were negative for both positive and negative controls. Sample denaturation with heat and/or detergents was also experimented in this ELISA format but all absorbance values remained null for positive and negative cell supernatants regardless of sample preparation (Fig 35. Graph 4).

Considering IFA results for NS1 protein detection were positive as well as results in Western blot, it can be deduced that detection problems in ELISA were not caused by the absence of binding between the antisera and the NS1 protein but rather related to the way an ELISA is constructed. In contrast to an IFA or WB assay, a sandwich ELISA requires antibodies both for capture and detection of the target antigen and sufficient affinity of the capture antibody to the antigen is necessary in order to maintain binding of the protein during the washing steps. In order to avoid false positive results, the capture and detection antibodies used should not bind to each other and the secondary antibody should not bind to the capture antibody. This problem can be avoided by coupling the detection antibody directly to the HRP enzyme thus avoiding the use of a secondary antibody which could bind

to the capture antibody. Direct coupling of purified IgG from the rabbit antiserum to the HRP enzyme was performed by Nina Stock during her PhD work [215] but testing results were not satisfying as the concentration of anti-NS1 antibodies dropped dramatically after the purification and coupling process. In order to further investigate the possibility of developing a YFV NS1 capture ELISA and avoid any unspecific binding between the secondary antibody and the capture antibody, IgG purification and HRP coupling of the guinea pig antiserum could be performed for use as a detection antibody.

However, the use of HRP-coupled secondary antibodies may still not be sufficient to avoid false positive results as these may rather be linked to the low specificity of polyclonal antibodies. For this study, polyclonal antibodies were selected to develop an ELISA as large quantities of polyclonal antibody are relatively quick and inexpensive to produce compared to monoclonal antibodies (Mabs). For general research applications, the advantages of polyclonal antibodies typically outweigh the few advantages that Mabs provide. The production of polyclonal antibodies was therefore considered the most appropriate approach for a first proof of principle in regard to the development of an ELISA for YFV NS1 detection. However, polyclonal antibodies are less specific than Mabs as they consist of a complex mixture of antibodies that differ in their affinity for the antigen. This non-specificity can be an advantage as polyclonal antibodies are capable of recognizing multiple epitopes of the target antigen which can lead to a higher affinity of the antibody preparation to the target antigen. However, this low specificity can also be a disadvantage in the development of a sandwich ELISA as the antiserum may bind to other components than the target antigen thus generating a high background and false positive results. In this case, the use of Mabs with high specificity may decrease background signals. In a polyclonal-monoclonal sandwich ELISA, often the polyclonal will be used as a capture antibody to attach a large amount of antigen and a monoclonal is used as the detection for specificity [206].

For this reason, the production of monoclonal antibodies has been planned based on the P1 and P2 peptides which we identified as efficient immunogens for the production of antibodies against YFV NS1 protein. Collaborators in France have planned the production of Mabs by immunization of mice with the P1 and P2 peptides. The Mabs should be available by end of 2014 and would allow the further development of a YFV NS1 capture ELISA.

In order to further investigate the possibility of developing a quantitative detection method for YFV NS1 protein, the availability of a purified and quantifiable source of YFV NS1 protein, such as a recombinant protein, would be of great value. For this study, cell supernatant of Vero cells infected with YFV-17D which was tested positive for YFV NS1 in Western blot was used as a positive control for YFV NS1 detection in ELISA. Positive controls composed of cell supernatant do not allow performing proper specificity testing as

the components of such samples are not well characterized. Sensitivity testing is also not possible with such samples as the amount of NS1 protein in the cell supernatant is not quantifiable. The development of most sandwich ELISAs involve the use of a recombinant protein based on the target antigen as a quantifiable and purified positive control suitable for specificity and sensitivity testing. Since YFV NS1 recombinant protein is not made available by the market of recombinant proteins or by research partners, its production has been planned and will be performed by Prof. Niedrigs' research team or ordered to a specialized company in the course of the year 2014.

The availability of a YFV NS1 recombinant protein and the production of mouse Mabs against P1 and P2 of YFV NS1 both represent significant and promising perspectives for the development of a novel ELISA-based quantitative detection method for YFV NS1 protein performing with the polyclonal antiserum developed and characterized in this study. For the time being, the rabbit anti-P1 and guinea pig anti-P2 sera can be successfully exploited in IFA and WB assays for the detection of YFV NS1 protein.

As there are no commercially available antibodies against the YFV-NS1 protein, the availability of such detection tools are of great value. The development of antibodies specific to the YFV-NS1 protein will allow investigating the role of NS1 in the pathogenesis and replication mechanisms during YFV infections and the potential use of the NS1 protein as a diagnostic marker for early YFV infections. Such advancements could have great implications in the study of flavivirus infections and very useful applications in field diagnostics potentially enabling an accurate and affordable diagnosis of YFV infections including in low-resource settings and remote endemic areas.

CHAPTER 3 DEVELOPMENT OF TOOLS FOR THE LIVE-CELL IMAGERY OF YELLOW FEVER INFECTIONS

A INTRODUCTION

To date, the disease mechanisms of yellow fever are poorly understood and have not been the subject of modern clinical research partly as a result of the occurrence of YF cases in remote areas without access to modern medical and laboratory facilities [129]. Since several years, the vaccine strain (YFV-17D) is being used as a model system for the study of all flaviviruses in order to identify and characterize components involved in viral pathogenesis and replication. By studying this model system, new insights may be acquired to understand functional significance of RNA replication, polyprotein processing, virus-host interaction and virion assembly and maturation of all flaviviruses. Better comprehension of all these mechanisms would be of great value as there is still no specific therapy available for YF and other flavivirus diseases.

Mechanisms of viral protein transport and replication in infected cells can be studied with site-specific fluorescent labeling of viral proteins. Recent advances in imaging techniques combined with the ability to visualize viral structural proteins by genetically encoded fluorescent tags have enabled to perform many studies on viral-cell interactions. The inclusion of such tags should not alter the biological functions of the protein and should allow studying the labeled proteins in intact cells [230]. The first genetically encoded fluorophore to be used was the jellyfish green fluorescent protein (GFP) which has been highly valuable for many years in understanding protein localization and dynamics in cell biology [231]. Numerous variants of GFP and other fluorescent proteins (xFP) were later developed providing a wide variety of new tools for biological imaging [232]. However, the relatively large size of these proteins (~27kDa) may result in the modification of the biological function of the target protein, thus limiting the applications of this approach. To reduce problems caused by xFP fusion, alternatives based on smaller genetically encoded tags have been developed such as AGT enzyme-based [233] or metal chelation-based strategies [234]. Another approach based on tetracysteine tag technology has been developed by Tsien and colleagues [235]. This method is based on the combination of a small genetically encoded peptide tag consisting of a tetracysteine (TC) motif and a small molecule probe, called FIAsh (Fluorescein Arsenical Hairpin). The general peptide sequence of the TC motif is Cys-Cys-Xaa-Xaa-Cys-Cys, in which Xaa is a noncysteine amino acid. Affinities in vitro

CHAPTER 3 – Introduction

and detection limits are optimized with Xaa-Xaa = Pro-Gly suggesting the preferred peptide conformation is a hairpin [236]. The FIAsh molecule is membrane-permeable and non-fluorescent. However, when specifically bound to the TC motif, it becomes highly fluorescent (Fig. 36). The specific tag can be genetically inserted into target protein sequences, so that the cells start expressing TC-containing proteins. Upon treatment of these cells with the FIAsh reagent, this molecule passes the cell membrane through diffusion and binds over four disulfide bridges specifically to the TC motif of the protein, activating the fluorescent of the complex [230, 235].

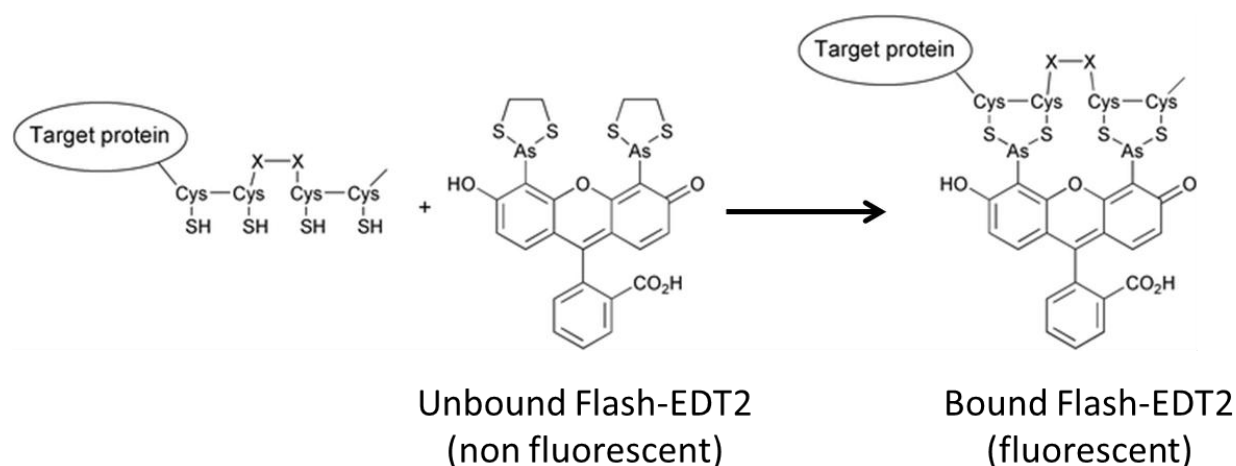


Figure 36: Structure of the fluorescein derivative, FIAsh-EDT2, which becomes fluorescent when bound to the peptide sequence CCXXCC. Source: Adams et al, 2008 [237]

Advantages of this technique are the small size of the peptide tag as well as the small size of the FIAsh molecule. Furthermore, it offers temporally controlled labeling, as FIAsh can be applied to the cells, which express the marked proteins at any time. Together with the property of FIAsh to pass cell membranes, this technique offers the possibility to investigate protein dynamics in living cells in real time. This technique has been used successfully to label and visualize the proteins of several viruses such as HIV, influenza and Ebola virus in living cells [238-241].

The objective of this project is to study the pathogenesis of YFV infections by live cell imaging microscopy through the fluorescent labeling of viral proteins of the 17D vaccine strain by using the tetracysteine tag technology. This project was initiated prior to this PhD work by Nina Stock and Panchali Roy Chowdhury, both students at that time in the research group of Prof. Niedrigs at the Robert Koch Institute [215, 242]. As part of their work, several insertion sites in the E- and the C-protein of YFV-17D have been chosen in order to avoid any modifications in the functionality of the tagged-proteins. As the structure of the E- and C-

protein of the YFV have not been determined by X-ray crystallography until now, the choice of insertion sites were based on the protein structure of other flaviviruses which all share common molecular and structural features. For the E-protein, the choice of three insertion sites was based on the crystal structure of the West Nile virus envelope glycoprotein [110] and for the C-protein, the choice of two insertion sites was based on the solution structure of dengue virus capsid protein [243].

Insertion sites selected for the tetracysteine (TC)-tag in the E-protein were:

- 17D-E1: between base 1120 and 1121 in domain I
- 17D-E2: between base 1600 and 1601 in domain II
- 17D-E3: between base 1378 and 1379 in domain I

For the C-protein, the selected insertion sites were:

- 17D-C1: between base 232 and 233 between domain α 1 and α 2
- 17D-C2: between base 334 and 335 between domain α 3 and α 4

To construct these five 17D clones we used a full-length infectious cDNA clone of the vaccine strain YF-17D named pACNR-FLYF-17D, which contains the entire YFV-17D sequence in a pACNR1181 plasmid. This plasmid was provided by Dr. Beate Kümmerer of the Bernhard Nocht Institute for Tropical Medicine in Hamburg and was constructed and described by Bredenbeek and colleagues [244]. The pACNR-FLYF-17D plasmid has a size of 13.451 kb and contains a SP6 promoter and a gene for ampicillin resistance (Fig. 37). Transcribed RNA of the plasmid resulted in a virus which exhibited growth kinetics, plaque morphology and proteolytic processing similar to the parental virus in cell culture [244].

Fragments of 1981 bp of the YFV-17D genome including the TC-tag in one of the insertion sites in the E or C protein were provided by the GeneArt® Plasmid Construction service and cloned into the pACNR-FLYF-17D plasmid. The cloning process was successful for all 17D clones except for the 17D-E2 clone which was not used in further experiments [215].

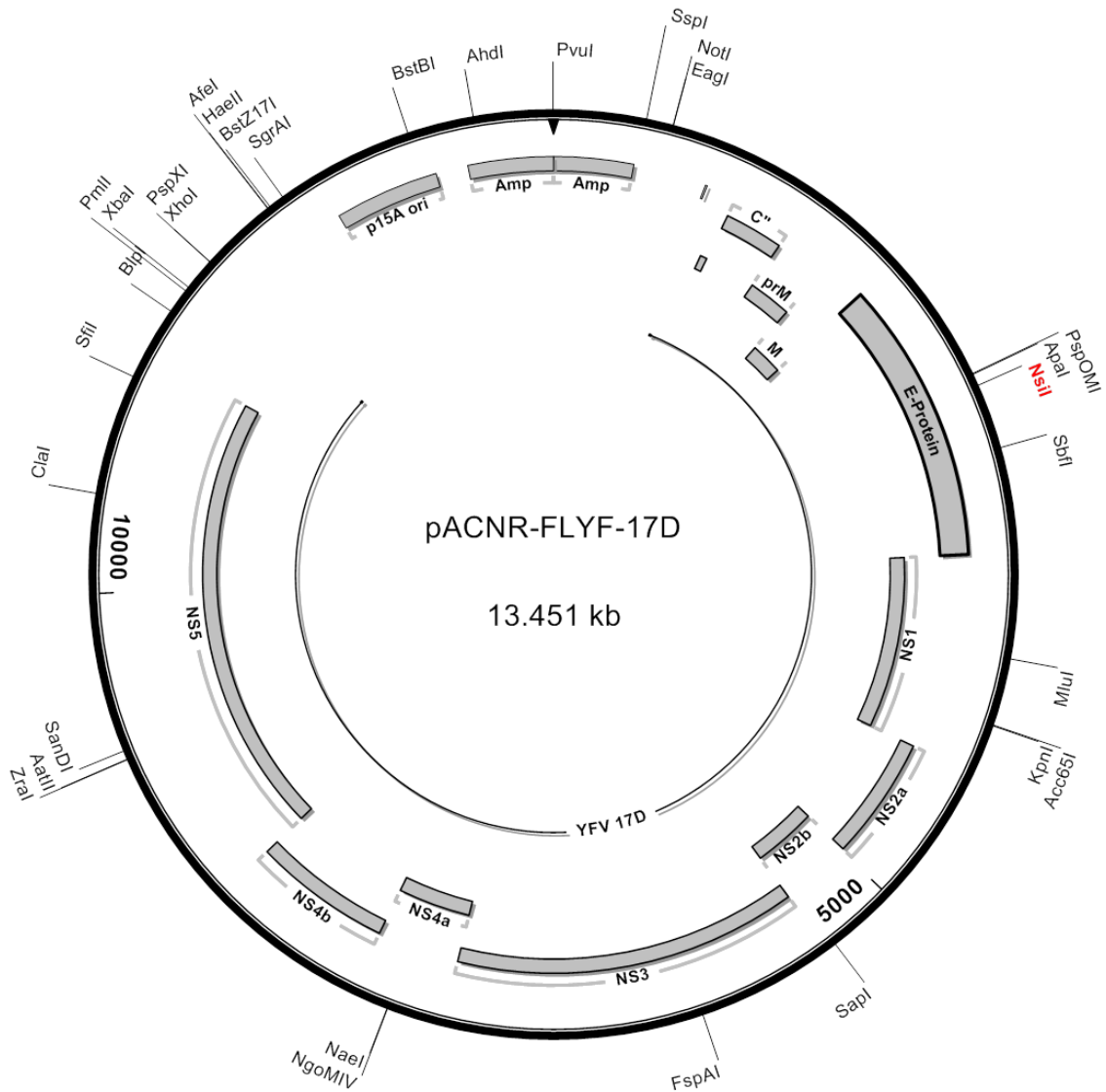


Figure 37: Schematic representation of the pACNR-FLYV-17D plasmid used for the construction of TC-tagged clones.

As part of this project on the fluorescent labeling of viral proteins of the YF-17D virus, the objective of the last chapter of this PhD dissertation was to investigate the potential use of the four YFV-17D clones (17D-E1, -E3, -C1 and -C2) previously produced as tools for the study of the pathogenesis of YFV infections in live cell imaging microscopy. More specifically, the successive objectives were to:

1. Check by sequencing if the four clones obtained each contained the correct genomic sequence with the TC-tag at the appropriate insertion site
2. Test whether the plasmid constructs were able to produce infectious clones after in-vitro transcription and transfection in Vero E6 cells

3. Compare whether the growth kinetics and plaque morphology produced by the obtained infectious clones were similar than for the parental virus
4. Test whether the 17D clones were able to produce fluorescence when put into contact with the biarsenical compounds from the TC-FIAsh™ II In-Cell Tetracysteine Tag Detection Kit (Invitrogen)
5. Use the produced 17D clones in live cell imaging microscopy for the study of the pathogenesis of YFV infections

The objectives 1 and 2 were completed as a joint work with Nina Stock and the corresponding results were presented in her PhD dissertation [215]. The methods and results parts corresponding to these two objectives are also presented in the following “Methods” chapter (§B.1 and §B.2) and “Results” chapter (§C.1 and §C.2).

B METHODS

B.1 SEQUENCING OF THE CDNA PLASMID CLONES

B.1.1 Polymerase chain reaction (PCR)

For amplification of the whole pACNR-FLYF-17D original plasmid, 12 PCRs were performed with the primers listed in Table 14. For the cloned plasmids, only the PCR N°1, 2 and 3 were performed in order to verify that the TC-tag was inserted at the appropriate position in the C- and E- protein. Each PCR reaction was performed using the Platinum Taq polymerase in a total volume of 20 µl with 1 µl of DNA template (Table 15). Once PCR was completed, the products were analyzed by gel electrophoresis.

Table 14: List of oligonucleotides used for PCR

PCR N°	Genome region	Forward primer	Reverse primer	Length (bp)
1	5'-End	U1s	U1as	800
2	M	U1cs	YF-Erev	1074
3	E	Unifor	E2as	1385
4	NS1	YF-Efor	3666as	1264
5	NS2	3597s	5375as	1789
6	NS3	NS3x1	NS3x2	815
7	NS3/NS4	98s	U7as	988
8	NS4	100s	U9bas	1343
9	NS4/NS5	U9cs	150as	1775
10	NS5	FU1	FD3	1084
11	3'-End	176s	176as	947
12	3'-Rest	U12s	U12as	757

Table 15: Reagents mixture for one PCR reaction and cyclers conditions

Reagents	Volume [μ L]	Time	T [$^{\circ}$ C]	Nr Cycles
dest. Water	9.6	5 min	94	40
10 x Taq-Buffer	2.0	30 sec	94	
dNTPs (10 mM)	2.0	30 sec	56	
MgCl ₂ (50 mM)	1.2	120 sec	72	
Forward Primer (10 μ M)	2.0	10 min	72	
Reverse Primer (10 μ M)	2.0			
Platinum®Taq (5 U/ μ L)	0.2			
DNA	1.0			
Total volume	20			

B.1.2 Agarose gel electrophoresis

Agarose gel electrophoresis is the most simple and common method for separation and analysis of DNA and their fragments based on their size. Gels were prepared in 1X TBE buffer with 1% agarose (w/v) and 0.025% ethidium bromide as a DNA staining dye. DNA samples were loaded on the gel with Gel Loading Dye, Blue (6X) and gel electrophoresis was run for 1h at 100 volts. After sufficient migration, the gel was observed under ultraviolet light and the size of DNA fragments determined by comparison with a molecular weight size marker (1 kb DNA Ladder, New England Biolabs).

B.1.3 Gel extraction for purification of DNA fragments

After gel electrophoresis, silica-membrane-based purification of DNA fragments from the gel was performed with a QIAquick Gel Extraction Kit from Qiagen according to the manufacturers' instructions. DNA was eluted in 50 µl H₂O and stored at -20°C.

B.1.4 Sample preparation for DNA sequencing

In order to determine the precise order of nucleotides, the chain-termination method, also called Sanger method, was applied to the purified DNA fragments. To sequence our DNA strands and plasmids, an automated dye-terminator sequencing method was performed by using the "BigDye® Terminator v3.1 Cycle Sequencing Kit" from Applied Biosystem. Dye-terminator sequencing utilizes labeling of the chain terminator ddNTPs, which allows sequencing in a single reaction. After samples are loaded onto the system's vertical gel system, they undergo electrophoresis, laser detection, and computer analysis. Data output is presented as fluorescent peak trace chromatograms. Table 16 indicates the conditions (reaction mixture and cyler conditions) for sample preparation before DNA sequencing. Sequencing was performed by the RKI internal sequencing service on a 3500 xL Dx Genetic Analyzer (Applied Biosystems).

Table 16: Reaction mixture for sequencing and cyler conditions

Reagents	Volume [µL]	Time	T [°C]	Nb. Cycles
dest. Water	5.5	2 min	96	25
5 x AVI buffer	2.0	10 sec	96	
BigDye 3.1 mix	1.0	5 sec	56	
Primer (10 µM)	0.5	4 min	60	
DNA template[10-20 ng]	1.0			
Total volume	10			

The sequences obtained were analyzed using the Lasergene SeqMan Pro® software (version 8.1.5) from DNASTAR, Inc. Each region of the DNA sequences was analyzed based on the sequencing results of at least two overlapping PCR products in order to obtain high sequence coverage and determine the correct base sequence.

B.2 PREPARATION OF VIRAL RNA FROM cDNA CLONES AND TRANSFECTION OF CELLS WITH THE VIRAL RNA

The pACNR-FLYF-17D original and cloned plasmids were first linearized by restriction reaction with the XhoI enzyme (§B.2.1). Subsequently, the linearized DNA was purified (§B.2.2) and in vitro-transcribed to obtain viral RNA (§B.2.3) before transfection of the obtained RNA in Vero E6 cells (§B.2.6).

B.2.1 Linearization of the cDNA plasmids

The original and cloned cDNA plasmids were linearized with the restriction enzyme XhoI from New England Biolabs (NEB) according to the manufacturers' instructions with BSA and Buffer 4 solutions delivered with the enzyme. Proportions of each reagent required to digest 2 µg of cDNA are listed in Table 14.

Table 14: Reaction mixture for restriction reaction with XhoI

Reagents	Volume [µL]
cDNA (500 ng/µl)	4
BSA (X100)	0.5
Buffer 4 (x10)	5
XhoI (20 U/µl)	1
dest. Water	39.5
Total volume	50

B.2.2 DNA purification

DNA was purified from the restriction enzyme mixture with the MSB® Spin PCRapace Kit (STRATEC Molecular GmbH) which can be used for PCR reaction mixture or restriction digestion mixture of DNA fragments from 80 bp to 30 kb in order to remove dNTPs, primers, enzymes, additives and salts from the DNA samples. DNA purification was performed according to the manufacturers' instructions. Purified DNA was eluted in 50 µl H₂O and stored at -20°C.

B.2.3 In-vitro transcription of the cDNA into viral RNA

In-vitro transcription was performed in order to obtain viral RNA from the linearized DNA obtained after restriction of the cDNA from each plasmid constructs. In vitro transcription requires a purified linear DNA template containing a promoter, ribonucleotide triphosphates, a buffer system that includes DTT and magnesium ions, and an appropriate phage RNA polymerase necessary. In-vitro transcription was performed with an Ambion SP6

polymerase (Life Technologies). A Cap Structure Analog m7G(5')ppp(5')G from New England Biolabs was included in the reaction mixture for co-transcriptional capping with SP6 RNA polymerase for ribosome binding and translation. The reaction was performed in a total volume of 25 µl for 1h at 40°C with the reaction mixture listed in Table 15.

Table 15: Reaction mixture for in-vitro transcription of DNA

Reagents	Volume [µL]
dest. Water	2.75
10 x SP6-Buffer (Ambion)	2.5
DTT (10 mM)	2.5
rNTPs (2.5 mM)	5
Cap (m7G(5')ppp(5')G) (10 mM)	1.25
RNAse Out (40 U/µl)	0.5
SP6 polymerase (15 U/µL)	0.5
Linear plasmid DNA (75 ng/µl)	10
Total volume	25

B.2.4 Determining the concentration of nucleic acids solution

Measurement of the optical density of a solution at 260 nm is a simple and fast method to determine its concentration of nucleic acids. The amount of protein contaminants can be estimated from the ratio OD_{260 nm} /OD_{280 nm} and the calculation of nucleic acid can be adjusted for a most accurate measurement. The concentration of nucleic acid in a solution was measured by a BioPhotometer from Eppendorf with the use of ultra-micro cuvettes by using distilled water as a blank.

B.2.5 Cell counting

The number of cells in a suspension is estimated by direct microscopic measurement using a haemocytometer or Neubauer counting chamber. The haemocytometer is designed so that the number of cells in one set of 16 corner squares is equivalent to the number of cells x 10⁴ / ml.

B.2.6 Transfection of viral RNA in Vero E6 cells

Transfection is defined as the introduction of foreign nucleic acids into eukaryotic cells. Transfection of in vitro-transcribed YFV-17D RNA (see §B.2.3) was performed in Vero E6 cells in order to produce viral particles. Lipid-based transfection was performed with Lipofectamine™ 2000, a reagent commercialized by Invitrogen which increases the

CHAPTER 3 – Methods

transfection efficiency of RNA or plasmid DNA into in vitro cell cultures. Lipofectamine reagent contains lipid subunits that can form liposomes which entrap the nucleic acids and transport them through the cell membrane.

Cultivation of adherent Vero cells was performed as described in Chapter 2 (§ B.2.4) and cells were seeded in 6-well plates so that they were ready for transfection the next day with 70 to 90% confluence. Different concentrations of Lipofectamine™ 2000 were tested based on the manufacturers' recommendations. The standard protocol in Figure 38 describes the preparation of solution 1 and 2. Both solutions were then incubated separately for 5 min at room temperature, then mixed together and incubated for another 20 minutes at room temperature to form complexes. Meanwhile, the cell monolayer was washed twice with OptiMEM after what 500 µl of the transfection mixture was added to each well. After 4h of incubation at 37°C with 5% CO₂ during which the viral RNA entered the cells, the medium was replaced with fresh DMEM culture medium supplemented with 10% FBS, 1% penicillin, 1% streptomycin and 1% glutamine.

The original plasmid pACNR-FLYF-17D was used as a positive control for all transfections and RNA-free transfection solution was used as a negative control.

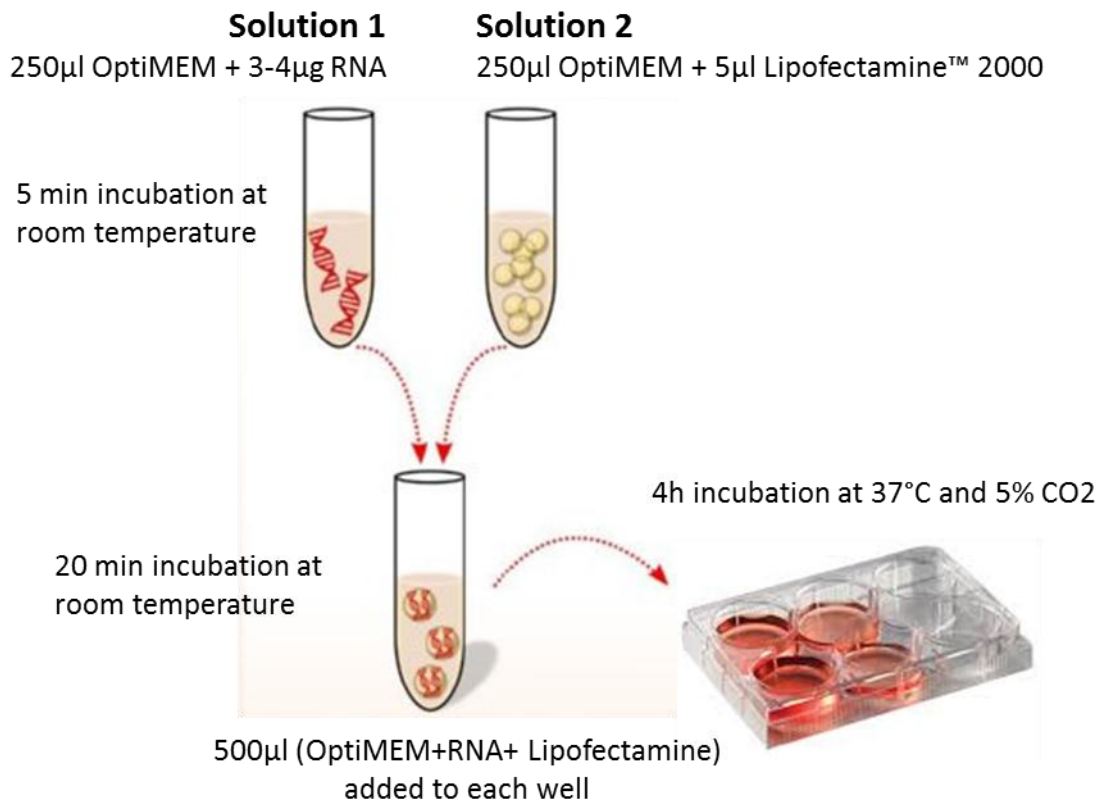


Figure 38: Schematic representation of the solution preparation for RNA transfection in Vero cells with Lipofectamine 2000.

B.3 MONITORING OF VIRUS PRODUCTION AFTER RNA TRANSFECTION

In order to verify the production of infectious viral particles after transfection of viral RNA in Vero E6 cells the production of viruses was monitored at day 3 and 6 after RNA transfection by real-time RT-PCR (§B.3.2), plaque assay (§B.3.3) and indirect immunofluorescence assay (§B.3.4).

B.3.1 Sampling procedure after transfection

The production of YFV-17D virus was monitored at day 3 and day 6 after RNA transfection. Two aliquots of 500 µl of cell supernatant were removed and stored at -80°C until use for testing in qRT-PCR as described in §B.3.2 or in plaque assay as described in §B.3.3. The cells were sampled in 500µl of supernatant, centrifuged at 4000 RPM for 3 minutes, resuspended in PBS and fixed on a slide for YFV detection in indirect immunofluorescence assay as described in §B.3.4.

B.3.2 Real-time reverse transcription polymerase chain reaction (RT-PCR)

Real-time RT-PCR testing was performed with the YFV-specific primers YFV FP/RP and probe YFV LNA2 in order to detect and quantify genomic RNA of YFV by using in-vitro transcribed RNA standards as described in § A.2.4 of Chapter 2 and by Weidmann and colleagues [131].

B.3.3 Viral titration by plaque assay

Plaque assay is the standard method to determine the concentration of infectious virus particles in a viral suspension. In principle, serial dilutions of the viral suspension are prepared and applied to a defined quantity of cells. CMC solution is added a few hours after viral infection to prevent further diffusion of the virus so that the virus can only spread from the infected cells to the adjacent cells. After a defined incubation time, plaques are formed in the cell monolayer as a result of the cytopathic effect of the virus. Each plaque is formed from a single infectious virion in the original suspension, thus allowing an accurate calculation of the virus titer. These plaques can be detected visually. The infectivity titer is expressed in PFU/ml and obtained by the following equation:

$$\text{Virus titer in PFU/ml} = \frac{\text{plaque number}}{\text{dilution} * \text{volume in ml}}$$

In the case of YFV titration, PS cells were used for viral infection and cultivation was performed as described in § B.2.4 of Chapter 2. A 10-fold serial dilution of viral suspension was prepared in dilution solution (L-15 medium with 5% FBS). Each well of a 24-well plate

was seeded with 200µl of PS cell suspension at 6×10^5 /ml and 200µl of virus dilution. For the negative control, the same amount of media was added to the well instead of the virus dilution. After 4 hours of incubation at 37°C, 400 µl of CMC overlay media (1.6% CMC in cell culture media) was added to each well. The plate was then incubated for 4 days at 37°C after which the media was removed from the well plate and cells are fixed with 3.7% formaldehyde for at least 15 minutes. Cells were then stained with Naphthalene black solution for 20 min and washed with tap water after staining. Once the plate has dried, plaques could be counted by naked eye.

B.3.4 Indirect immunofluorescence assay

To perform indirect immunofluorescence assay (IFA) after transfection, Vero E6 cells were scraped from cell culture wells and suspended in 500 µl of PBS. The cell suspension was transferred in an Eppendorf tube and centrifuged at 4000 rpm for 3 min in order to pellet the cells. Cells were resuspended in 50 µl of supernatant and 20 µl of cell suspension was dropped on a glass slide and let to dry out. The cells were then fixed for at least 10 min in cold acetone at -20°C. This process fixates the cells and also inactivates the virus.

To detect YFV-17D, the slides were incubated for 1h at room temperature with MAB6330 (mouse anti-YFV antibody [216]) primary antibodies diluted at 1:100 in 1x PBST. After 1h incubation, all slides were washed 3 times with PBST and let to dry. The glass slides were then incubated for 1h at room temperature in the dark with FITC labeled anti-mouse secondary antibodies diluted at 1:200 in 1 x PBST in order to detect bound primary antibodies. After the second incubation, slides were washed 3 times with PBST and let to dry. The slides were covered with ProLong® Gold Antifade Reagent with DAPI, a fluorescent dye which stains the cell nuclei, and then mounted with a glass cover slip. A fluorescence microscope was used to analyze the immunofluorescence of the secondary antibodies (FITC – green filter) and cell nucleus (DAPI – blue filter).

B.3.5 Preparation of virus stock

If test results were positive for the presence of infectious YFV-17D virus, the corresponding viral suspension was used to prepare a virus stock by infecting Vero E6 cells in a 150 cm² flask. For comparison and characterization of the modified viruses, a 150 cm² flask of Vero E6 cells were infected with the wild strain YFV-17D (RKI Reference charge 354/1) as well. Vero E6 cells confluent at 80% were infected with virus at an MOI of 1, incubated during 1h and then washed 2 times with PBS before fresh medium was added. After 8 days of infection, the cell supernatant was collected while the cells were frozen at -80°C for 5 minutes and then thawed, mixed to the supernatant and centrifuged at 4000 RPM for 15 minutes. This procedure allowed to break the cells and collect the viruses contained

inside the cells. A virus stock composed of 500 µl aliquots of viral suspension was stored at -80°C until further use and characterization.

B.4 VIRUS CHARACTERIZATION BY GROWTH KINETICS ON VERO CELLS

The modified viruses obtained by transfection of the TC-tagged YFV plasmids in Vero cells were characterized by comparing their growth kinetics to the native YF-17D virus. The kinetic were performed in 12-well plates, one plate was used per virus strain and one was left uninfected as a negative control. In each well, 1.5×10^5 cells were seeded and left to grow for 4h at 37°C with 5% CO₂. Cells were then infected with 1.5×10^3 PFU of virus per well corresponding to a MOI of 0.01. The viral suspension was incubated 1h at 37°C on the Vero cells after what the medium was removed, cells were washed with PBS and 2 ml of fresh culture medium was added to each well. The first harvest was performed at this time point considered as the starting point of the growth curve, T0. Further harvests were performed at 17, 24, 47, 71, 95, 119, 143, 168 and 191 hours after T0. All harvests were performed as described in Figure 39 and performed in duplicate for each virus.

The supernatants were removed and frozen in 3 aliquots of 500µl at -80°C until further testing by plaque assay and RT-PCR. Plaque assay for viral titration in the cell supernatants was performed as described in §B.3.3. Isolation of viral RNA of cell supernatants for further RT-PCR testing was performed with the “QIAamp ® Viral RNA Mini Kit” from Qiagen according to manufacturer’s instructions. RNA was eluted in 50 µl of Rnase-free H₂O and stored until further use at -80°C. Real-time RT-PCR for YFV RNA detection could then be performed as described in §B.3.2.

In order to quantify intracellular viruses as well, 350µl of RLT buffer with β-mercaptoethanol was added to each well and cells were scrapped on the bottom of the well. The resulting cell suspension was stored at -80°C until RNA extraction from cells with the Rneasy Mini Kit (Qiagen) performed according to the manufacturer’s instructions. RNA was eluted in 50 µl of Rnase-free H₂O and stored at -80°C until RT-PCR YFV RNA detection (§B.3.2).

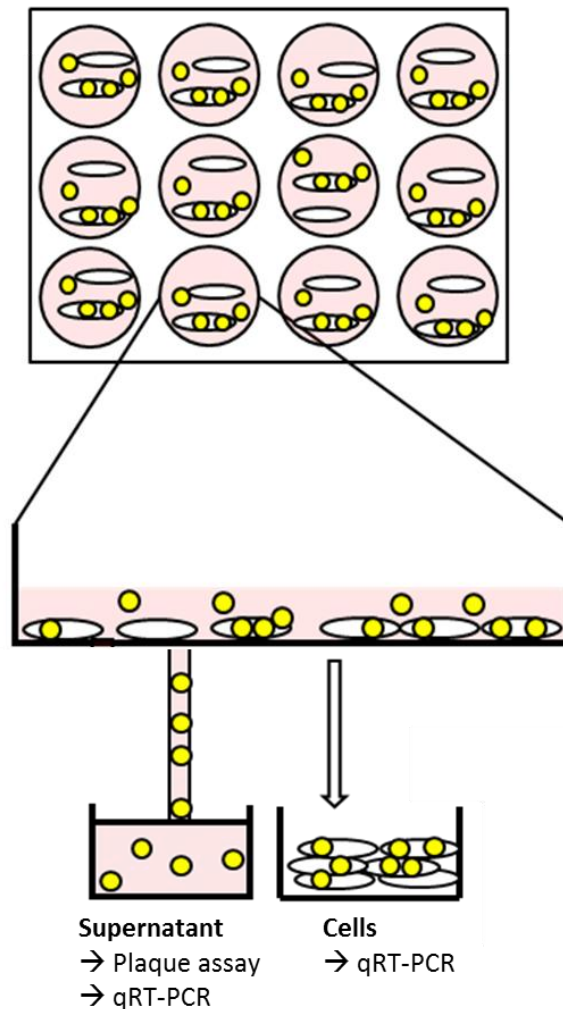


Figure 39: Schematic representation of a harvest for the growth kinetics of YFV-17D clones. The supernatants were removed and stored at -80°C until use in plaque assay (§B.3.3) or qRT-PCR (§B.3.2). The cells were scrapped, resuspended in RLT buffer with β -mercaptoethanol from the Rneasy Mini Kit (Qiagen) and stored at -80°C until further testing in qRT-PCR.

B.5 LABELING OF THE TC-TAGGED VIRUS WITH FLASH REAGENT

Vero E6 cells were cultivated as described in § B.2.4 of Chapter 2 and seeded in a 24-well plate with $5 \cdot 10^4$ cells per well. Cells were infected with the original YFV-17D virus and the TC-tagged virus at a MOI of 1. Dilution and cultivation medium was DMEM supplemented with 5% FBS. Cells were incubated overnight at 37°C and 5% CO_2 for virus absorption. Cells were then washed once with PBS and once with OptiMEM medium. The biarsenical reagent from the TC-FIAsh™ II In-Cell Tetracysteine Tag Detection Kit (Invitrogen) was diluted in OptiMEM medium and tested in several dilutions (1 μM , 2.5 μM , 5 μM and 10 μM). The reagent was incubated 30 minutes accordingly to the manufacturers' instructions. The cells

were then washed twice with 500 μ l of BAL wash buffer (250 μ M) and 500 μ l of OptiMEM was added to each well.

A fluorescence microscope was used to analyze the immunofluorescence of the FIAsH reagent binding to the TC-tagged viruses with the FITC filter set. The Vero cells infected with the parental and the TC-tagged YFV-17D were also incubated with a polyclonal antibody against the YFV C-protein (anti-YFV-C serum) produced in rabbits and characterized by Nina Stock in her PhD dissertation [215].

C RESULTS

C.1 SEQUENCING OF THE CDNA PLASMID CLONES

The first objective of this project was to confirm the correctness of the viral sequence of the YFV plasmids and in particular to check whether the TC-tags were inserted in the correct insertion sites. First of all, the full length YFV plasmid (pACNR-FLYF-17D) used for our constructions was entirely sequenced and its sequence was compared to the original sequence described by Dr. Kümmerer of BNI Hamburg. Sequencing results demonstrated some differences between the sequence of the previously described full-length YFV-17D plasmid and the sequence of the YFV-17D plasmid used to construct the cloned plasmids. Six point mutations were observed, one of which was not included in the YFV genome sequence and two others were silent mutations. The three last point mutations resulted in amino acid (aa) modifications at aa position 1065 in the YFV genome sequence placed in the NS2A protein where a valine was mutated in a methionine; at position aa 2439 in the NS4B protein where a glutamine was mutated in a lysine and at position aa 3484 in the NS5 protein where an alanine was changed to a threonine.

Secondly, the four plasmids containing the TC-tag in the E- or the C-protein (17D-E1, -E3, -C1 and -C2) were sequenced in the inserted DNA region in order to confirm that the TC-tag were inserted in the plasmid at the correct position. Sequencing results demonstrated no mutations between the TC-tagged plasmids and the original full length YFV plasmid used to construct the clones. Results also showed that all four TC-tag sequences were inserted at the correct position for each cloned plasmid.

C.2 TRANSFECTION OF CELLS WITH THE VIRAL RNA FROM CDNA CLONES

In order to transfect cells with viral RNA obtained from our YFV-17D plasmids, the plasmids were first linearized with the XhoI restriction enzyme (§B.2.1) and in-vitro transcribed with a SP6-polymerase (§B.2.2). Linearization of cDNA of all plasmids and in-

in vitro transcription of the linearized DNA into RNA was performed successfully although the initial amount of cDNA was very low. In fact the full length YFV plasmids are low copy plasmids and plasmid preparations could not yield cDNA concentrations over 16 ng/μl for 17D-C2 and 74 ng/μl for 17D-C1. After linearization of cDNA, purification of the resulting DNA and in-vitro transcription, the final RNA concentrations used for transfection ranged from 63 to 70 ng/μl. Transfection of Vero E6 cells was performed with 3.1 to 3.4 μg of this viral RNA as described in Figure 38 (§B.2.6).

C.3 MONITORING OF VIRUS PRODUCTION AFTER RNA TRANSFECTION

In order to verify the production of infectious viral particles after transfection, monitoring of virus production was performed at day 3 and 6 after transfection by RT-PCR (§B.3.2), plaque assay (§B.3.3) and IFA (§B.3.4).

RT-PCR results demonstrated the presence of YFV RNA in all samples including the negative control. As a negative control during transfection, supernatant from cells transfected with RNA-free transfection solution was sampled simultaneously than the RNA transfected cells. Based on the RT-PCR results, transfections with each of the modified YFV-17D RNA appear to have led to the production of viruses demonstrating YFV RNA concentrations ranging from 1.65E+08 genome equivalents (Geq) per ml for 17D-E1 to 2.52E+09 Geq/ml for 17D-C1 at day 3 after transfection (Table 16). RNA concentrations were not higher at day 6 after transfection and even appeared to be slightly lower than on day 3 after transfection .

Plaque assay results were negative for transfection with viral RNA of the YFV clones 17D-E1, 17D-E3 and 17D-C2 as plaque forming units (PFU) were not observed during testing of the corresponding cell supernatants. Only transfection with 17D-C1 RNA demonstrated the presence of plaque forming units by testing the cell supernatant in plaque assay which indicated a viral titer of 5.23E+05 PFU/ml at day 3 and 4.32E+05 PFU/ml at day 6 after transfection (Table 16). Similarly to the RT-PCR results, plaque assay results showed no increase in the number of infectious viral particles from day 3 to day 6 after transfection.

IFA results were consistent with plaque assay results, demonstrating the presence of YFV infection in Vero cells transfected with 17D-C1 RNA at day 3 and day 6 after transfection. After transfections with 17D-E1, 17D-E3 and 17D-C2 RNA, IFA demonstrated negative results regarding the detection of YFV-protein at day 3 and day 6. Figure 40 shows all IFA results at day 3 after transfection.

CHAPTER 3 – Results

Table 16: Real-time RT-PCR and plaque assay results after transfection of Vero E6 cells with viral RNA of the YFV clones 17D-E1, -E3, -C1 and -C2 at day 3 and day 6 after transfection. Vero cells treated with the transfection reagent but without viral RNA were cultivated simultaneously and used as negative control (NC).

Transfected clone	qRT-PCR results in Geq/ml		Plaque assay results in PFU/ml	
	Day 3	Day 6	Day 3	Day 6
17D-E1	1.65E+08	1.57E+08	0	0
17D-E3	3.21E+08	2.05E+07	0	0
17D-C1	2.52E+09	9.80E+08	5.23E+05	4.32E+05
17D-C2	2.53E+08	9.16E+07	0	0
NC	6.56E+03	4.86E+04	0	0

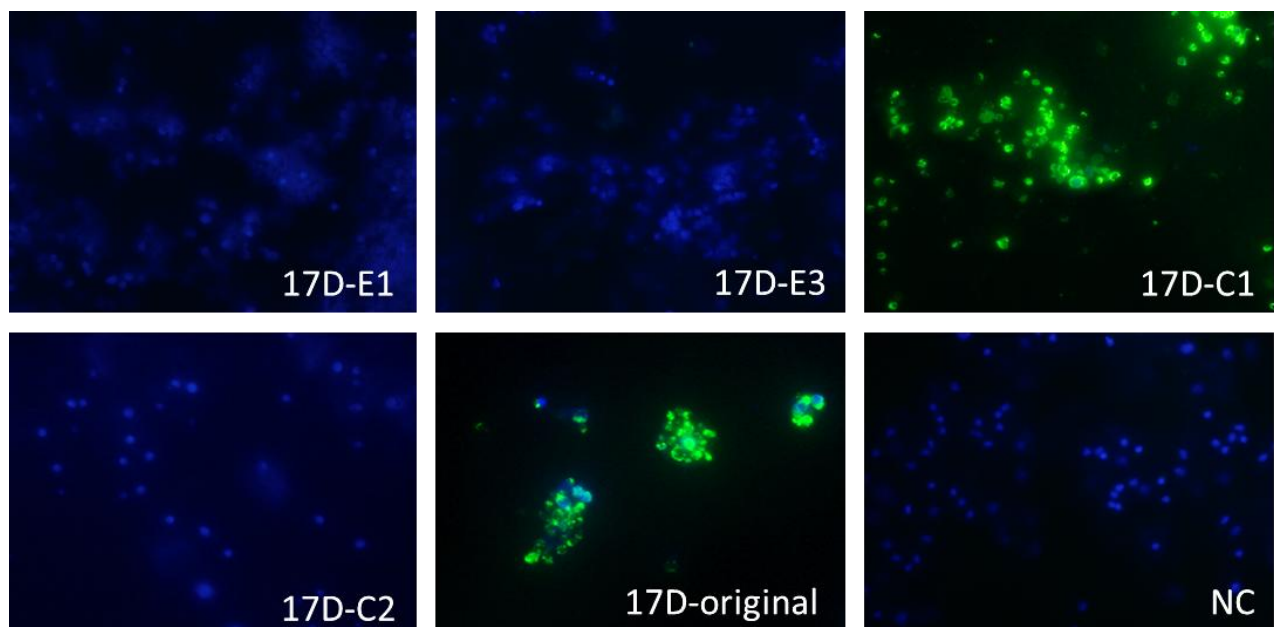


Figure 40: IFA images of Vero E6 cells transfected with viral RNA of the YFV clones 17D-E1, -E3, -C1 and -C2 at day 3 after transfection. The original 17D plasmid was used as a positive control for the whole transfection process. Vero cells treated with the transfection reagent but without viral RNA were cultivated in parallel and used as negative control (NC). The slides were covered with ProLong® Gold Antifade Reagent with DAPI, a fluorescent dye which stains the cell nuclei, and mounted with a glass cover slip. The secondary antibodies coupled with FITC were observed with the green filter and cell nucleus stained with DAPI with the blue filter. Image magnification: X10. These images have already been presented in the dissertation of Nina Stock [215]

C.4 VIRUS CHARACTERIZATION BY GROWTH KINETICS ON VERO CELLS

As the results of the previous paragraph showed, the 17D-C1 plasmid was the only one able to produce infectious virus particles after transfection in Vero cells. To examine whether the addition of the TC-tag in the virus sequence of the 17D-C1 clone altered viral replication, growth behavior or plaque morphology, the growth kinetics of the modified virus was compared to the parental YFV-17D. Growth kinetics of the parental YFV-17D strain and the 17D-C1 clone were performed *in vitro* and monitored daily for 8 days by qRT-PCR (§B.3.2) and by plaque assay (§B.3.3) as described by Figure 39.

The qRT-PCR results obtained for the detection of intracellular and extracellular viral RNA supernatants demonstrated very similar trends during infection with the modified and the parental YF-17D viruses (Fig. 41). The concentrations of Geq/ml in the cell fraction increased during infection until reaching over 10^9 Geq/ml after 191 hours of infection. For the detection of extracellular RNA, the amount of RNA was slightly lower during infection with the TC-tagged virus than with the parental virus. Although the curve for the clone shows a slight delay compared to the curve for the parental virus, both curves show an analogous progression. For the detection of intracellular RNA, both curves are coincident (Figure 41).

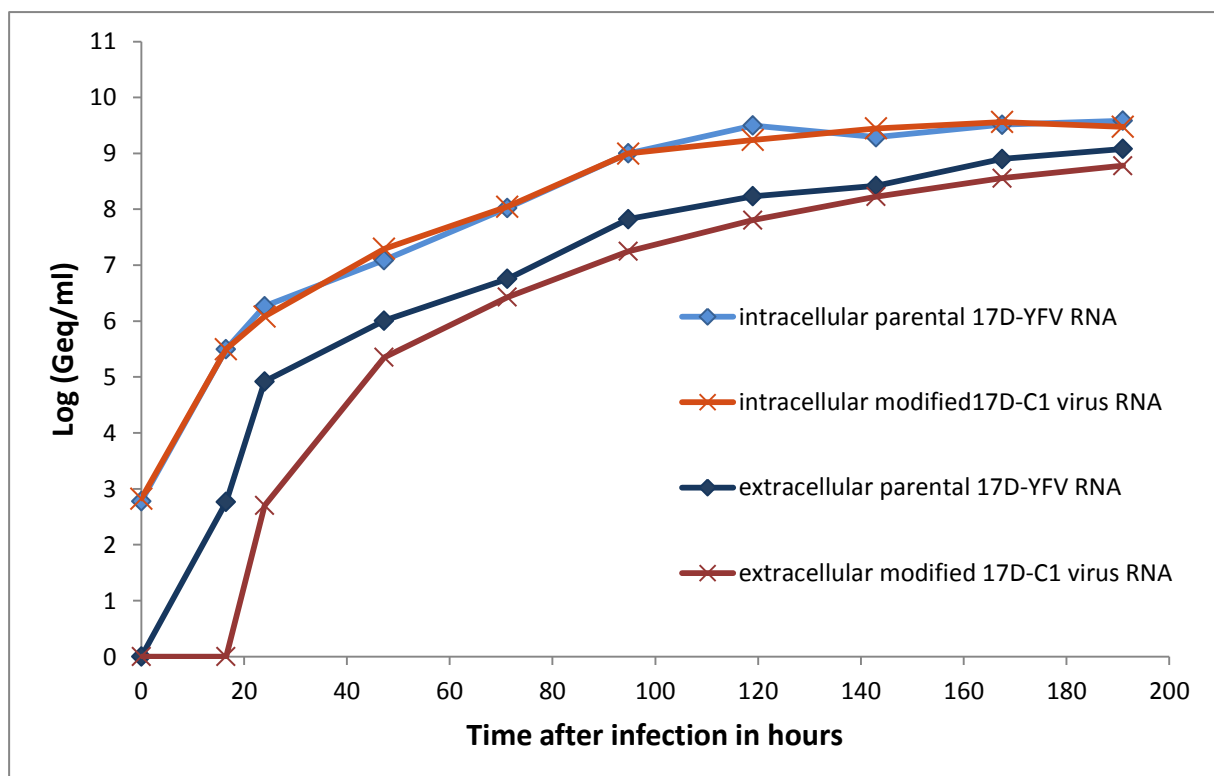


Figure 41: RT-PCR results of the growth kinetics of the parental YF-17D virus and the modified 17D-C1 virus for intracellular and extracellular YFV RNA.

The production of infectious viral particles determined by plaque assay (§B.3.3) was also comparable for the parental YFV-17D and the modified YF-17D C1 virus. Viral titers increased steadily from 17h after infection until 95h, where both virus strains reached viral titers of circa $5 \cdot 10^5$ PFU/ml. After this point, viral titers stagnated until the end of the 8-day experiment (Fig. 42). The morphology of the plaques observed on PS cells was also comparable for the parental and TC-tagged virus (Fig. 43).

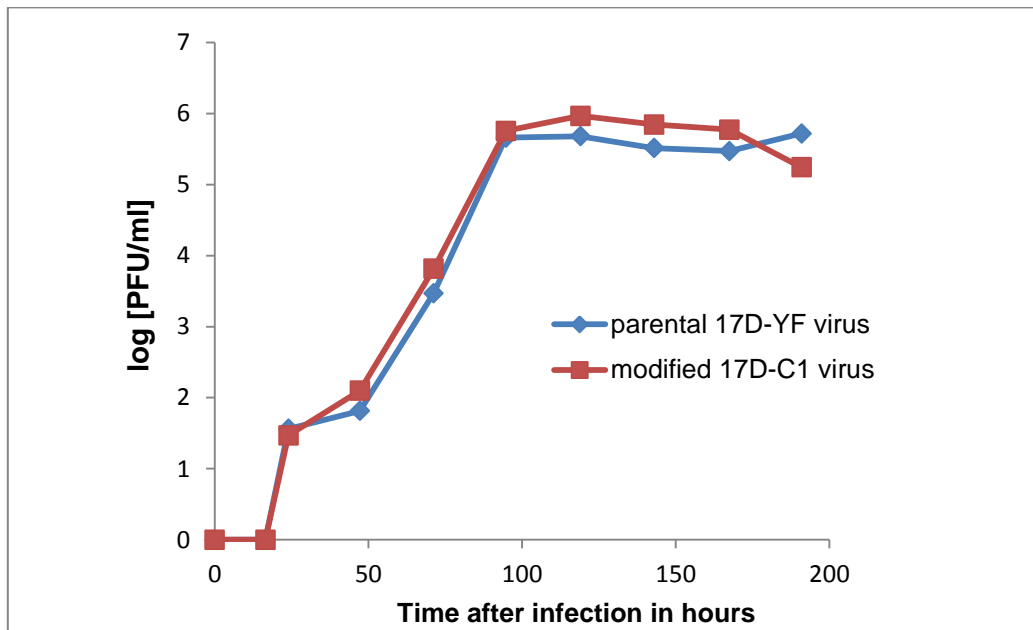


Figure 42: Plaque assay results demonstrating the viral titer during the growth kinetics of the YF-17D parental virus and 17D-C1 modified virus.

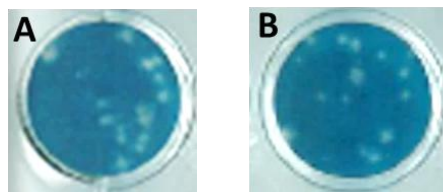


Figure 43: Plaque morphology of the YF-17D parental virus (A) and 17D-C1 modified virus (B) obtained with a 1:106 dilution of viral suspension after 4 days of infection on PS cells and inhibiting virus diffusion by overlay media (§B.3.3)

C.5 LABELING OF THE TC-TAGGED VIRUS WITH FLASH REAGENT

During 8 days of infection in Vero cells, RT-PCR and plaque assay results showed comparable growth behavior and plaque morphology for the native and the TC-tagged YFV-17D viruses. These results indicate that the 17D-C1 modified virus with the TC-tag in the C-protein can be considered as a viable tool for the pathogenesis study of YFV-17D.

Finally, it was tested whether the TC-tagged virus could produce fluorescence when put into contact with the biarsenical compound from the TC-FIAsh™ II In-Cell Tetracysteine Tag Detection Kit of Invitrogen (§B.5). The fluorescence intensity observed with the TC-tagged virus was compared to the fluorescence observed in Vero E6 cells transfected with the original YFV-17D RNA as a negative control.

Several experiments were performed with different concentrations of FIAsh reagent and with different times of incubation but all experimental conditions resulted in a high fluorescence background with Vero cells infected with the original YFV-17D virus and also with the TC-tagged virus.

The Vero cells infected with the parental and the TC-tagged YFV-17D were also incubated with a polyclonal antibody against the YFV C-protein (anti-YFV-C serum) in a 1/50 dilution and a goat-anti-rabbit secondary antibody labeled with FITC was used for detection by fluorescence microscopy (see IFA protocol in §B.3.4 of this chapter). This test was performed as a positive control for the presence of YFV C-protein in the Vero cells. Immunofluorescence results with the anti-YFV-C serum could demonstrate the presence of the YFV C-protein in the Vero cells infected with the parental virus (Fig.44 A) and the TC-tagged virus (Fig.44 B). Cells imaged after labeling with the FIAsh reagent demonstrated the same background fluorescence in the Vero cells infected with the parental virus (Fig.44 C) and the TC-tagged virus (Fig.44 D). No specific fluorescence could be observed from the labeling of the FIAsh reagent to the TC-tag in the C-protein of the 17D-C1 clone.

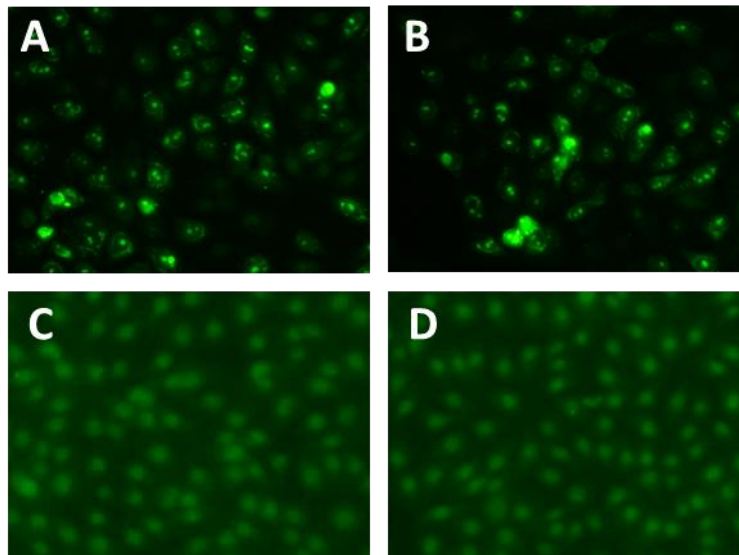


Figure 44: Specific labeling of the C-protein of the YFV-17D in Vero E6 cells 24 h after infection at a MOI of 1. Image magnification: X20. **A:** Vero cells infected with the parental virus and labeling with the anti-YFV-C serum (1:50) and a goat-anti-rabbit-FITC antibody (1:200); **B:** Vero cells infected with the TC-tagged virus and labeling with the anti-YFV-C serum (1:50) and a goat-anti-rabbit-FITC antibody (1:200); **C:** Vero cells infected with the parental virus and labeling during 45 min with 2.5 μ M FIAsh reagent; **D:** Vero cells infected with the TC-tagged virus and labeling during 45 min with 2.5 μ M FIAsh reagent.

D DISCUSSION

Due to its small size and versatility, the tetracysteine (TC-) tag technology is an attractive method to fluorescently label proteins for investigations with live cell imaging. In the field of virology, it has shown to be a useful technique for the study of viral protein localization, virus-cell interactions, virus entry and egress for several viruses [239, 241, 245-248]. However, until now this technology has not been applied to the study of pathogenesis of flavivirus infections. The vaccine strain (YFV-17D) is commonly used as a model system for all flaviviruses in order to identify and characterize components involved in viral pathogenesis and replication. Moreover the YFV-17D full length infectious complementary DNA (cDNA) clone offers an easy platform for molecular biological experiments [244].

A project initiated at the Robert Koch Institute by Nina Stock and Panchali Roy Chowdhury [215, 242] aimed to study the pathogenesis of YFV infections in live cell imaging microscopy by fluorescent labeling of viral proteins of the 17D vaccine strain by using the biarsenical-tetracysteine system. In their PhD and Master thesis [215, 242], they were able to construct four YFV-17D full length plasmids with the TC-tag in the envelope (E) or the capsid

(C) protein by using the full-length infectious cDNA clone of YFV-17D named pACNR-FLYF-17D and constructed by Bredenbeek and colleagues [244].

The last chapter of this PhD dissertation aimed to investigate the potential use of the four YFV-17D clones as tools for the study of the pathogenesis of YFV infections in live cell imaging microscopy.

The first objective was to check by sequencing whether the four TC-tagged plasmids each contained the correct genomic sequence with the TC-tag at the appropriate insertion site. The whole sequence of the full-length plasmid used to construct the cloned plasmids was sequenced and compared to the sequence of the previously described full-length YFV-17D plasmid, pACNR-FLYF-17D [244]. Sequencing results demonstrated the presence of six point mutations, one of which was not included in the YFV genome sequence and two others were silent mutations. Three amino-acid changes were therefore detected in the sequence of the original YFV-17D plasmid and were localized in the NS2A, NS4B and NS5 protein sequences (§C.1). While performing further experiments using this plasmid, it was recalled that these mutations could potentially affect the replication or growth behavior of the generated viruses.

The sequencing results for the four YFV-17D clones indicated that all TC-tags were inserted at the appropriate position of the plasmid sequence and the E and C regions of the plasmids were all mutation-free compared the original full length YFV plasmid sequence (§C.1). It was therefore decided to use the plasmid constructs for further experiments and test whether they were able to produce infectious clones after in-vitro transcription and transfection in Vero E6 cells.

In-vitro transcription and transfection in Vero E6 cells were performed in parallel for the parental and all cloned plasmids (§C.2). Monitoring of virus production during transfection with IFA, RT-PCR and plaque assay revealed that transfection was successful and could generate live infectious virus particles 3 days after transfection with the parental plasmid and with one cloned plasmid with the TC-tag in the C protein (§C.3).

The obtained modified virus, 17D-C1, was further characterized in order to verify its potential use as a model for YFV-17D pathogenesis investigations. For that purpose, a growth kinetics comparing the replication of the obtained infectious clone 17D-C1 and the parental virus 17D was performed on Vero E6 cells and viral production was monitored by RT-PCR and plaque assay (§C.4).

Daily monitoring of viral RNA detection performed by RT-PCR demonstrated the presence of YFV RNA in all samples including the negative control which included supernatant from cells transfected with RNA-free transfection solution. An additional negative

control was tested during the RNA extraction procedure and revealed similar RNA concentrations suggesting that the low amount of YFV RNA present in the negative controls are due to RNA contamination during the extraction as very high concentrations of RNA were present in the samples tested.

Daily monitoring of viral infection was also performed by plaque assay for measurement of the viral titer. Overall, all RT-PCR and plaque assay results revealed similar growth behaviour and plaque morphology of both viruses indicating that the TC-tagged virus can be used as a tool for the study of the pathogenesis of YFV infections in live cell imaging microscopy (§C.4). The results of viral titer and RNA quantification during the growth kinetics performed in Vero E6 cells demonstrated similar patterns than for YFV-17D growth kinetics in other cell lines, such as human cell line Hep G2 and insect cell line AP 61, as described by Nina Stock [215].

Before the TC-tagged virus could be used in live cell imaging microscopy, it was tested whether YFV-17D-C1 was able to produce fluorescence when exposed to the biarsenical reagent from the TC-FIAsh II In-Cell Tetracysteine Tag Detection Kit (Invitrogen). Vero E6 cells transfected with the non-tagged YFV-17D RNA were labeled as well and used as negative control to be sure that the fluorescence observed is due to the labeling of the target protein containing the TC-tag. Non-transfected cells are not a proper control as transfection can produce unspecific fluorescence staining due to the presence of cellular debris [249]. Unfortunately, all experiments performed in different conditions with several concentrations of FIAsh reagent and several times of incubation resulted in a similar fluorescence background with the TC-tagged virus and with the native 17D virus infected in Vero E6 cells (§C.5).

The nonappearance of specific fluorescence cannot be attributed to the unavailability of C protein as the presence of C protein in the infected cells has been verified by using a polyclonal serum against the YFV-C protein detected by a FITC labeled secondary antibody. Unsuccessful fluorescent labeling may be due to the non-accessibility of the biarsenical reagent to the tetracysteine tag and non-optimal positioning of the TC-tag in the protein. Undetectable fluorescence after FIAsh labelling may also be explained by a too low concentration and too brief exposure of C the protein inside the infected cells.

Despite its successful use in several studies, the specificity of this biarsenical substrate is less than ideal due to the presence of naturally occurring cysteine-rich sequences in proteins other than the target protein. Moreover, nonspecific hydrophobic interactions with the fluorogenic substrate do not allow the detection of proteins expressed at low levels and/or during a short time. It has been reported that the major drawback of the biarsenical-tetracysteine method for protein labeling in mammalian cell lines is the appearance of a high

CHAPTER 3 – Discussion

unspecific fluorescence background [249, 250]. The high level of background associated with the labeling of low-abundance TC tagged proteins has significantly limited its applicability in many virus systems. Another limitation of the biarsenical-tetracysteine system is the fact that the target cysteines in the TC-tag must be in their reduced form in order to bind to the biarsenical dyes. Therefore, previous studies of TC-tagged viruses tried to improve the signal to background ratio by using a higher contrast twelve-amino acids TC motif or by labeling the TC-tagged proteins outside the cells under acutely reducing conditions or by increasing the number of available TC tagged proteins inside the target cell via pseudotyped viruses [251]. Unfortunately none of these options were applicable at this stage of the project. As none of the constructs at our disposal at this point were suitable for the study of YFV pathogenesis and the development of new YFV plasmids constructs was not foreseen, the project was not further conducted.

GENERAL CONCLUSION

Vector-borne viruses are causing a large variety of diseases with a high impact on the health of populations independent of age, sex, social status and origin. In the course of environmental, social and demographic changes combined with the effects of an increasing globalization and worldwide mobility, the risk posed to humans and to animals by newly emerging vector-borne diseases is very difficult to predict. Therefore, it is of outmost importance to provide a systematic approach for analyzing, assessing and managing health risks linked to this emergence.

For this reason, public health efforts to strengthen vector-borne viral disease detection, surveillance and control have been intensified in recent years. In this effort, clinicians and clinical microbiology laboratories play an important role in the early detection of disease, identification of the infectious agent, and notification of cases to the appropriate authorities depend on them. To be effective in this role, laboratories must be prepared to handle viral agents with the appropriate biosafety measures and must implement rapid and accurate diagnostic procedures. Since laboratory diagnostic methods for vector-borne viral infections are often not standardized and based on in-house assays, it is essential to evaluate and improve the quality of diagnostic methods currently in use by developing quality control measures.

For this purpose, external quality assurance (EQA) programs provide comparative testing of multiple number-coded samples which allows analyzing the accuracy of the entire testing process from receipt of sample and testing of sample to reporting of results. Upon reception of the EQA results, the participating laboratories can evaluate their routine tests compared to other laboratories and identify the corrective measures to apply in order to improve their performance.

The first chapter of this dissertation describes five EQAs performed, as part of the ENIVD (European Network for Imported Viral Diseases) activities, in order to assess the molecular or serological detection methods for hantavirus, yellow fever virus, Crimean-Congo hemorrhagic fever virus and Rift Valley fever virus diagnostics [177-180]. In total over 80 laboratories from 44 different countries combined (27 EU member states and 17 non-EU member states) participated and response rates for all studies were over 90%. Although this is already a great achievement, it is crucial to further encourage laboratories situated in endemic countries to participate in quality assurance programs as they are first-line diagnostic sites. An increased participation would promote the availability of reliable and timely diagnostic results directly in all countries concerned with vector-borne viral infections.

GENERAL CONCLUSION

Several general observations and recommendations could be made by summarizing the results of all five EQAs. First of all, although commercial tests have the advantage of being standardized, they did not reveal better overall performances than in-house assays. Therefore, at this point, it is not recommended to use one type of assay rather than the other.

Results from the three molecular EQAs revealed that real-time RT-PCR performed better than conventional or nested RT-PCR. For YFV molecular testing, three published protocols [135, 178, 179] could only detect the YFV-17D vaccine strain and therefore are not recommended for the identification of suspected YFV infections with wild type strains [177]. Finally the results from molecular EQAs revealed that most laboratories do not include standards in their real-time RT-PCR procedures. This issue is mainly due to the lack of international standards and indicates the need to develop and provide such reference material in order to enable quantification of genome copies for all laboratories performing molecular testing of vector-borne viral infections.

The main observation arising from the two serological EQAs concerned IgM detection since part of the participating laboratories did not include IgM detection in their diagnostic routine and results from laboratories testing for the presence of IgM antibodies revealed a low sensitivity. Such deficiencies in IgM detection indicate a considerable risk of overlooking acute infections in hantavirus or YFV infected patients. For this reason, these studies have identified the development of reliable assays for IgM detection as a priority in order to strengthen laboratory capacity for hantavirus and YFV diagnostics.

Finally, in all the EQA studies presented, performances varied greatly even when laboratories were using the same technique. The reasons for such variations in performance are difficult to identify as many parameters (e.g. type of kits, instruments and reagents used) are involved in testing procedures but they can be minimized by optimizing testing conditions, including the use of adequate controls and standardized protocols. Such great variations of performance among participating laboratories clearly demonstrate the need to perform EQA programs for vector-borne viral diseases on a more regular basis. Given the demand for biological preparedness, regular participation in EQA programs will become increasingly important for laboratories worldwide. In this process, ENIVD's role is essential as it provides international EQA programs for a number of rare, imported or emerging viral agents that are usually not addressed by commercial organizations. Nevertheless, the current configuration of EQA programs would clearly need further development and requires wider proficiency panels, but at present financial and technical limitations such as the difficulty of providing a sufficient amount of the required reference material are impeding the preparation of wider panels.

GENERAL CONCLUSION

The next chapters of the dissertation focus on the study and the development of diagnostic tools for the yellow fever virus (YFV). Despite the use of a safe and effective vaccine, YFV is still causing hundreds of thousands of infections and tens of thousands of deaths every year mostly in Africa. As the disease is difficult to distinguish from other illnesses during its early stage, it is necessary to develop reliable, rapid and simple diagnostic methods to confirm YF cases. The availability of methods for early detection of cases would enable an effective response to outbreaks through vaccination and vector control and would also enable a more accurate assessment of the burden of YF on the health of affected populations.

Within this scope, the second chapter describes the development of new diagnostic methods for the detection of YFV infections. The development of an isothermal molecular method for YFV detection using recombinase polymerase amplification (RPA) is first described. The real-time RT-RPA assay proved to be a specific and sensitive detection method for YFV during testing in laboratory conditions with a low detection limit (<21 genome equivalent copies per reaction) and rapid processing time (<20 minutes) using a portable and easy-to-use instrument setup [191]. The real-time RT-RPA assay was operated in 2013 by German and Senegalese colleagues in field conditions in Senegal using a battery charged by solar panels as electricity source. The results of this testing confirmed that the real-time RT-RPA assay for YFV detection is a suitable technique which performs with the same efficiency and accuracy under field conditions as that of cutting-edge laboratory settings. Therefore the RPA method can provide an affordable alternative to current PCR-based technologies in established laboratories but also in low-resource field settings. Since its development, the RPA assay for YFV detection has already been implemented in several laboratories in Africa and will allow rapid response measures to YFV outbreaks and local disease surveillance in endemic countries. RPA for the detection of other viruses such as dengue, chikungunya, Rift valley fever, Ebola, Marburg and West Nile viruses have also been developed [190, 201] or are currently in development and will allow a complete and rapid differential diagnosis for arboviral and hemorrhagic fever diseases in areas where several viruses circulate.

In a second part, the chapter on the development of new diagnostic methods aimed at developing a serological method for the early detection of yellow fever infections. Serological methods are affordable diagnostic techniques that can easily be implemented in low-resource settings. However, serological approaches in YFV diagnostic are mostly based on antibody detection and often confronted with a high level of antigenic cross-reactivity among flaviviruses. Moreover, antibody detection is not applicable during the early course of infection before the appearance of an immune response. A complementary approach has recently been successfully developed for dengue diagnosis, in which the viral NS1 protein was used as an early diagnostic marker [206, 222].

GENERAL CONCLUSION

In this project, the possibility of using NS1 detection for the diagnosis of yellow fever infections was investigated by developing specific tools for the detection of the YFV-NS1 protein and to investigate their potential use for YFV diagnostics. YFV-specific polyclonal antisera against the NS1 protein were produced by immunization of guinea pigs with antigenic peptides selected from the NS1 protein sequence. All three polyclonal antisera produced were able to detect the YFV NS1 protein through Western blot and immunofluorescence assay by producing specific signals. However, one of the antisera produced better performances in all tests and was used for further experiments.

The possibility of developing a “sandwich ELISA” with this guinea pig antiserum in combination with another anti-NS1 serum produced previously in rabbit was then investigated [215]. Despite the use of antisera of two distinct species for capture and detection, the presence of false positive results could not be prevented. Even though the establishment of an ELISA for the specific detection of the YFV NS1 protein could not be completed within the frame of this study, the preliminary results provide a basis for further development of the method. The production of monoclonal antibodies (Mabs) based on results obtained in this study is currently being performed by collaborators in France and the Mabs should be available in 2014. Moreover, a commercial recombinant YFV NS1 protein was recently made available by a company and has been ordered in order to progress in the development of an ELISA with characterized and quantifiable positive controls.

This project led to the production and characterization of polyclonal antibodies specific for the detection of the YFV NS1 with good performances in IFA and WB. The availability of such detection tools is of great value as there are no commercially available antibodies against the YFV NS1 protein. The developed anti-NS1 guinea pig sera along with the previously produced rabbit antiserum will allow investigating the role of NS1 in the pathogenesis and replication mechanisms during YFV infections. Results from this project also indicate that such tools have a strong potential for useful applications in field diagnostics enabling an accurate and affordable diagnosis of YFV infections including in low-resource settings and remote endemic areas.

The third and last chapter of this dissertation describes the development of a project previously initiated at the Robert Koch Institute [215, 242] aiming to study the pathogenesis of YFV infections in live cell imaging microscopy through fluorescent labeling of viral proteins of the 17D vaccine strain by using the tetracysteine (TC-) tag technology (FIAsH). Due to its small size and versatility, the TC-tag system has proven to be a useful technique in the field of virology for the study of viral protein localization and virus-cell interactions. This project aimed at applying this technology for the first time to the study of the pathogenesis of flavivirus infections by using the vaccine strain (YFV-17D) as a model system for all

GENERAL CONCLUSION

flaviviruses. Prior to this work, four YFV-17D full length plasmids with the TC-tag in the envelope (E) or the capsid (C) protein were constructed by using a full-length infectious cDNA clone of YFV-17D [215].

The objective of this work was to investigate the potential use of the four YFV-17D plasmids previously constructed as tools for the study of the pathogenesis of YFV infections in live cell imaging microscopy. In-vitro transcription and transfection in Vero E6 cells were performed with the four plasmids and monitoring of virus production after transfection with IFA, RT-PCR and plaque assay revealed that transfection was successful and could generate live infectious viral particles for one of the plasmids with the TC-tag in the C protein (YFV-17D-C1). In order to verify its potential use as a model for YFV-17D pathogenesis investigations, the modified virus obtained was further characterized by performing growth kinetics comparing its replication to the parental virus 17D. RT-PCR and plaque assay results revealed similar growth behaviour and plaque morphology of both viruses indicating that the TC-tagged virus can be used as a tool for the study of the pathogenesis of YFV infections.

Unfortunately, further experiments revealed that the YFV-17D-C1 virus was not able to produce fluorescence when exposed to the biarsenical reagent. Several testing conditions with different concentrations of FIAsH reagent and times of incubation resulted in a similar fluorescence background after staining Vero E6 cells infected with the TC-tagged virus and with the native 17D virus. As none of the constructs at our disposal at this point were suitable for the study of YFV pathogenesis and the development of new YFV plasmids constructs was not foreseen, the project was ended at this stage. In the future, another labeling strategy might be applied to the YFV-17D full-length infectious cDNA plasmid and the choice of technology will be founded on detailed literature research concerning newest updates in the field of live cell imaging microscopy by fluorescent labeling of viral proteins.

In conclusion, this PhD dissertation contributed to the international quality assessment of diagnostic methods for vector-borne viral infections by identifying weak points and recommendations regarding the serological and molecular detection of hantavirus, yellow fever virus, Rift Valley fever virus and Crimean-Congo hemorrhagic fever virus. General observations have been formulated about the current configuration of EQAs and enhancements for their future development have been proposed.

In a second part, this PhD work focuses on the yellow fever virus by contributing to the development of molecular and serological diagnostic methods for YFV infections. A rapid, sensitive and easy-to-use isothermal molecular assay was established and new specific antibodies were produced and characterized for the future development of a serological

GENERAL CONCLUSION

assay based on NS1 protein detection. The implementation of these two new diagnostic strategies will enable an early, accurate and affordable diagnosis of YFV infections even in low-resource settings and remote endemic areas.

REFERENCES

1. Barker, J., D. Stevens, and S.F. Bloomfield, *Spread and prevention of some common viral infections in community facilities and domestic homes*. J Appl Microbiol, 2001. **91**(1): p. 7-21.
2. Henderson, D.A., *The eradication of smallpox--an overview of the past, present, and future*. Vaccine, 2011. **29 Suppl 4**: p. D7-9.
3. Dobler, G., *Arboviruses causing neurological disorders in the central nervous system*. Arch Virol Suppl, 1996. **11**: p. 33-40.
4. Lambrechts, L. and T.W. Scott, *Mode of transmission and the evolution of arbovirus virulence in mosquito vectors*. Proc Biol Sci, 2009. **276**(1660): p. 1369-78.
5. Kuno, G. and G.J. Chang, *Biological transmission of arboviruses: reexamination of and new insights into components, mechanisms, and unique traits as well as their evolutionary trends*. Clin Microbiol Rev, 2005. **18**(4): p. 608-37.
6. Carver, S., et al., *Influence of hosts on the ecology of arboviral transmission: potential mechanisms influencing dengue, Murray Valley encephalitis, and Ross River virus in Australia*. Vector Borne Zoonotic Dis, 2009. **9**(1): p. 51-64.
7. *Arthropod-borne and rodent-borne viral diseases. Report of a WHO Scientific Group*. World Health Organ Tech Rep Ser, 1985. **719**: p. 1-116.
8. Gubler, D.J., *Human arbovirus infections worldwide*. Ann N Y Acad Sci, 2001. **951**: p. 13-24.
9. Weaver, S.C. and A.D. Barrett, *Transmission cycles, host range, evolution and emergence of arboviral disease*. Nat Rev Microbiol, 2004. **2**(10): p. 789-801.
10. Davies, F.G., K.J. Linthicum, and A.D. James, *Rainfall and epizootic Rift Valley fever*. Bull World Health Organ, 1985. **63**(5): p. 941-3.
11. Jones, K.E., et al., *Global trends in emerging infectious diseases*. Nature, 2008. **451**(7181): p. 990-3.
12. Weaver, S.C. and W.K. Reisen, *Present and future arboviral threats*. Antiviral Res, 2010. **85**(2): p. 328-45.
13. Pfeffer, M. and G. Dobler, *Emergence of zoonotic arboviruses by animal trade and migration*. Parasit Vectors, 2010. **3**(1): p. 35.
14. Kilpatrick, A.M. and S.E. Randolph, *Drivers, dynamics, and control of emerging vector-borne zoonotic diseases*. Lancet, 2012. **380**(9857): p. 1946-55.
15. Gould, E.A. and S. Higgs, *Impact of climate change and other factors on emerging arbovirus diseases*. Trans R Soc Trop Med Hyg, 2009. **103**(2): p. 109-21.
16. LaBeaud, A.D., *Why arboviruses can be neglected tropical diseases*. PLoS Negl Trop Dis, 2008. **2**(6): p. e247.
17. Josseran, L., et al., *Chikungunya disease outbreak, Reunion Island*. Emerg Infect Dis, 2006. **12**(12): p. 1994-5.
18. Sambri, V., et al., *The 2007 epidemic outbreak of Chikungunya virus infection in the Romagna region of Italy: a new perspective for the possible diffusion of tropical diseases in temperate areas?* New Microbiol, 2008. **31**(3): p. 303-4.
19. Franco-Paredes, C., et al., *Neurotoxicity due to antimalarial therapy associated with misdiagnosis of malaria*. Clin Infect Dis, 2005. **40**(11): p. 1710-1.
20. Amexo, M., et al., *Malaria misdiagnosis: effects on the poor and vulnerable*. Lancet, 2004. **364**(9448): p. 1896-8.
21. Kumar, C.J., et al., *The socioeconomic impact of the chikungunya viral epidemic in India*. Open Med, 2007. **1**(3): p. e150-2.
22. Cleton, N., et al., *Come fly with me: Review of clinically important arboviruses for global travelers*. J Clin Virol, 2012.

REFERENCES

23. Ergonul, O., *Crimean-Congo hemorrhagic fever virus: new outbreaks, new discoveries*. *Curr Opin Virol*, 2012. **2**(2): p. 215-20.
24. Appannanavar, S.B. and B. Mishra, *An update on crimean congo hemorrhagic Fever*. *J Glob Infect Dis*, 2011. **3**(3): p. 285-92.
25. Tomori, O., et al., *Bwamba virus infection: a sero-survey of veterbrates in five ecological zones in Nigeria*. *Trans R Soc Trop Med Hyg*, 1974. **68**(6): p. 461-5.
26. Lutwama, J.J., et al., *Isolations of Bwamba virus from south central Uganda and north eastern Tanzania*. *Afr Health Sci*, 2002. **2**(1): p. 24-8.
27. Mabey, D., *The Encyclopedia of Arthropod-Transmitted Infections*. *BMJ*, 2002. **324**(7335): p. 490.
28. Tauro, L.B., et al., *First case of human infection with a Bunyamwera serogroup virus in Argentina*. *J Clin Virol*, 2012. **54**(1): p. 98-9.
29. Gerrard, S.R., et al., *Ngari virus is a Bunyamwera virus reassortant that can be associated with large outbreaks of hemorrhagic fever in Africa*. *J Virol*, 2004. **78**(16): p. 8922-6.
30. Morvan, J.M., et al., *Ilesha virus: a new aetiological agent of haemorrhagic fever in Madagascar*. *Trans R Soc Trop Med Hyg*, 1994. **88**(2): p. 205.
31. Briese, T., et al., *Batai and Ngari viruses: M segment reassortment and association with severe febrile disease outbreaks in East Africa*. *J Virol*, 2006. **80**(11): p. 5627-30.
32. Haddow, A.D., D. Bixler, and A.J. Schuh, *The demographic and socioeconomic factors predictive for populations at high-risk for La Crosse virus infection in West Virginia*. *PLoS One*, 2011. **6**(9): p. e25739.
33. Haddow, A.D. and A. Odoi, *The incidence risk, clustering, and clinical presentation of La Crosse virus infections in the eastern United States, 2003-2007*. *PLoS One*, 2009. **4**(7): p. e6145.
34. Hubalek, Z., *Mosquito-borne viruses in Europe*. *Parasitol Res*, 2008. **103 Suppl 1**: p. S29-43.
35. Lundstrom, J.O., *Mosquito-borne viruses in western Europe: a review*. *J Vector Ecol*, 1999. **24**(1): p. 1-39.
36. Aguilar, P.V., et al., *Guaroa virus infection among humans in Bolivia and Peru*. *Am J Trop Med Hyg*, 2010. **83**(3): p. 714-21.
37. Forshey, B.M., et al., *Arboviral etiologies of acute febrile illnesses in Western South America, 2000-2007*. *PLoS Negl Trop Dis*, 2010. **4**(8): p. e787.
38. Vasconcelos, H.B., et al., *Oropouche fever epidemic in Northern Brazil: epidemiology and molecular characterization of isolates*. *J Clin Virol*, 2009. **44**(2): p. 129-33.
39. Azevedo, R.S., et al., *Reemergence of Oropouche fever, northern Brazil*. *Emerg Infect Dis*, 2007. **13**(6): p. 912-5.
40. Fagbami, A.H. and O. Tomori, *Tataguine virus isolations from humans in Nigeria, 1971-1975*. *Trans R Soc Trop Med Hyg*, 1981. **75**(6): p. 788.
41. Boshra, H., et al., *Rift valley fever: recent insights into pathogenesis and prevention*. *J Virol*, 2011. **85**(13): p. 6098-105.
42. Pepin, M., et al., *Rift Valley fever virus(Bunyaviridae: Phlebovirus): an update on pathogenesis, molecular epidemiology, vectors, diagnostics and prevention*. *Vet Res*, 2010. **41**(6): p. 61.
43. Cusi, M.G., G.G. Savellini, and G. Zanelli, *Toscana virus epidemiology: from Italy to beyond*. *Open Virol J*, 2010. **4**: p. 22-8.
44. Charrel, R.N., et al., *Emergence of Toscana virus in Europe*. *Emerg Infect Dis*, 2005. **11**(11): p. 1657-63.
45. Dionisio, D., et al., *Epidemiological, clinical and laboratory aspects of sandfly fever*. *Curr Opin Infect Dis*, 2003. **16**(5): p. 383-8.

REFERENCES

46. Gardner, C.L. and K.D. Ryman, *Yellow fever: a reemerging threat*. Clin Lab Med, 2010. **30**(1): p. 237-60.
47. Staples, J.E. and T.P. Monath, *Yellow fever: 100 years of discovery*. JAMA, 2008. **300**(8): p. 960-2.
48. Barnett, E.D., *Yellow fever: epidemiology and prevention*. Clin Infect Dis, 2007. **44**(6): p. 850-6.
49. Wilder-Smith, A., et al., *Update on dengue: epidemiology, virus evolution, antiviral drugs, and vaccine development*. Curr Infect Dis Rep, 2010. **12**(3): p. 157-64.
50. Thomas, S.J., D. Strickman, and D.W. Vaughn, *Dengue epidemiology: virus epidemiology, ecology, and emergence*. Adv Virus Res, 2003. **61**: p. 235-89.
51. Campbell, G.L., et al., *West Nile virus*. Lancet Infect Dis, 2002. **2**(9): p. 519-29.
52. Murray, K.O., C. Walker, and E. Gould, *The virology, epidemiology, and clinical impact of West Nile virus: a decade of advancements in research since its introduction into the Western Hemisphere*. Epidemiol Infect, 2011. **139**(6): p. 807-17.
53. Sambri, V., et al., *Diagnosis of West Nile Virus Human Infections: Overview and Proposal of Diagnostic Protocols Considering the Results of External Quality Assessment Studies*. Viruses, 2013. **5**(10): p. 2329-2348.
54. Endy, T.P. and A. Nisalak, *Japanese encephalitis virus: ecology and epidemiology*. Curr Top Microbiol Immunol, 2002. **267**: p. 11-48.
55. Ghosh, D. and A. Basu, *Japanese encephalitis-a pathological and clinical perspective*. PLoS Negl Trop Dis, 2009. **3**(9): p. e437.
56. Reisen, W.K., *Epidemiology of St. Louis encephalitis virus*. Adv Virus Res, 2003. **61**: p. 139-83.
57. McCarthy, M., *St. Louis Encephalitis and West Nile Virus Encephalitis*. Curr Treat Options Neurol, 2001. **3**(5): p. 433-438.
58. Evans, I.A., L. Hueston, and S.L. Doggett, *Murray Valley encephalitis virus*. N S W Public Health Bull, 2009. **20**(11-12): p. 195-6.
59. Knox, J., et al., *Murray Valley encephalitis: a review of clinical features, diagnosis and treatment*. Med J Aust, 2012. **196**(5): p. 322-6.
60. Donoso Mantke, O., et al., *Tick-borne encephalitis in Europe, 2007 to 2009*. Euro Surveill, 2011. **16**(39).
61. Petri, E., D. Gniel, and O. Zent, *Tick-borne encephalitis (TBE) trends in epidemiology and current and future management*. Travel Med Infect Dis, 2010. **8**(4): p. 233-45.
62. Pavri, K., *Clinical, clinicopathologic, and hematologic features of Kyasanur Forest disease*. Rev Infect Dis, 1989. **11 Suppl 4**: p. S854-9.
63. Adhikari Prabha, M.R., et al., *Clinical study of 100 cases of Kyasanur Forest disease with clinicopathological correlation*. Indian J Med Sci, 1993. **47**(5): p. 124-30.
64. Memish, Z.A., et al., *Alkhurma viral hemorrhagic Fever virus: proposed guidelines for detection, prevention, and control in Saudi Arabia*. PLoS Negl Trop Dis, 2012. **6**(7): p. e1604.
65. Memish, Z.A., et al., *Seroprevalence of Alkhurma and other hemorrhagic fever viruses, Saudi Arabia*. Emerg Infect Dis, 2011. **17**(12): p. 2316-8.
66. Venegas, E.A., et al., *Ilheus virus infection in human, Bolivia*. Emerg Infect Dis, 2012. **18**(3): p. 516-8.
67. Cruz, A.C., et al., *Ilheus virus (Flaviviridae, Flavivirus) is closely related to Japanese encephalitis virus complex*. Intervirology, 1997. **40**(4): p. 220-5.
68. Romero, J.R. and K.A. Simonsen, *Powassan encephalitis and Colorado tick fever*. Infect Dis Clin North Am, 2008. **22**(3): p. 545-59, x.
69. Liu, H., et al., *Banna virus, China, 1987-2007*. Emerg Infect Dis, 2010. **16**(3): p. 514-7.

REFERENCES

70. Burt, F.J., et al., *Chikungunya: a re-emerging virus*. Lancet, 2012. **379**(9816): p. 662-71.
71. Jaffar-Bandjee, M.C., et al., *Emergence and clinical insights into the pathology of Chikungunya virus infection*. Expert Rev Anti Infect Ther, 2010. **8**(9): p. 987-96.
72. Queyriaux, B., et al., *Clinical burden of chikungunya virus infection*. Lancet Infect Dis, 2008. **8**(1): p. 2-3.
73. Tesh, R.B., et al., *Mayaro virus disease: an emerging mosquito-borne zoonosis in tropical South America*. Clin Infect Dis, 1999. **28**(1): p. 67-73.
74. Izurieta, R.O., et al., *Hunting in the Rainforest and Mayaro Virus Infection: An emerging Alphavirus in Ecuador*. J Glob Infect Dis, 2011. **3**(4): p. 317-23.
75. Bessaud, M., et al., *O'nyong-nyong Virus, Chad*. Emerg Infect Dis, 2006. **12**(8): p. 1248-50.
76. Posey, D.L., et al., *O'Nyong-nyong fever in West Africa*. Am J Trop Med Hyg, 2005. **73**(1): p. 32.
77. Powers, A.M., et al., *Re-emergence of Chikungunya and O'nyong-nyong viruses: evidence for distinct geographical lineages and distant evolutionary relationships*. J Gen Virol, 2000. **81**(Pt 2): p. 471-9.
78. Barber, B., J.T. Denholm, and D. Spelman, *Ross River virus*. Aust Fam Physician, 2009. **38**(8): p. 586-9.
79. Jacups, S.P., P.I. Whelan, and B.J. Currie, *Ross River virus and Barmah Forest virus infections: a review of history, ecology, and predictive models, with implications for tropical northern Australia*. Vector Borne Zoonotic Dis, 2008. **8**(2): p. 283-97.
80. Deresiewicz, R.L., et al., *Clinical and neuroradiographic manifestations of eastern equine encephalitis*. N Engl J Med, 1997. **336**(26): p. 1867-74.
81. Zacks, M.A. and S. Paessler, *Encephalitic alphaviruses*. Vet Microbiol, 2010. **140**(3-4): p. 281-6.
82. Kurkela, S., et al., *Clinical and laboratory manifestations of Sindbis virus infection: prospective study, Finland, 2002-2003*. J Infect Dis, 2005. **191**(11): p. 1820-9.
83. Kurkela, S., et al., *Sindbis virus infection in resident birds, migratory birds, and humans, Finland*. Emerg Infect Dis, 2008. **14**(1): p. 41-7.
84. Weaver, S.C., et al., *Venezuelan equine encephalitis*. Annu Rev Entomol, 2004. **49**: p. 141-74.
85. Valassina, M., M.G. Cusi, and P.E. Valensin, *A Mediterranean arbovirus: the Toscana virus*. J Neurovirol, 2003. **9**(6): p. 577-83.
86. Hang, V.T., et al., *Diagnostic accuracy of NS1 ELISA and lateral flow rapid tests for dengue sensitivity, specificity and relationship to viraemia and antibody responses*. PLoS Negl Trop Dis, 2009. **3**(1): p. e360.
87. Guzman, M.G., et al., *Dengue: a continuing global threat*. Nat Rev Microbiol, 2010. **8**(12 Suppl): p. S7-16.
88. Mansfield, K.L., et al., *Flavivirus-induced antibody cross-reactivity*. J Gen Virol, 2011. **92**(Pt 12): p. 2821-9.
89. Sampath, A. and R. Padmanabhan, *Molecular targets for flavivirus drug discovery*. Antiviral Res, 2009. **81**(1): p. 6-15.
90. Geiss, B.J., et al., *Focus on flaviviruses: current and future drug targets*. Future Med Chem, 2009. **1**(2): p. 327-44.
91. Sautto, G., et al., *Possible future monoclonal antibody (mAb)-based therapy against arbovirus infections*. Biomed Res Int, 2013. **838491**(10): p. 22.
92. Kumar, P., et al., *A single siRNA suppresses fatal encephalitis induced by two different flaviviruses*. PLoS Med, 2006. **3**(4): p. 14.
93. Sbrana, E., et al., *Efficacy of post-exposure treatment of yellow fever with ribavirin in a hamster model of the disease*. Am J Trop Med Hyg, 2004. **71**(3): p. 306-12.

REFERENCES

94. Julander, J.G., et al., *Treatment of yellow fever virus with an adenovirus-vectored interferon, DEF201, in a hamster model*. *Antimicrob Agents Chemother*, 2011. **55**(5): p. 2067-73.
95. Wilke, A.B. and M.T. Marrelli, *Genetic control of mosquitoes: population suppression strategies*. *Rev Inst Med Trop Sao Paulo*, 2012. **54**(5): p. 287-92.
96. Javed, S., F. Khan, and S.K. Tyring, *Bites and mites: prevention and protection of vector-borne disease*. *Curr Opin Pediatr*, 2013. **25**(4): p. 488-91.
97. Falzarano, D. and H. Feldmann, *Vaccines for viral hemorrhagic fevers--progress and shortcomings*. *Curr Opin Virol*, 2013. **3**(3): p. 343-51.
98. Ray, D. and P.Y. Shi, *Recent advances in flavivirus antiviral drug discovery and vaccine development*. *Recent Pat Antiinfect Drug Discov*, 2006. **1**(1): p. 45-55.
99. Iyer, A.V. and K.G. Kousoulas, *A review of vaccine approaches for West Nile virus*. *Int J Environ Res Public Health*, 2013. **10**(9): p. 4200-23.
100. Gould, E.A. and T. Solomon, *Pathogenic flaviviruses*. *Lancet*, 2008. **371**(9611): p. 500-9.
101. WHO, *Yellow fever fact sheet*. *Wkly Epidemiol Rec*, 2010. **85**(5): p. 33-6.
102. Labeaud, A.D., F. Bashir, and C.H. King, *Measuring the burden of arboviral diseases: the spectrum of morbidity and mortality from four prevalent infections*. *Popul Health Metr*, 2011. **9**(1): p. 1.
103. *Yellow fever in the WHO African and American Regions, 2010*. *Wkly Epidemiol Rec*, 2011. **86**(34): p. 370-6.
104. Yuill, T.M., J.P. Woodall, and S. Baekeland, *Latest outbreak news from ProMED-mail. Yellow fever outbreak-Darfur Sudan and Chad*. *Int J Infect Dis*, 2013. **17**(7): p. e476-8.
105. Markoff, L., *Yellow fever outbreak in Sudan*. *N Engl J Med*, 2013. **368**(8): p. 689-91.
106. Barrett, A.D. and T.P. Monath, *Epidemiology and ecology of yellow fever virus*. *Adv Virus Res*, 2003. **61**: p. 291-315.
107. Robertson, S.E., et al., *Yellow fever: a decade of reemergence*. *JAMA*, 1996. **276**(14): p. 1157-62.
108. Luca, V.C., et al., *Crystal structure of the Japanese encephalitis virus envelope protein*. *J Virol*, 2012. **86**(4): p. 2337-46.
109. Nayak, V., et al., *Crystal structure of dengue virus type 1 envelope protein in the postfusion conformation and its implications for membrane fusion*. *J Virol*, 2009. **83**(9): p. 4338-44.
110. Nybakken, G.E., et al., *Crystal structure of the West Nile virus envelope glycoprotein*. *J Virol*, 2006. **80**(23): p. 11467-74.
111. Kanai, R., et al., *Crystal structure of west nile virus envelope glycoprotein reveals viral surface epitopes*. *J Virol*, 2006. **80**(22): p. 11000-8.
112. Elahi, M., et al., *High resolution crystal structure of dengue-3 envelope protein domain III suggests possible molecular mechanisms for serospecific antibody recognition*. *Proteins*, 2013. **81**(6): p. 1090-5.
113. Kiermayr, S., K. Stiasny, and F.X. Heinz, *Impact of quaternary organization on the antigenic structure of the tick-borne encephalitis virus envelope glycoprotein E*. *J Virol*, 2009. **83**(17): p. 8482-91.
114. Heinz, F.X. and K. Stiasny, *Flaviviruses and flavivirus vaccines*. *Vaccine*, 2012. **30**(29): p. 4301-6.
115. Beck, C., et al., *Flaviviruses in europe: complex circulation patterns and their consequences for the diagnosis and control of west nile disease*. *Int J Environ Res Public Health*, 2013. **10**(11): p. 6049-83.
116. Jones, C.T., et al., *Flavivirus capsid is a dimeric alpha-helical protein*. *J Virol*, 2003. **77**(12): p. 7143-9.

REFERENCES

117. Allison, S.L., et al., *Mutational evidence for an internal fusion peptide in flavivirus envelope protein E*. J Virol, 2001. **75**(9): p. 4268-75.
118. Stiasny, K., S. Kiermayr, and F.X. Heinz, *Entry functions and antigenic structure of flavivirus envelope proteins*. Novartis Found Symp, 2006. **277**: p. 57-65; discussion 65-73, 251-3.
119. Li, L., et al., *The flavivirus precursor membrane-envelope protein complex: structure and maturation*. Science, 2008. **319**(5871): p. 1830-4.
120. Muller, D.A. and P.R. Young, *The flavivirus NS1 protein: Molecular and structural biology, immunology, role in pathogenesis and application as a diagnostic biomarker*. Antiviral Res, 2013. **98**(2): p. 192-208.
121. Leung, J.Y., et al., *Role of nonstructural protein NS2A in flavivirus assembly*. J Virol, 2008. **82**(10): p. 4731-41.
122. Murray, C.L., C.T. Jones, and C.M. Rice, *Architects of assembly: roles of Flaviviridae non-structural proteins in virion morphogenesis*. Nat Rev Microbiol, 2008. **6**(9): p. 699-708.
123. Davidson, A.D., *Chapter 2. New insights into flavivirus nonstructural protein 5*. Adv Virus Res, 2009. **74**: p. 41-101.
124. Gillespie, L.K., et al., *The endoplasmic reticulum provides the membrane platform for biogenesis of the flavivirus replication complex*. J Virol, 2010. **84**(20): p. 10438-47.
125. Mukhopadhyay, S., R.J. Kuhn, and M.G. Rossmann, *A structural perspective of the flavivirus life cycle*. Nat Rev Microbiol, 2005. **3**(1): p. 13-22.
126. Diallo, M., J. Thonnon, and D. Fontenille, *Vertical transmission of the yellow fever virus by Aedes aegypti (Diptera, Culicidae): dynamics of infection in F1 adult progeny of orally infected females*. Am J Trop Med Hyg, 2000. **62**(1): p. 151-6.
127. Fontenille, D., et al., *First evidence of natural vertical transmission of yellow fever virus in Aedes aegypti, its epidemic vector*. Trans R Soc Trop Med Hyg, 1997. **91**(5): p. 533-5.
128. Barrett, A.D. and S. Higgs, *Yellow fever: a disease that has yet to be conquered*. Annu Rev Entomol, 2007. **52**: p. 209-29.
129. Monath, T.P. and A.D. Barrett, *Pathogenesis and pathophysiology of yellow fever*. Adv Virus Res, 2003. **60**: p. 343-95.
130. Monath, T.P., *Yellow fever: an update*. Lancet Infect Dis, 2001. **1**(1): p. 11-20.
131. Quaresma, J.A., et al., *Immunity and immune response, pathology and pathologic changes: progress and challenges in the immunopathology of yellow fever*. Rev Med Virol, 2013. **23**(5): p. 305-18.
132. Houghton-Triviño, N., D. Montaña, and J. Castellanos, *Dengue-yellow fever sera cross-reactivity; challenges for diagnosis*. Rev Salud Publica (Bogota), 2008. **10**: p. 299-307.
133. Koraka, P., et al., *Reactivity of serum samples from patients with a flavivirus infection measured by immunofluorescence assay and ELISA*. Microbes Infect, 2002. **4**(12): p. 1209-15.
134. Weidmann, M., et al., *Improved LNA probe-based assay for the detection of African and South American yellow fever virus strains*. J Clin Virol, 2010. **48**(3): p. 187-92.
135. Nunes, M.R., et al., *Evaluation of two molecular methods for the detection of Yellow fever virus genome*. J Virol Methods, 2011. **174**(1-2): p. 29-34.
136. Dash, P.K., et al., *Development of a SYBR green I based RT-PCR assay for yellow fever virus: application in assessment of YFV infection in Aedes aegypti*. Virol J, 2012. **9**(1): p. 27.
137. Drosten, C., et al., *Rapid detection and quantification of RNA of Ebola and Marburg viruses, Lassa virus, Crimean-Congo hemorrhagic fever virus, Rift Valley fever virus,*

REFERENCES

- dengue virus, and yellow fever virus by real-time reverse transcription-PCR.* J Clin Microbiol, 2002. **40**(7): p. 2323-30.
138. Bae, H.G., et al., *Detection of yellow fever virus: a comparison of quantitative real-time PCR and plaque assay.* J Virol Methods, 2003. **110**(2): p. 185-91.
139. Kwallah, A.O., et al., *A Real-Time Reverse Transcription Loop-Mediated Isothermal Amplification Assay For The Rapid Detection Of Yellow Fever Virus.* J Virol Methods, 2013. **193**(1): p. 23-7.
140. Domingo, C., et al., *Advanced yellow fever virus genome detection in point-of-care facilities and reference laboratories.* J Clin Microbiol, 2012.
141. Weaver, S.C., *Urbanization and geographic expansion of zoonotic arboviral diseases: mechanisms and potential strategies for prevention.* Trends in Microbiology, 2013. **21**(8): p. 360-363.
142. van den Hurk, A.F., et al., *Impact of *Wolbachia* on Infection with Chikungunya and Yellow Fever Viruses in the Mosquito Vector *Aedes aegypti*.* PLoS Negl Trop Dis. **6**(11): p. e1892.
143. *Yellow fever preparedness.* Lancet, 2008. **371**(9615): p. 786.
144. Frierson, J.G., *The yellow fever vaccine: a history.* Yale J Biol Med, 2010. **83**(2): p. 77-85.
145. Theiler, M. and H.H. Smith, *The Use of Yellow Fever Virus Modified by in Vitro Cultivation for Human Immunization.* J Exp Med, 1937. **65**(6): p. 787-800.
146. Norrby, E., *Yellow fever and Max Theiler: the only Nobel Prize for a virus vaccine.* J Exp Med, 2007. **204**(12): p. 2779-84.
147. Roukens, A.H. and L.G. Visser, *Yellow fever vaccine: past, present and future.* Expert Opin Biol Ther, 2008. **8**(11): p. 1787-95.
148. Barrett, A.D. and D.E. Teuwen, *Yellow fever vaccine - how does it work and why do rare cases of serious adverse events take place?* Curr Opin Immunol, 2009. **21**(3): p. 308-13.
149. Stock, N.K., et al., *The phylogeny of yellow fever virus 17D vaccines.* Vaccine, 2012. **30**(6): p. 989-94.
150. Poland, J.D., et al., *Persistence of neutralizing antibody 30-35 years after immunization with 17D yellow fever vaccine.* Bull World Health Organ, 1981. **59**(6): p. 895-900.
151. Jiang, X., et al., *Yellow fever 17D-vectored vaccines expressing Lassa virus GP1 and GP2 glycoproteins provide protection against fatal disease in guinea pigs.* Vaccine, 2011. **29**(6): p. 1248-57.
152. Barban, V., et al., *Broad neutralization of wild-type dengue virus isolates following immunization in monkeys with a tetravalent dengue vaccine based on chimeric yellow fever 17D/dengue viruses.* Virology, 2012. **429**(2): p. 91-8.
153. Guy, B., et al., *Preclinical and clinical development of YFV 17D-based chimeric vaccines against dengue, West Nile and Japanese encephalitis viruses.* Vaccine, 2010. **28**(3): p. 632-49.
154. Franco, D., et al., *Evaluation of yellow fever virus 17D strain as a new vector for HIV-1 vaccine development.* Vaccine, 2010. **28**(35): p. 5676-85.
155. Bonaldo, M.C., P.C. Sequeira, and R. Galler, *The yellow fever 17D virus as a platform for new live attenuated vaccines.* Hum Vaccin Immunother, 2014. **10**(5).
156. Breugelmans, J.G., et al., *Adverse events following yellow fever preventive vaccination campaigns in eight African countries from 2007 to 2010.* Vaccine, 2013.
157. Thomas, R.E., et al., *The Safety of Yellow Fever Vaccine 17D or 17DD in Children, Pregnant Women, HIV+ Individuals, and Older Persons: Systematic Review.* Am J Trop Med Hyg, 2012. **86**(2): p. 359-72.

REFERENCES

158. Thomas, R.E., et al., *Active and passive surveillance of yellow fever vaccine 17D or 17DD-associated serious adverse events: systematic review*. *Vaccine*, 2011. **29**(28): p. 4544-55.
159. Domingo, C. and M. Niedrig, *Safety of 17D derived yellow fever vaccines*. *Expert Opin Drug Saf*, 2009. **8**(2): p. 211-21.
160. Barrett, A.D., M. Niedrig, and D.E. Teuwen, *International laboratory network for yellow fever vaccine-associated adverse events*. *Vaccine*, 2008. **26**(43): p. 5441-2.
161. Hayes, E.B., *Is it time for a new yellow fever vaccine?* *Vaccine*, 2010. **28**(51): p. 8073-6.
162. Monath, T.P., et al., *Inactivated yellow fever 17D vaccine: development and nonclinical safety, immunogenicity and protective activity*. *Vaccine*, 2010. **28**(22): p. 3827-40.
163. Monath, T.P., et al., *An inactivated cell-culture vaccine against yellow fever*. *N Engl J Med*, 2011. **364**(14): p. 1326-33.
164. Bueno-Mari, R. and R. Jimenez-Peydro, *Global change and human vulnerability to vector-borne diseases*. *Front Physiol*, 2013. **4**: p. 158.
165. Vorou, R.M., V.G. Papavassiliou, and S. Tsiodras, *Emerging zoonoses and vector-borne infections affecting humans in Europe*. *Epidemiol Infect*, 2007. **135**(8): p. 1231-47.
166. Pugliese, A., T. Beltramo, and D. Torre, *Emerging and re-emerging viral infections in Europe*. *Cell Biochem Funct*, 2007. **25**(1): p. 1-13.
167. Lobermann, M., et al., *[Emerging viral diseases in Europe]*. *Dtsch Med Wochenschr*, 2012. **137**(17): p. 900-5.
168. Vaheri, A., et al., *Hantavirus infections in Europe and their impact on public health*. *Rev Med Virol*, 2013. **23**(1): p. 35-49.
169. Ertugrul, B., et al., *An outbreak of Crimean-Congo hemorrhagic fever in western Anatolia, Turkey*. *Int J Infect Dis*, 2009. **13**(6): p. e431-6.
170. Sotelo, E., J. Fernandez-Pinero, and M.A. Jimenez-Clavero, *[West Nile fever/encephalitis: re-emergence in Europe and the situation in Spain]*. *Enferm Infecc Microbiol Clin*, 2012. **30**(2): p. 75-83.
171. Charatan, F., *Organ transplants and blood transfusions may transmit West Nile virus*. *BMJ*, 2002. **325**(7364): p. 566.
172. Paty, M.C., *[The expansion of vector-borne diseases and the implications for blood transfusion safety: The case of West Nile Virus, dengue and chikungunya]*. *Transfus Clin Biol*, 2013. **20**(2): p. 165-73.
173. Diseases of, E., P. Zoonotic Origin Team European Centre for Disease, and Control, *Chikungunya in Italy: actions in and implications for the European Union*. *Euro Surveill*, 2007. **12**(9): p. E070906 2.
174. *Outbreak news. Dengue fever in Madeira, Portugal*. *Wkly Epidemiol Rec*, 2012. **87**(43): p. 413.
175. Gould, E.A., et al., *First cases of autochthonous dengue fever and chikungunya fever in France: from bad dream to reality!* *Clin Microbiol Infect*, 2010. **16**(12): p. 1702-4.
176. Marchand E, P.C., Jeannin C, Lafont E, Bergmann T, Flusin O, Rizzi J, Roux N, Busso V, Deniau J, Noel H, Vaillant V, Leparç-Goffart I, Six C, Paty MC, *Autochthonous case of dengue in France, October 2013*. *Euro Surveill.*, 2013(18(50):pii=20661).
177. Domingo, C., et al., *First international external quality assessment study on molecular and serological methods for yellow fever diagnosis*. *PLoS One*, 2012. **7**(5): p. e36291.
178. Escadafal, C., et al., *Second external quality assurance study for the serological diagnosis of hantaviruses in Europe*. *PLoS Negl Trop Dis*, 2012. **6**(4): p. e1607.

REFERENCES

179. Escadafal, C., et al., *First international external quality assessment of molecular detection of Crimean-Congo hemorrhagic fever virus*. PLoS Negl Trop Dis, 2012. **6**(6): p. e1706.
180. Escadafal, C., et al., *International external quality assessment of molecular detection of rift valley Fever virus*. PLoS Negl Trop Dis, 2013. **7**(5): p. e2244.
181. Mantel, N., et al., *Standardized quantitative RT-PCR assays for quantitation of yellow fever and chimeric yellow fever-dengue vaccines*. J Virol Methods, 2008. **151**(1): p. 40-6.
182. Brown, T.M., et al., *Detection of yellow fever virus by polymerase chain reaction*. Clin Diagn Virol, 1994. **2**(1): p. 41-51.
183. Domingo, C., et al., *2nd International external quality control assessment for the molecular diagnosis of dengue infections*. PLoS Negl Trop Dis, 2010. **4**(10): p. 0000833.
184. Biel, S.S., et al., *Quality control measures for the serological diagnosis of hantavirus infections*. J Clin Virol, 2003. **28**(3): p. 248-56.
185. Niedrig, M., et al., *International diagnostic accuracy study for the serological detection of chikungunya virus infection*. Clin Microbiol Infect, 2009. **15**(9): p. 880-4.
186. Sanchini, A., et al., *Second international diagnostic accuracy study for the serological detection of west nile virus infection*. PLoS Negl Trop Dis, 2013. **7**(4): p. e2184.
187. Donoso Mantke, O. and H. Zeichhardt, *Final Report External Quality Assessment Scheme (EQAS) on Virus Immunology - Hantaviruses*. Gesellschaft zur Förderung der Qualitätssicherung in medizinischen Laboratorien e. V (I N S T A N D e. V.), 2013.
188. Piepenburg, O., et al., *DNA detection using recombination proteins*. PLoS Biol, 2006. **4**(7): p. e204.
189. TwistDx, *Appendix to the TwistAmp reaction kit manuals*.
190. Euler, M., et al., *Recombinase polymerase amplification assay for rapid detection of Rift Valley fever virus*. J Clin Virol, 2012. **54**(4): p. 308-12.
191. Escadafal, C., et al., *Rapid Molecular Assays for the Detection of Yellow Fever Virus in Low-Resource Settings*. PLoS Negl Trop Dis, 2014. **8**(3): p. e2730.
192. Diallo, D., et al., *Landscape ecology of sylvatic chikungunya virus and mosquito vectors in southeastern Senegal*. PLoS Negl Trop Dis, 2012. **6**(6): p. e1649.
193. Euler, M., et al., *Recombinase polymerase amplification assay for rapid detection of Rift Valley fever virus*. J Clin Virol, 2012.
194. Euler, M., et al., *Recombinase Polymerase Amplification Assay for Rapid Detection of Francisella tularensis*. J Clin Microbiol, 2012. **50**(7): p. 2234-8.
195. Linke, S., et al., *Detection of West Nile virus lineages 1 and 2 by real-time PCR*. J Virol Methods, 2007. **146**(1-2): p. 355-8.
196. Achazi, K., et al., *Detection and differentiation of tick-borne encephalitis virus subtypes by a reverse transcription quantitative real-time PCR and pyrosequencing*. J Virol Methods, 2011. **171**(1): p. 34-9.
197. Patel, P., et al., *Development of one-step quantitative reverse transcription PCR for the rapid detection of flaviviruses*. Virol J, 2013. **10**: p. 58.
198. Weidmann, M., et al., *Rapid detection of important human pathogenic Phleboviruses*. J Clin Virol, 2008. **41**(2): p. 138-42.
199. Weidmann, M., E. Muhlberger, and F.T. Hufert, *Rapid detection protocol for filoviruses*. J Clin Virol, 2004. **30**(1): p. 94-9.
200. Domingo, C., et al., *Detection of yellow fever 17D genome in urine*. J Clin Microbiol, 2011. **49**(2): p. 760-2.
201. Euler, M., et al., *Development of a panel of recombinase polymerase amplification assays for detection of biothreat agents*. J Clin Microbiol, 2013. **51**(4): p. 1110-7.

REFERENCES

202. Brandt, W.E., et al., *Partial purification and characterization of a dengue virus soluble complement-fixing antigen*. J Immunol, 1970. **105**(6): p. 1565-8.
203. Mackenzie, J.M., M.K. Jones, and P.R. Young, *Immunolocalization of the dengue virus nonstructural glycoprotein NS1 suggests a role in viral RNA replication*. Virology, 1996. **220**(1): p. 232-40.
204. Lindenbach, B.D. and C.M. Rice, *trans-Complementation of yellow fever virus NS1 reveals a role in early RNA replication*. J Virol, 1997. **71**(12): p. 9608-17.
205. Youn, S., et al., *Non-structural protein-1 is required for West Nile virus replication complex formation and viral RNA synthesis*. Virol J, 2013. **10**(1): p. 339.
206. Young, P.R., et al., *An antigen capture enzyme-linked immunosorbent assay reveals high levels of the dengue virus protein NS1 in the sera of infected patients*. J Clin Microbiol, 2000. **38**(3): p. 1053-7.
207. Alcon, S., et al., *Enzyme-linked immunosorbent assay specific to Dengue virus type 1 nonstructural protein NS1 reveals circulation of the antigen in the blood during the acute phase of disease in patients experiencing primary or secondary infections*. J Clin Microbiol, 2002. **40**(2): p. 376-81.
208. Zainah, S., et al., *Performance of a commercial rapid dengue NS1 antigen immunochromatography test with reference to dengue NS1 antigen-capture ELISA*. J Virol Methods, 2009. **155**(2): p. 157-60.
209. Wang, S.M. and S.D. Sekaran, *Evaluation of a commercial SD dengue virus NS1 antigen capture enzyme-linked immunosorbent assay kit for early diagnosis of dengue virus infection*. J Clin Microbiol, 2010. **48**(8): p. 2793-7.
210. Thomas, L., et al., *Relationship between nonstructural protein 1 detection and plasma virus load in Dengue patients*. Am J Trop Med Hyg, 2010. **83**(3): p. 696-9.
211. Libraty, D.H., et al., *High circulating levels of the dengue virus nonstructural protein NS1 early in dengue illness correlate with the development of dengue hemorrhagic fever*. J Infect Dis, 2002. **186**(8): p. 1165-8.
212. Chung, K.M. and M.S. Diamond, *Defining the levels of secreted non-structural protein NS1 after West Nile virus infection in cell culture and mice*. J Med Virol, 2008. **80**(3): p. 547-56.
213. Geysen, H.M., R.H. Meloen, and S.J. Barteling, *Use of peptide synthesis to probe viral antigens for epitopes to a resolution of a single amino acid*. Proc Natl Acad Sci U S A, 1984. **81**(13): p. 3998-4002.
214. Geysen, H.M., S.J. Barteling, and R.H. Meloen, *Small peptides induce antibodies with a sequence and structural requirement for binding antigen comparable to antibodies raised against the native protein*. Proc Natl Acad Sci U S A, 1985. **82**(1): p. 178-82.
215. Stock, N., *Molekularepidemiologische Analysen von Gelbfiebertvirusisolaten und Entwicklung neuer Nachweismethoden zur Untersuchung und Diagnostik von Gelbfiebertviren*. PhD Dissertation submitted at the Freien Universität Berlin, 2014: p. 199.
216. Gelderblom, H.R., et al., *Comparative immunoelectron microscopy with monoclonal antibodies on yellow fever virus-infected cells: pre-embedding labelling versus immunocytochemistry*. J Virol Methods, 1985. **10**(3): p. 225-39.
217. Kozuch, O. and V. Mayer, *Pig kidney epithelial (PS) cells: a perfect tool for the study of flaviviruses and some other arboviruses*. Acta Virol, 1975. **19**(6): p. 498.
218. Macdonald, J., et al., *NS1 protein secretion during the acute phase of West Nile virus infection*. J Virol, 2005. **79**(22): p. 13924-33.
219. Erra, E.O., et al., *Dengue in Travelers: Kinetics of Viremia and NS1 Antigenemia and Their Associations with Clinical Parameters*. PLoS One, 2013. **8**(6).

REFERENCES

220. Li, Y.Z., et al., *A specific and sensitive antigen capture assay for NS1 protein quantitation in Japanese encephalitis virus infection*. J Virol Methods, 2012. **179**(1): p. 8-16.
221. Hsieh, C.J. and M.J. Chen, *The commercial dengue NS1 antigen-capture ELISA may be superior to IgM detection, virus isolation and RT-PCR for rapid laboratory diagnosis of acute dengue infection based on a single serum sample*. J Clin Virol, 2009. **44**(1): p. 102.
222. Lima Mda, R., et al., *Comparison of three commercially available dengue NS1 antigen capture assays for acute diagnosis of dengue in Brazil*. PLoS Negl Trop Dis, 2010. **4**(7): p. e738.
223. Schlesinger, J.J., M.W. Brandriss, and E.E. Walsh, *Protection against 17D yellow fever encephalitis in mice by passive transfer of monoclonal antibodies to the nonstructural glycoprotein gp48 and by active immunization with gp48*. J Immunol, 1985. **135**(4): p. 2805-9.
224. Gould, E.A., et al., *Neutralizing (54K) and non-neutralizing (54K and 48K) monoclonal antibodies against structural and non-structural yellow fever virus proteins confer immunity in mice*. J Gen Virol, 1986. **67** (Pt 3): p. 591-5.
225. Schlesinger, J.J., et al., *Protection against yellow fever in monkeys by immunization with yellow fever virus nonstructural protein NS1*. J Virol, 1986. **60**(3): p. 1153-5.
226. Krishna, V.D., M. Rangappa, and V. Satchidanandam, *Virus-specific cytolytic antibodies to nonstructural protein 1 of Japanese encephalitis virus effect reduction of virus output from infected cells*. J Virol, 2009. **83**(10): p. 4766-77.
227. Diamond, M.S., T.C. Pierson, and D.H. Fremont, *The structural immunology of antibody protection against West Nile virus*. Immunol Rev, 2008. **225**: p. 212-25.
228. Chung, K.M., et al., *Antibodies against West Nile Virus nonstructural protein NS1 prevent lethal infection through Fc gamma receptor-dependent and -independent mechanisms*. J Virol, 2006. **80**(3): p. 1340-51.
229. Chung, K.M., et al., *Antibody recognition of cell surface-associated NS1 triggers Fc-gamma receptor-mediated phagocytosis and clearance of West Nile Virus-infected cells*. J Virol, 2007. **81**(17): p. 9551-5.
230. Hoffmann, C., et al., *Fluorescent labeling of tetracysteine-tagged proteins in intact cells*. Nat Protoc, 2010. **5**(10): p. 1666-77.
231. Tsien, R.Y., *The green fluorescent protein*. Annu Rev Biochem, 1998. **67**: p. 509-44.
232. Shaner, N.C., P.A. Steinbach, and R.Y. Tsien, *A guide to choosing fluorescent proteins*. Nat Meth, 2005. **2**(12): p. 905-909.
233. Gautier, A., et al., *An engineered protein tag for multiprotein labeling in living cells*. Chem Biol, 2008. **15**(2): p. 128-36.
234. Soh, N., *Selective Chemical Labeling of Proteins with Small Fluorescent Molecules Based on Metal-Chelation Methodology*. Sensors, 2008. **8**(2): p. 1004-1024.
235. Griffin, B.A., S.R. Adams, and R.Y. Tsien, *Specific covalent labeling of recombinant protein molecules inside live cells*. Science, 1998. **281**(5374): p. 269-72.
236. Adams, S.R., et al., *New biarsenical ligands and tetracysteine motifs for protein labeling in vitro and in vivo: synthesis and biological applications*. J Am Chem Soc, 2002. **124**(21): p. 6063-76.
237. Adams, S.R. and R.Y. Tsien, *Preparation of the membrane-permeant biarsenicals FLaSH-EDT2 and ReAsH-EDT2 for fluorescent labeling of tetracysteine-tagged proteins*. Nat. Protocols, 2008. **3**(9): p. 1527-1534.
238. Pereira, C.F., et al., *Labeling of multiple HIV-1 proteins with the biarsenical-tetracysteine system*. PLoS One, 2011. **6**(2): p. e17016.
239. Li, Y., et al., *Genetically engineered, biarsenically labeled influenza virus allows visualization of viral NS1 protein in living cells*. J Virol, 2010. **84**(14): p. 7204-13.

REFERENCES

240. Panchal, R.G., et al., *In vivo oligomerization and raft localization of Ebola virus protein VP40 during vesicular budding*. Proc Natl Acad Sci U S A, 2003. **100**(26): p. 15936-41.
241. Arhel, N.J. and P. Charneau, *Bisarsenical labeling of HIV-1 for real-time fluorescence microscopy*. Methods Mol Biol, 2009. **485**: p. 151-9.
242. Roy Chowdhury, P., *Establishment of a Yellow fever virus neutralization assay and FLAsH labelling of virus proteins*. Diploma Thesis submitted at the Technical University of Berlin, 2010.
243. Ma, L., et al., *Solution structure of dengue virus capsid protein reveals another fold*. Proceedings of the National Academy of Sciences of the United States of America, 2004. **101**(10): p. 3414-3419.
244. Bredenbeek, P.J., et al., *A stable full-length yellow fever virus cDNA clone and the role of conserved RNA elements in flavivirus replication*. J Gen Virol, 2003. **84**(Pt 5): p. 1261-8.
245. Whitt, M.A. and C.E. Mire, *Utilization of fluorescently-labeled tetracysteine-tagged proteins to study virus entry by live cell microscopy*. Methods, 2011. **55**(2): p. 127-36.
246. Rutkowska, A., C.H. Haering, and C. Schultz, *A FLAsH-based cross-linker to study protein interactions in living cells*. Angew Chem Int Ed Engl, 2011. **50**(52): p. 12655-8.
247. Sun, S., et al., *Visualizing hepatitis B virus with biarsenical labelling in living cells*. Liver Int, 2013.
248. Zheng, Y. and M. Kielian, *Imaging of the alphavirus capsid protein during virus replication*. J Virol, 2013. **87**(17): p. 9579-89.
249. Griffin, B.A., et al., *Fluorescent labeling of recombinant proteins in living cells with FLAsH*. Methods Enzymol, 2000. **327**: p. 565-78.
250. Stroffekova, K., C. Proenza, and K.G. Beam, *The protein-labeling reagent FLASH-EDT2 binds not only to CCXXCC motifs but also non-specifically to endogenous cysteine-rich proteins*. Pflugers Arch, 2001. **442**(6): p. 859-66.
251. Turville, S.G., et al., *Resolution of de novo HIV production and trafficking in immature dendritic cells*. Nat Methods, 2008. **5**(1): p. 75-85.
252. Gaunt, M.W. and E.A. Gould, *Rapid subgroup identification of the flaviviruses using degenerate primer E-gene RT-PCR and site specific restriction enzyme analysis*. J Virol Methods, 2005. **128**(1-2): p. 113-27.

LIST OF MATERIALS

CHEMICALS

Acetone	Carl Roth, Karlsruhe
Agar	Invitrogen, Karlsruhe
Agarose	Biozym, Oldendorf
Amido Black	Carl Roth, Karlsruhe
Ammonium peroxodisulfate (APS)	Carl Roth, Karlsruhe
β -Mercaptoethanol	Sigma-Aldrich, Munich
Bovine Serum Albumin solution (100x)	New England Biolabs
Bromphenol blue	Merck, Darmstadt
Cap Analog (m7G(5')ppp(5')G)	Applied Biosystems, USA
Carboxymethylcellulose (CMC)	BDH Chemicals, Poole, UK
Dimethylsulfoxid (DMSO)	Merck, Darmstadt
Dinatriumhydrogenphosphate (Na_2HPO_4)	Merck, Darmstadt
Desoxyribonucleosidtriphosphat-Mix (dNTP-Mix)	Eppendorf, Hamburg
Dithiothreitol (DTT)	Invitrogen, Karlsruhe
Ethanol	Carl Roth, Karlsruhe
Ethidium bromide, 0,025 %	Carl Roth, Karlsruhe
Ethylenediaminetetraacetic acid (EDTA)	Merck, Darmstadt
Formaldehyde	Carl Roth, Karlsruhe
Glycerin	Merck, Darmstadt
IIFT-mounting medium	EUROIMMUN AG, Lübeck
Isopropanol	Merck, Darmstadt
Lipofectamin™ 2000	Invitrogen, Karlsruhe
Magnesium acetate (280 mM)	TwistDx Limited, Cambridge
Magnesium chloride solution (50 mM)	Eppendorf, Hamburg
Methanol	Carl Roth, Karlsruhe
Milchpulver	Carl Roth, Karlsruhe
Sodium acetate	Sigma-Aldrich, Munich
Sodium bicarbonate	Merck, Darmstadt
Sodium carbonate decahydrate	Merck, Darmstadt
Sodium chloride	Merck, Darmstadt
Sodium hydroxide	Merck, Darmstadt
Polyacrylamide (PAA) (Rotiphorese® Gel 30; 37.5:1)	Carl Roth, Karlsruhe
Prolong® Gold antifade reagent with DAPI	Invitrogen, Karlsruhe
Ribonucleoside triphosphate-Mix (rNTP-Mix)	Invitrogen, Karlsruhe
Sulphuric acid	Merck, Darmstadt
Sodium dodecyl sulfate (SDS)	Serva, Heidelberg
Select Agar	Invitrogen, Karlsruhe
N, N, N', N'-Tetramethylethylenediamine (TEMED)	Carl Roth, Karlsruhe
Tris-Hydroxymethyl-Aminomethane (Tris)	Carl Roth, Karlsruhe
tRNA	Sigma-Aldrich, Munich
Tryptose-Phosphate Broth	Sigma-Aldrich, Munich
Tween® 20	Merck, Darmstadt
Water (RNase free for molecular use)	Eppendorf, Hamburg

LIST OF MATERIALS

KITS

BigDye [®] Terminator v3.1 Cycle Sequencing Kit	Applied Biosystems, USA
IIFT Flavivirus Mosaic 3	EUROIMMUN AG,Lübeck
IIFT Yellow fever virus	EUROIMMUN AG,Lübeck
Invisorb Spin Plasmid Mini Two Kit	STRATEC Molecular, Berlin
QIAamp [®] Viral RNA Mini Kit	Qiagen, Hilden
QIAshredder columns	Qiagen, Hilden
RNeasy [®] Mini Kit	Qiagen, Hilden
Pierce ECL Western Blotting Substrate	Pierce, Rockford, IL, USA
Invisorb [®] Spin DNA Extraction Kit	STRATEC Molecular, Berlin
QIAquick Gel Extraction Kit	Qiagen, Hilden
QuantiTect Virus + ROX Vial Kit	Qiagen, Hilden
QIAquick PCR Purification Kit	Qiagen, Hilden
MSB Spin PCRapace	STRATEC Molecular, Berlin
QIAGEN Plasmid Maxi Kit	Qiagen, Hilden
HiSpeed Plasmid Maxi Kit	Qiagen, Hilden
TMB Peroxidase ELISA Substrate Kit	BioRad,Laboratories,USA
TwistAmp [®] exo and nfo	TwistDx Limited, Cambridge

ENZYMES AND INHIBITORS

Nsil restriction enzyme	New England Biolabs [®] , Frankfurt/Main
NotI restriction enzyme	New England Biolabs [®] , Frankfurt/Main
XhoI restriction enzyme	New England Biolabs [®] , Frankfurt/Main
Platinum [®] Taq DNA-Polymerase (5 U/μl)	Invitrogen, Karlsruhe
AmpliTaq Gold [®] DNA-Polymerase	Applied Biosystems, Carlsbad, CA, USA
SP6 RNA Polymerase (20 U/μl)	Applied Biosystems, Carlsbad, CA, USA
SuperScript [™] III Reverse Transcriptase	Invitrogen, Karlsruhe
T4-DNA-Ligase (5 U/μl)	Fermentas, St. Leon-Rot
RNasin [®] Ribonuclease-Inhibitor	Promega, Madison, USA
RNase Out (RNase-Inhibitor) (40 U/μl)	Invitrogen, Karlsruhe
Cap Structure Analog m7G(5')ppp(5')G	New England Biolabs [®] , Frankfurt/Main

LIST OF PROTEIN AND DNA MARKERS

Quick-Load [®] 1 kb DNA Ladder	New England Biolabs [®] , Frankfurt/Main
Prestained Protein Marker, Page Ruler	Fermentas, St. Leon-Roth

LIST OF MATERIALS

OLIGONUCLEOTIDES

Table 0-1: Primers used for YFV PCR and sequencing

YFV prot.	Primer	Orientation	Sequence (5'→3')	5'-pos. in YFV genome	3'-pos. in YFV genome	5'-pos. in YFV clone	3'-Pos. in YFV clone
	E-S0 [#]	sense	GTT CCG CGC ACA TTT CC	-	-	513	529
	Not1_hin [#]	sense	TGA CGT GTC GAC GCG GCC G	-	-	545	563
5'NTR	U1 s	sense	AGT AAA TCC TGT GTG CTA ATT GAG GT	1	26	809	834
	E-S1 [#]	sense	GCG TCA ATA TGG TAC GAC GAG	152	172	960	980
C	U1b as	antisense	TGT TTG ACA AGG AGC GAA CTC CT	172	194	980	1002
	U1c s	sense	ATG CTG GAC CCA AGA CAA GGC T	329	350	1137	1158
	U1d s	sense	AGA GAG TGG TGG CCA GTT TGA T	372	393	1180	1201
	E-S2 [#]	sense	GTA CTG GTG CCC AGA CTC AAT G	594	615	1402	1423
prM	U2 s	sense	AAC GTT AGA GTC GCA TAT GGT AAG T	689	713	1497	1521
	U1 as	antisense	TTT CTT GCC GGG TCT TCA AAC CAT	777	800	1585	1608
M	E-S3 [#]	sense	GTT GGT CCG GCC TAC TCA	955	972	1763	1780
	E-as6 [#]	antisense	TGA GTA GGC CGG ACC AAC	955	972	1763	1780
	E-S4 [#]	sense	CAA TGC GTG CAA GCG CAC	1239	1256	2047	2064
	E-as5 [#]	antisense	GTG CGC TTG CAC GCA TTG	1239	1256	2047	2064
	164 s	sense	GCC AAA TTC ACT TGT GTC AAA TTC AT	1322	1347	2130	2155
	YF-Erev [#]	antisense	GCA ATT GTG CTC TGA TGA C	1385	1403	2193	2211
	U2 as	antisense	CTG ATA GTG CAT CAA ACT TGA GAG T	1445	1469	2253	2277
	E-S5 [#]	sense	GCT CCC AGG AAG TCG AGT TC	1469	1488	2277	2296
	E-as4 [#]	antisense	GAA CTC GAC TTC CTG GGA GC	1469	1488	2277	2296
	U3 s	sense	CCT GCC ATG GCA GAG TGG AAG T	1615	1636	2423	2444
	E-S6 [#]	sense	CAA CTG ACA CTG GCC ATG	1901	1918	2709	2726
	E-as3 [#]	antisense	CAT GGC CAG TGT CAG TTG	1901	1918	2709	2726
E	E1 s	sense	TGG CAC AAA GAG GGG AGT TCA ATA GGA	2138	2164	2946	2972
	U4 s	sense	CTC CGC TGG AGG GTT CTT CAC T	2236	2257	3044	3065
	U4b s	sense	CTC CGC TGG AGG GTY CTT CAC T	2236	2257	3044	3065
	164 as	antisense	CCA ACC GAA GTG AAG AAC CCT CCA	2242	2265	3050	3073
	E-S7 [#]	sense	GTT TGG CTC TGC CTT TCA G	2283	2301	3091	3109
	E-as2 [#]	antisense	CTG AAA GGC AGA GCC AAA C	2283	2301	3091	3109
	U3 as	antisense	TGT TAT CCA GTT CAA GCC GCC AAA T	2308	2332	3116	3140
	U4c s	sense	ATT TGG CGG CTT GAA CTG GAT AAC A	2308	2332	3116	3140
	YF-Efor [#]	sense	CAT GAT CTT GGT AGG AGT G	2401	2419	3209	3227
	E-S8 [#]	sense	GAG ACT CTG ATG ACT GG	2519	2535	3327	3343
	E-as1 [#]	antisense	CCA GTC ATC AGA GTC TC	2519	2535	3327	3343
NS1	E2 s	sense	ATG AGA TGT GGA GAA GCA GGG CAG AT	2646	2671	3454	3479
	E2 as	antisense	ATC TGC CCT GCT TCT CCA CAT CTC AT	2646	2671	3454	3479
	U2b as	antisense	CCC GTC CCA AAC TCC TCT ATC T	2913	2934	3721	3742

LIST OF MATERIALS

	Mlu1_rück #	antisense	ATG TAC ACG CGT GTG GTG AA	2938	2957	3746	3765
	E-as0 #	antisense	CGC AGT CTA TGG TGT ATT C	2971	2989	3779	3797
	76 s	sense	GGA GGC CCA GTT AGC TCT CAC AAT CAT A	3194	3221	4002	4029
	U4c as	antisense	CCT CAC TTC TAG TGG TAC CTG CAT	3257	3278	4065	4086
	E1 as	antisense	GGA CAC GCT TCT CTC CTC ACT TCT A	3270	3288	4078	4096
	U4 as	antisense	CTG GAC ACG CTT CTC TCC TCA CT	3274	3296	4082	4104
	U4b as	antisense	CCC GCT ATC CGT GGT GGA TC	3348	3367	4156	4175
	76b as	antisense	ACC ACT TCC ATT GCT ATC ATC ATG C	3543	3567	4351	4375
	3597 s	sense	ATG CTG GTT GGA GGA GTG GTG CT	3596	3618	4404	4426
	3666 as	antisense	TCA GCA AAT CAA GGA GAG TTA CCT G	3644	3665	4452	4473
	U5 s	sense	GCT GAG GTG AGA CTT GCC GCA AT	3989	4011	4797	4819
NS2a	76 as	antisense	AGT GTG AGG GCC ACC AGA GGT ATA GTC TT	4076	4104	4884	4912
	119 s	sense	TGC ATT TCT GGC AAC CCG CAT	4147	4167	4955	4975
NS2b	U5 as	antisense	GAA AGC CAG TCC TGC CAG CAC T	4225	4245	5033	5053
	FJb s	sense	AGG TTC AGT TGA TTG CTG CTG T	4857	4878	5665	5686
	U6 s	sense	CTA CCC GAG TGG CAC TTC AGG AT	4966	4988	5774	5796
	119 as	antisense	GAC ACG AAG GAG TTG TCA CCG ACA A	5043	5067	5851	5875
	5375 as	antisense	TAA GTT AGG GTG GCA TGG CAC AT	5363	5385	6171	6193
	98 s	sense	TGG ATC CAG CTA GCA TAG CCG CT	5451	5473	6259	6281
NS3	U6 as	antisense	CTG GGT ATG TCC GTT TGAACA TCT	5583	5607	6391	6415
	U3b s	sense	ACG GCA TGG TTC CTT CCA TCC AT	5657	5679	6465	6487
	U7 s	sense	GAC CAG CCG GTA TGG CTT TCG T	6203	6224	7011	7032
	98 as	antisense	CTT GGG CGC AGA GGC TTC TTT G	6345	6366	7153	7174
	100 s	sense	AAA GAA GCC TCT GCG CCC AAG G	6346	6367	7154	7175
	U7 as	antisense	CCT CCT ACC TTC AGC AAA CTT GAT	6419	6439	7227	7247
	U8 s	sense	CTT ACC GCA ATG CAC TAT CAA TGA T	6555	6579	7363	7387
	U9b s	sense	GAA TAG CCC AGT CAG CCT CAG T	7092	7113	7900	7921
NS4a	U9 s	sense	CAT AAT GCT GCT GGT CAG TGG CT	7165	7187	7973	7995
	100 as	antisense	GGT AAA ATG AGA GAC CAG TGG AGC ATG GC	7232	7260	8040	8068
	U8 as	antisense	GTA AAA TGA GAG ACC AGT GGA GCA T	7235	7259	8043	8067
NS4b	U9c s	sense	TGG CTG AAG GCA TTG TCC TAG CAT	7464	7487	8272	8295
	U9b as	antisense	AGA TTC AGT TCC CTC TTC CAG ACT	7666	7689	8474	8497
	U10 s	sense	TTT ACT CTT GGA AGA GAC GGC CAT	7943	7966	8751	8774
NS5	U9 as	antisense	GTT TTG TCC TTG AAG GTG ATG ATG T	8001	8025	8809	8833
	U9c as	antisense	TGT GAC GCA TGA CGA TGA TGA CT	8082	8104	8890	8912
	150 s	sense	CCC GCA GCA ATG TCA CAT TTA CTG T	8310	8334	9118	9142
	U10 as	antisense	GGT CCC TTG TCT GTC TCA ACA CT	8429	8451	9237	9259

LIST OF MATERIALS

	U11 s	sense	GTG TCG GAC TTG TGT GTA CAA CAT GAT	8977	9003	9785	9811
	150 as	antisense	CAT CCG CGT AGA ATC CAC CAC C	9218	9239	10026	10047
	U14s #	sense	GAATGGCAGAAAGCAGAGATG	9504	9523	10312	10331
	U14as #	antisense	CATCTCTGCTTCTGCCATTC	9504	9523	10312	10331
	176 s	sense	ATT GTG GTG CCT TGC CGA GAA CA	9818	9840	10626	10648
	U11 as	antisense	CAC ATG TTG GCA TAG GCC TTG CT	9911	9933	10719	10741
	U12 s	sense	XAC CAA CAA CCC ACA CAT GCA GGA	10102	10125	10910	10933
	U13s #	sense	GACCTGCAACCGGGTGAGCTTATC	10328	10351	11136	11159
	U13as #	antisense	GATAAGCTCACCCGGTTGCAGGTC	10328	10351	11136	11159
	U12b s	sense	CTC CAC ACA TTG AGA CAG AAG AAG T	10511	10535	11319	11343
	U15s #	sense	CTGGTTTCTGGGACCTCCAC	10625	10645	11433	11453
3'NTR	U15as #	antisense	GTGGGAGGTCCCAGAAACCAG	10625	10645	11433	11453
	176 as	antisense	CCT GGC GTC AAT ATG GTC CCA CT	10743	10765	11551	11573
	U12 as	antisense	GGT TTT GTG TTT GTC ATC CAA AGG T	10835	10859	11643	11667

Table 0-2: Flavivirus universal primers

Name	Orientation	Sequence (5' → 3')	YFV prot.	Ref.
Unifor	sense	TGG GGN AAY SRN TGY GGN YTN TTY GG	E	[252]
Unirev	antisense	CCN CCH RNN GAN CCR AAR TCC CA	E	

Table 0-3: FIAsh tag primers

Name	Orientation	Sequence (5' → 3')	Target	Provider
Flash-for	sense	TGT TGT CCC GGG TGT TGT	TC-Tag	Invitrogen
Flash-back	antisense	ACA ACA CCC GGG ACA ACA	TC-Tag	Invitrogen

Table 0-4: Oligonucleotides for real-time YFV RT-PCR

Name	Orientation	Sequence (5' → 3')	YFV protein	Reference
YFV FP	sense	ATT GAG GTG CAT TGG TCT GC	5'-NTR	
YFV RP	antisense	GTC RGT TCT CTG CTA ATC GCT CA	5'-NTR	[134]
YFV LNA2	probe	AGTTGCTARGCA+AT+A+A+A	5'-NTR	

LIST OF MATERIALS

Table 0-5: Oligonucleotides for YFV RPA

RPA format	Name	Orientation	Sequence (5' → 3')
Lateral-flow strip RT-RPA	YFV RF2	sense	AAATCCTGTGTGCTAATTGAGGTGYATTGG
	YFV RR2-Bio	antisense	Biotin- ACATDWTCTGGTCARTTCTCTGCTAATCGC
	YFV Rprobe nfo	sense	FAM-CTGCAAATCGAGTTGCTAGGCAATAAACAC-[THF] TTTGGATT-AATTTTRATCGTT-Ph
Real-time RT-RPA	YFV RF2	sense	AAATCCTGKGTGCTAATTGAGGTGYATTGG
	YFV RR2	antisense	ACATDWTCTGGTCARTTCTCTGCTAATCGC
	YFV Rprobe exo	sense	gCAAATCgAgTTgCTAggCAATAAACACATT [BHQdT]g[THF]A[FAMdT]TAATTTTRATCgTTC-Ph

ANTIBODIES AND CORRESPONDING ANTIGENIC PEPTIDES

Table 0-6: Peptides for Immunization

Name	Target protein	Peptide sequence	Provider
R1	YFV NS1	C-KQK TKQ IGN RPG PSR	Eurogentec, Belgium
RC	YFV-C	QDP KNV YQR GTH PFS-C	Eurogentec, Belgium
P1	YFV NS1	RKN GSF IID GKS RKE-C	Eurogentec, Belgium
P2	YFV NS1	VNG KKS AHG SPT FWM-C	Eurogentec, Belgium

Table 0-7: Polyclonal antibodies

Name	Target	Specification	Provider
Anti-YFV NS1 R1	YFV NS1	Rabbit serum	-
Anti-YFV-C RC	YFV-C	Rabbit serum	-
Anti-YFV NS1 R1 IgG	YFV NS1	Rabbit-IgG	Eurogentec, Belgium
Anti-YFV NS1 R1 IgG-HRP	YFV NS1	Rabbit-IgG	Eurogentec, Belgium
Anti-YFV NS1 R1 IgG-Biotin	YFV NS1	Rabbit-IgG	Eurogentec, Belgium
Anti-YFV NS1 P1	YFV NS1	Guinea pig serum	Eurogentec, Belgium
Anti-YFV NS1 P2	YFV NS1	Guinea pig serum	Eurogentec, Belgium
Anti-YFV NS1 P1/2	YFV NS1	Guinea pig serum	Eurogentec, Belgium

LIST OF MATERIALS

Table 0-8: Monoclonal antibodies

Name	Target protein	Specification	Concentration	Provider
MAB6330	YFV-E	monoclonal mouse antibody	1,2 mg/ml	[216]

Table 0-9: Secondary labeled antibodies

Name	Target	Specification	Provider
goat-anti-mouse FITC	Mouse-IgG	Polyclonal goat-anti-mouse antibody	Dianova
goat-anti-rabbit FITC	Rabbit-IgG	Polyclonal goat-anti-mouse antibody	Dianova
goat-anti-guinea pig-HRP	Guinea pig-IgG	Polyclonal goat-anti-GP antibody	Pierce
goat-anti-mouse HRP	Mouse-IgG	Polyclonal goat-anti-mouse antibody	Pierce
goat-anti-rabbit poly-HRP	Rabbit-IgG	Polyclonal goat-anti-mouse antibody	Pierce
Streptavidin-HRP	Biotin	Streptavidin-HRP	Sigma

VIRUS STRAINS

Table 0-10: Virus strains used for sequence analysis of the NS1 protein

Type of strain	Accession number	Virus
YFV vaccine	U21055.1	YFU21055 Yellow fever virus French neurotropic strain
	U17066.1	YFU17066 Yellow fever virus vaccine strain 17DD
	DQ118157.1	Yellow fever virus isolate YF-AVD2791-93F/04 from Spain
	NC_002031.1	Yellow fever virus (NCBI Reference, YFV-17D-204, USA)
	DQ100292.1	Yellow fever virus strain 17DD-Brazil
	X03700.1	Yellow fever virus complete genome, (YFV-17D-204_1 (USA))
	X15062.1	Yellow fever virus genomic RNA (YFV-17D-204_2 (Pasteur))
YFV wild strains	AY640589.1	Yellow fever virus strain ASIBI
	AY603338.1	Yellow fever virus strain Ivory Coast 1999
	AY572535.1	Yellow fever virus strain Gambia 2001
	U21056.1	YFU21056 Yellow fever virus French viscerotropic strain
	AF094612.1	Yellow fever virus strain Trinidad 79A isolate 788379
	U54798.1	YFU54798 Yellow fever virus strain 85-82H Ivory Coast
	DQ235229.1	Yellow fever virus strain Couma
	AY968065.1	Yellow fever virus strain Uganda48a
	AY968064.1	Yellow fever virus strain Angola71
Other flaviviruses	NC_001477	Dengue virus 1
	NC_001474	Dengue virus 2
	NC_001475	Dengue virus 3
	NC_001672	Tick-borne encephalitis virus (FSME-Virus)
	NC_007580	St.Louis encephalitis virus
	NC_001437	Japanese encephalitis virus
	NC_001563	West Nile virus

LIST OF MATERIALS

CELL LINES

Table 0-11: Cells lines used with their corresponding culture medium

Cell line	Source	Culture medium
Vero E6	African green monkey kidney cells	D-MEM + 5 % FCS + 1% Glutamine
PS	Pig kidney cells	L-15 + 5 % FCS + 1 % Glutamine

CELL CULTURE MEDIUM

D-MEM (Dulbecco's Modified Eagle Medium)	GIBCO Invitrogen, Karlsruhe
Leibovitz-Medium (L 15)	GIBCO Invitrogen, Karlsruhe
Opti-Mem® I Reduced Serum-Medium	GIBCO Invitrogen, Karlsruhe
Trypsin/EDTA-solution	PAN Biotech GmbH, Aidenbach
L-Glutamine	PAA Laboratories, Linz, Austria
Penicilline/Streptomycine-Mix	PAA Laboratories, Linz, Austria
Fetal bovine serum (FBS)	PAA Laboratories, Linz, Austria

COMPOSITION OF BUFFERS

DNA sample buffer (6x)	New England Biolabs®, Frankfurt/Main
Naphthaline Black	1 g Amido black 13,6 g Sodium acetate 60 ml acetic acid complete to 1L with H ₂ O Invitrogen, Karlsruhe
PCR Buffer (10x)	TwistDx Limited, Cambridge
RPA buffer (10x)	New England Biolabs®, Frankfurt/Main
Buffer for restriction enzymes	Thermo Fisher Scientific Inc., Waltham, MA, USA
Lane Marker Sample Buffer (5x) (Western blot)	Fermentas, St. Leon-Rot
Ligase Buffer (10x)	140 mM NaCl 2 mM KCl 10 mM Na ₂ HPO ₄ 2 mM KH ₂ PO ₄
Phosphate buffered saline (PBS)	50 mM Tris; pH 6.8 40% Glycerin 8% β-Mercaptoethanol 4 g/l Bromphenolblue 80 g/l SDS
SDS sample buffer 4x) (Western blot) (with or without β-Mercapthoethanol)	

LIST OF MATERIALS

SDS running buffer (5x) (Western blot)	15 g/l Tris 72 g/l Glycine 5 g/l SDS
Transfer buffer (Western blot)	25 mM Tris 150 mM Glycine 10% Methanol
0,1 M Carbonate buffer, pH 9,8 (ELISA)	5,6 g sodium hydrogen carbonate 9,53 g Sodium carbonate decahydrate complete to 1L with H ₂ O EUROIMMUN AG, Lübeck
IIFT-sample buffer	

EQUIPMENT

Autoclave automat 21/2

Webeco, Bad Schwartau

Centrifuges

- 1-13
- 1-15 K
- 3-K30 C
- Centrifuge 5415R
- Sigma 2K15 Kühlzentrifuge

Sigma Laborzentrifugen,
Osterode am Harz
Sigma Laborzentrifugen,
Osterode am Harz
Sigma Laborzentrifugen,
Osterode am Harz
Eppendorf, Hamburg
B. Braun, Melsungen
Bio-Rad, Munich
Tecan Group Ltd.,
Männedorf, Switzerland

ChemiDoc XRS + system

ELISA-Reader Infinite[®]200

Freezers

- -20 °C
- -80 °C

Bosch, Stuttgart
Heraeus, Hanau
Christ, Hanau
Bosch, Stuttgart

Freeze-dryer Alphal-5

Fridges

Gel electrophoresis system

- ComPhor Mini/Midi
- Mini Protean[®] 3

Biozym, Oldendorf
Bio-Rad, Munich

Heating and stirring plaques

- IKA[®] RH basic 2
- IKA KM02

Ika Werk, Staufen
Ika Werk, Staufen

Incubators

- for bacterial culture
- for cell culture

New Brunswick Scientific,
Edison, NJ, USA
Heraeus, Hanau

Laminar flow hoods

LIST OF MATERIALS

• Safe 2020	Thermo Fisher Scientific Inc., Waltham, MA, USA
• HeraSafe	Heraeus, Hanau
Microscopes	
• Fluoreszenzmikroskop (Axiovert 200)	Carl Zeiss, Jena
• EUROStarII	EUROIMMUN, Lübeck
• Biozero	Keyence Deutschland GmbH, Neu-Isenburg
• PrimoVert	Carl Zeiss, Jena
Photometer (Bio-Photometer)	Eppendorf, Hamburg
Pipettes (bis 10 µl, 100 µl, 200 µl, 1.000 µl)	Eppendorf, Hamburg
Pipette Controller (Accujet®)	Gilson Inc., Middleton, USA
Sequencer 3500xL Dx Genetic Analyzer	Brand, Wertheim
Tension devices	Applied Biosystems, Carlsbad, CA, USA
Thermoblock (Thermomixer comfort)	Biometra, Göttingen
Tube Scanner ESEQuant	Bio-Rad, Munich
Thermocyclers	Eppendorf, Hamburg
• Biometra T Gradient	Qiagen, Hilden
• Biometra T Personal	Biometra, Göttingen
• Biometra T Professional Basic Gradient	Biometra, Göttingen
• Stratagene MX3000P / MX3005P	Agilent Technologies, Inc, Santa Clara, CA, USA
Tube Scanner ESEQuant	Qiagen, Hilden
UV Transilluminator TC-312A	Spectroline, Westbury, USA
Vortex®	Carl Roth, Karlsruhe
Western Blot Module (Fastblot B 34)	Biometra, Göttingen
X-raying film development system Curix 60	Agfa-Gevaert Group, Mortsel, Belgium

ADDITIONAL MATERIAL

Cell scraper	TPP, Trasadingen, CH
Cooling box	Nunc, Wiesbaden
Cryo tubes (1,8 ml)	Nunc, Wiesbaden
Development cassette for X-ray (Western blot)	Appligene, Heidelberg
Disposable cuvettes	Eppendorf, Hamburg
ELISA Maxisorb 96-well plates	Nunc, Wiesbaden
Eppendorf tubes (0,5 ml; 1,5 ml; 2,0 ml)	Eppendorf, Hamburg
Falcon tubes (15 ml; 50 ml)	VWR International
Flasks for cell culture with and without filters	Nunc, Wiesbaden
Glassware	Schott Glas, Mainz
Glass slides for IFA	EUROIMMUN, Lübeck
HybriDetect lateral flow stripe (LFS)	Milenia Biotec, Giessen
Membranes (Western blot)	

LIST OF MATERIALS

• Westran [®] PVDF (0,2 µm/0,45 µm)	Schleicher & Schuell, Dassel
• Nitrocellulose (0,2 µm/0,45 µm)	Schleicher & Schuell, Dassel
Pipette tips with filter (10 µl, 20 µl, 100 µl, 200 µl, 1000 µl)	Biozym, Oldenburg Eppendorf, Hamburg Molecular Bioproducts Eppendorf, Hamburg
Pipette tips without filter (10 µl, 20 µl, 100 µl, 200 µl, 1000 µl)	
PCR Plates with 96 wells for TaqMan PCR and RPA tubes	Abgene, Epsom, UK
• 0,2 ml; 0,5 ml	
• 0,2 ml 8-tube strips with attached caps	Eppendorf, Hamburg Nunc, Wiesbaden Thermo Fisher Scientific Inc., Waltham, MA, USA Thermo Fisher Scientific Inc., Waltham, MA, USA Nunc, Wiesbaden
Ready-to-Use gels - 12 wells (Western blot)	
8-16% Precise Tris-HEPES - 4% polyacrylamide	
Sterile pipettes (1 ml; 5 ml; 10 ml; 25 ml, 50 ml)	B. Braun Aesculap, Tuttlingen
Scalpel	Carl Roth, Karlsruhe Nunc, Wiesbaden
Sterile filters (0,22 und 0,45 µm)	
Well plates (6er, 12er, 24er, 48er, 96er)	Schleicher & Schuell, Dassel
Whatman Blotting paper (Western blot)	
X-ray film CL-XPosure TM (Western blot)	Thermo Fisher Scientific Inc., Waltham, MA, USA

SOFTWARE

Adobe [®] Photoshop [®] CS3 Extended Version 10	Adobe Systems Inc. Munich
Lasergene [®] SeqMan Pro Software (Version 8.1.5)	DNASTAR Inc., Madison, WI, USA
MS Office	Microsoft Deutschland GmbH, Unterschleißheim
MxPro 4.10 QPCR Software	Agilent Technologies, Inc. Santa Clara, CA, USA
SDS 1.9.1 (ABI Prism [®] Sequence Detector)	Applied Biosystems, Carlsbad, CA, USA
Geneious Pro TM Version 5.3.4	Biomatters LTD, Auckland, New Zealand
Endnote X5	Thomson Reuters, Carlsbad, CA, USA
Image Lab	Bio-Rad, Munich
Adobe Acrobat Reader	Adobe Systems Inc., Munich
ESEQuant Tube Scanner Software	Qiagen, Hilden
ZEN lite	Carl Zeiss AG, Germany

CURRICULUM VITAE

For reasons of data protection, the curriculum vitae is not included in the online version.

For reasons of data protection, the curriculum vitae is not included in the online version.